The T-box Transcription Factor Eomesodermin Governs Hemogenic Competence of Yolk-Sac Mesodermal Progenitors

Luke T.G. Harland[1], Claire S. Simon [1,7], Anna D. Senft [1,8], Ita Costello[1], Lucas Greder[2], Ivan Imaz-Rosshandler [3,4], Berthold Gottgens[3], John C. Marioni[4,5,6], Elizabeth K. Bikoff [1], Catherine Porcher[2], Marella de Bruijn [2,9] and Elizabeth J. Robertson [1,9]

1.Sir William Dunn School of Pathology, University of Oxford, South Parks Road, Oxford, OX1 3RE, UK

2.MRCMolecular Haematology Unit, MRC Weatherall Institute of Molecular Medicine, University of Oxford, John Radcliffe Hospital, Oxford, OX3 9DS, UK

3.Wellcome-MRC Cambridge Stem Cell Institute, Jeffrey Cheah Biomedical Centre, University of Cambridge, Cambridge, CB2 0AW, UK

4.European Molecular Biology Laboratory, European Bioinformatics Institute (EMBL-EBI), Wellcome Genome Campus, Cambridge, CB10 1SD, UK.

5.Wellcome Sanger Institute, Wellcome Genome Campus, Cambridge, CB10 1SA, UK.

6.CRUK Cambridge Institute, University of Cambridge, Robinson Way, Cambridge, CB2 0RE, UK.

7.Current address: Developmental Biology Program, Memorial Sloan Kettering Cancer Centre, New York, NY10065, USA

8.Current address: National Institutes of Health/NICHD, 6 Center Drive, Bethesda, MD 20892, USA

9.Corresponding authors. (E.J.R Elizabeth.robertson@path.ox.ac.uk; M.dB marella.debruijn@imm.ox.ac.uk)

Abstract

Extra-embryonic mesoderm (ExM), the earliest cells that traverse the primitive streak (PS), give rise to the endothelium as well as hematopoietic progenitors in the developing yolk-sac (YS). How a specific subset of ExM becomes committed to a hematopoietic fate remains unclear. Here we demonstrate using an embryonic stem cell (ESC) model that transient expression of the T-box transcription factor Eomesodermin (Eomes) governs hemogenic competency of ExM. Eomes regulates the accessibility of enhancers that SCL normally utilizes to specify primitive erythrocytes and is essential for the normal development of Runx1^{+} hemogenic endothelium. Single-cell-RNA-seq suggests that Eomes loss-of-function profoundly blocks formation of blood progenitors but not specification of Flk-1^{+} hematoendothelial progenitors. Our findings place Eomes at the top of the transcriptional hierarchy regulating early blood formation and suggest that hemogenic competence is endowed earlier during embryonic development than previously appreciated.

Introduction

The process of gastrulation generates the three primary embryonic germ layers, namely mesoderm, ectoderm and definitive endoderm. Beginning at embryonic day 6 (E6.0), in response to local signaling cues, pluripotent epiblast cells on the prospective posterior side of the embryo undergo a process of epithelial-to-mesenchymal transition allowing them to delaminate and migrate within the PS[1]. The first cells that traverse the PS include progenitors of the ExM that migrate proximally to generate the developing YS[1-3]. ExM subsequently differentiates into endothelial cells that form the YS vasculature as well blood progenitors that sustain growth and development of the post-implantation embryo[3, 4].

Hematopoietic progenitors initially form at E7.5 to generate nucleated primitive erythrocytes within the distally located YS blood islands (BI)[3]. A day later a second wave of blood progenitors arise from a subset of endothelial cells present within the developing YS vasculature[5]. This so-called hemogenic endothelium (HE) undergoes an endothelial-to-hematopoietic transition (EHT) whereby cells round up, detach from the endothelial layer and enter the blood stream[6-8]. Hematopoietic progenitors derived from YS HE at E8.25 have restricted erythro-myeloid potential and generate enucleated erythrocytes[9] and are therefore designated ‘definitive’. Subsequently, at E10.5 a third wave of hematopoietic progenitors including definitive hematopoietic stem cells (HSC) arise from HE in vascular beds of the dorsal aorta and vitelline/umbilical arteries[7, 10].

Understanding the transcriptional hierarchy that guides hematopoiesis during embryogenesis is essential for the generation of hematopoietic progenitors from pluripotent stem cell sources *in vitro*[11, 12]. Of particular interest is how HE is specified as this represents a critical early step in the generation of definitive hematopoietic cells including the HSC. Only a few transcriptional regulators that impact hematopoietic output from HE have been identified, including the transcription factors (TF) SCL and Runx1 that play key roles during embryonic hematopoiesis. SCL is required for the specification of the blood fate and the generation of HE and all hematopoietic cells[13-17]. In contrast, Runx1 is non-essential for the generation of HE or primitive erythrocytes/megakaryocytes but is essential for EHT and the production of all definitive hematopoietic stem and progenitor cells[18].

Here we report that the T-box TF Eomes is transiently expressed in ExM progenitors that generate virtually all YS hematopoietic and endothelial cells. Using an ESC differentiation system, we find that Eomes is essential for the production of primitive erythrocytes and Runx1^{+} HE. Eomes is expressed prior to both SCL and Runx1 during mesoderm patterning. Single-cell RNA-seq (scRNAseq) comparisons to *in vivo* hematoendothelial development strongly suggest the block in hematopoietic development in Eomes loss-of-function cultures occurs after the specification of Flk-1^{+}/SCL^{+} hematoendothelial progenitors. ATAC-Seq experiments reveal that Eomes governs the accessibility of Runx1 enhancers as well as *cis*-regulatory regions that SCL normally utilizes to specify primitive erythrocytes. ChIP-seq experiments demonstrate that Eomes occupies Runx1 *cis*-regulatory regions and coordinates the development of hemogenic competent mesoderm in the context of Activin/Nodal and Tead-Yap signaling. Finally, re-expression of Runx1 in Eomes-null endothelial cultures is sufficient to rescue the block in EHT and definitive blood production. Collectively, these experiments demonstrate that Eomes sits at the top of the transcriptional hierarchy, functioning upstream of Runx1 expression and SCL functional activity, to promote hemogenic competence of the YS mesodermal lineage.

Results

Eomes expression transiently marks the proximal epiblast, PS and Flk-1^{+} ExM progenitors that give rise to hematopoietic and endothelial lineages of the YS

The first wave of cells to traverse the PS give rise to ExM that migrates proximally, displacing the overlying extra-embryonic ectoderm (ExE) to form the inner layer of the developing YS[2, 3]. Subsequently these cells generate the BI containing primitive erythrocytes and endothelial cells that give rise to the YS vascular network[3] (Fig. 1a). The T-box TF factor brachyury (T) is expressed in the PS and nascent mesoderm, including the hemangioblast, a multipotent progenitor that generates hematopoietic and endothelial cells[19]. Flk-1 also marks the hemangioblast[19] and *in vivo* fate mapping studies demonstrate that YS hematopoietic and endothelial cells are derived from Flk-1^{+} ExM[20].

Here we observed that Eomes expression is detectable in proximal epiblast/PS cells at early/mid PS stages (E6.5) prior to widespread T expression (Fig. 1b,c). Additionally, at mid-streak (E6.5) stages a population of Flk-1^{+} migratory mesoderm co-expressed Eomes in the extraembryonic region (Extended Data Fig. 1a). To test whether Eomes expressing progenitors contribute to the ExM at later stages we performed short-term lineage tracing experiments using an Eomes$^{GFP/+}$ reporter line[21]. At E7.5 Eomes-GFP^{+} cells detected within the YS BIs co-expressed Flk-1 (Fig. 1d) and the ExM/hematopoietic marker Runx1 (Fig. 1e). However, this reflects GFP perdurance as endogenous Eomes protein was no longer detectable in Eomes-GFP^{+} (Fig. 1f) or Flk-1^{+} cells in the YS at this stage (Extended Data Fig. 1b).

To examine contributions made by Eomes-expressing cells to YS vascular and hematopoietic lineages we generated an *Eomes^{iCre}* reporter allele (Extended Data Fig. 2a-e) and performed long-

term lineage tracing experiments. *Eomes*$^{iCre/+}$ males were mated to females carrying the *ROSA26*^{R} allele[22] and the resulting embryos stained for LacZ expression. At E8.5 and E9.5 virtually all the YS hematopoietic and endothelial cells in *Eomes*^{iCre}*; ROSA26*^{R} embryos were LacZ^{+} (Fig. 1g). Thus, we conclude that transient Eomes expression marks ExM progenitors that give rise to the YS hematopoietic and endothelial compartments.

To assess Eomes functional contributions we analyzed E7.5 embryos carrying an epiblast-specific *Eomes* deletion (*Eomes*$^{CA/N}$;Sox2.Cre)[23] that disrupts delamination of nascent mesoderm[23]. In contrast to wild-type embryos, *Eomes*$^{\Delta Epi}$ mutant embryos fail to induce expression of Flk-1 and ER71, genes essential for YS hematopoiesis and vasculogenesis[24-26] (Extended Data Fig. 2f). Thus, Eomes expression in the epiblast is essential for the generation of ExM.

Eomes is expressed transiently in hematovascular progenitors prior to the onset of SCL and Runx1 expression during hematopoietic differentiation

To circumvent *in vivo* morphogenetic defects caused by Eomes functional loss, we exploited an *in vitro* ESC differentiation protocol[27, 28] to promote the formation of YS-like hematopoietic and endothelial progenitors via the staged addition of growth factors to embryoid bodies (EB) under serum free conditions (Fig. 2a-c). Eomes[21], SCL[29] and Runx1 (Extended Data Fig. 3a,b) expression were analyzed utilizing ESC reporter lines. Dissociated EBs were stained for Flk-1 and PdgfRa, markers that distinguish hematovascular mesoderm (Flk-1^{hi}/PdgfRa^{-}), primitive/cardiac mesoderm (Flk-1^{+}/PdgfRa^{+}), and paraxial mesoderm (Flk-1^{-}/PdgfRa^{+}) and the hematopoietic marker CD41[26, 30-34] (Fig. 2d,e). Eomes-GFP was detectable at day 3 prior to expression of Flk-1/PdgfRa. The majority of cells at day 4, including the Flk-1^{hi}/PdgfRa^{-} hematovascular mesoderm compartment, express Eomes-GFP (Fig. 2d). 24 hours later Eomes-GFP^{+} cells comprise roughly half the Flk-1^{hi}/PdgfRa^{-} compartment (Fig. 2d). In contrast, developing CD41^{+} hematopoietic cells are predominantly Eomes-GFP$^{lo/-}$ (Fig. 2e).

At day 4 SCL-mCherry is exclusively expressed within the Flk-1^{hi}/PdgfRa^{-} compartment (Fig. 2d). At day 5 hematopoietic cells co-express CD41 and SCL-mCherry and downregulate Flk-1 expression (Fig. 2d,e). Runx1-Venus is also expressed in CD41^{+} hematopoietic cells (Fig. 2e). However, in contrast to SCL-mCherry, Runx1-Venus expression is restricted to cells that weakly express Flk-1 within the Flk-1^{hi}/PdgfRa^{-} compartment at day 4/5 (Fig. 2d).

Consistent with above results, differentiation trajectories constructed using scRNAseq data from E6.5 to E8.5 mouse embryos[15] reveal dynamic Eomes expression in mesoderm/hematoendothelial progenitors that give rise to SCL and Runx1 expressing hematopoietic and endothelial cells (Fig. 2f). Thus, we conclude Eomes is transiently expressed, prior to SCL and Runx1, in hematovascular mesoderm progenitors.

Eomes functional loss disrupts primitive and definitive hematopoiesis but not endothelial development

Next, we examined the ability of Eomes-null ESC[23] to generate hematovascular mesoderm (Fig. 3a). Eomes-null EBs contain a detectable but decreased number of Flk-1^{hi}/PdgfRa^{-} cells at day 4/5 and lack Flk-1^{+}/PdgfRa^{+} progenitors at day 4, reflecting Eomes requirements for cardiac mesoderm specification[35, 36] (Fig. 3b). RNA-Seq experiments performed at day 4 reveal that Eomes-null Flk-1^{hi}/PdgfRa^{-} cells express SCL, ER71, Gata2, Lmo2, Tek, Cdh5, Fli1 and CD31 (Fig. 3c), suggesting that Eomes is non-essential for specification of hematovascular mesoderm. In contrast, EHT regulators including Runx1 and Gfi1b, and genes expressed in erythroid cells (Gata1 and Hbb-bh1) were downregulated (Fig. 3c).

To further examine Eomes functional requirements we cultured EBs for three more days in pro-hematopoietic conditions (Fig. 3a, red). Wild-type cultures robustly form hematopoietic progenitors co-expressing c-Kit, and/or CD41 and CD45, and generate primitive/definitive erythrocyte and myeloid/mixed hematopoietic colonies (Fig. 3d,e). In contrast, Eomes-null cultures lack the ability to form CD41^{+}/CD45^{+} cells and hematopoietic colonies (Fig. 3d,e). These cultures contain CD31^{+}/Cdh5^{+} endothelial cells (Fig. 3f) and express normal levels of endothelial marker genes Cdh5, Flk-1, Flt-1 and Fli-1 (Fig. 3,g). However, SCL, Runx1, PU.1, Gata1 and Hbb-bh1 transcripts at day 6 were markedly downregulated confirming a block in hematopoiesis (Fig. 3g).

To further explore Eomes functional contributions Flk-1^{hi} cells were isolated at day 5 and plated on Matrigel under conditions known to promote HE development[37] (Fig. 3a, blue). By day 8 wild-type Flk-1^{hi} cells give rise to patches of adherent Cdh5^{+}/c-Kit^{+} HE cells that actively undergo EHT to generate semi-adherent and floating CD41^{+}/CD45^{+} hematopoietic cells (Fig. 3h,i). Eomes-null Flk-1^{hi} cells generate Cdh5^{+}/c-Kit^{+} endothelium but these cells fail to efficiently undergo EHT and lack expression of the hematopoietic markers CD41/CD45 (Fig. 3i). Thus, we conclude Eomes is dispensable for the generation of endothelial cells but is essential for both primitive and definitive hematopoietic development.

Eomes is essential for the generation of Runx1^{+} hemogenic endothelium

Defects observed above in Eomes-null ESCs closely resemble those reported for SCL mutants[13]. Therefore, next we re-generated the Eomes-null allele in ESCs that contain an SCL reporter allele[29] (Extended Data Fig. 4a-c) to directly test Eomes requirements for SCL expression. At day 5 of differentiation many Eomes-null Flk-1^{hi}/PdgfRa^{-} cells are SCL-mCherry^{+} (Fig. 4a) and a day later a high proportion of c-Kit^{+}/Cdh5^{+} cells expressed wild-type levels of SCL-mCherry (Fig. 4b). Thus, the

block in primitive and definitive hematopoiesis observed in Eomes-null cultures cannot be explained simply due to loss of SCL expression.

Runx1 expression is required for EHT and the generation of definitive hematopoietic cells[18]. To assess whether the block in definitive hematopoiesis in Eomes-null cultures reflects the absence of HE, we disrupted Eomes expression in the Runx1-Venus reporter ESCs (Extended Data Fig. 4a-c). At day 5 Eomes-null EBs almost entirely lack Runx1-Venus expression (Fig. 4c). At day 8, Runx1-Venus expression normally marks a $CD41^{-/lo}$ HE subset within the c-Kit^{+}/$Cdh5^{+}$ compartment (Fig. 4d, blue gate). Upon EHT, cells upregulate CD41, generating Runx1-$Venus^{+}$/$CD41^{+}$ hematopoietic cells (Fig. 4d, green gate). Strikingly, Eomes-null EHT cultures lack Runx1-$Venus^{+}$cKit^{+}/$Cdh5^{+}$ HE (Fig4d, blue gate). Eomes-null Runx1-Venus day 5 EBs and day 8 EHT cultures lack clonogenic progenitors for primitive erythrocyte and definitive erythro-myeloid lineages, respectively (Fig. 4e), as well as $Cdh5^{-}$ /$CD41^{+}$/Runx1-$Venus^{+}$ cells (Fig. 4d, orange gate) and budding cells (Fig. 4f). We conclude that the block in definitive hematopoiesis in Eomes-null EHT cultures is associated with the loss of Runx1+ HE.

To test whether Eomes regulates Runx1 expression in a cell autonomous fashion, we performed co-culture experiments. Wild-type ESCs were mixed with Runx1-Venus or Eomes-null Runx1-Venus ESCs (Extended Data Fig. 3c). Wild-type:Runx1-Venus co-cultures at day 6 contain $CD41^{+}$ hematopoietic cells that are Runx1-$Venus^{+}$. In contrast, Runx1-Venus expression in $CD41^{+}$ cells is barely detectable in Eomes-null Runx1-Venus:wild-type co-cultures. These results strongly suggest that Eomes promotes robust induction of Runx1 expression in a cell-autonomous fashion during hematopoiesis.

Eomes influences chromatin accessibility at SCL bound enhancers in hematovascular mesoderm

To investigate Eomes-dependent chromatin accessibility we performed ATAC-Seq[38] analysis of day 4 wild-type and Eomes-null Flk-1^{hi}/PdgfRa^{-} hematovascular mesoderm. We identified changes at 4180 genomic locations corresponding to ~7% of all accessible sites (Fig. 5a). The majority of sites (>85%) showing reduced chromatin accessibility in Eomes-null cells were located in distal intergenic regions (Fig. 5a) and are enriched for binding motifs for hematopoietic regulators such as Gata1/2, SCL, Erg, Ets1, Fli1, Runx1, Meis1 and Gfi1b (Fig. 5b). Strikingly, when these peaks were compared to published ChIP-Seq datasets from Flk-1^{+} cells generated using a hematopoietic differentiation protocol[39], we found that the majority of Eomes-dependent sites with reduced accessibility were

enriched for enhancer marks (H3K4Me1 and H3K27Ac) and SCL occupancy (Fig. 5c). Moreover, sites showing reduced accessibility that correlate with SCL occupancy are enriched for genes related to hematopoietic development (Fig. 5d). Of these 231 are associated with downregulated genes in Eomes-null Flk-1^{hi}/PdgfRa^{-} cells including Gata1 and Nfe2, which are critical for primitive erythrocyte development and those governing EHT and definitive hematopoiesis, namely Runx1, Gfi1/1b, Ikzf1 and Myb (Fig. 5e). Many of the changes in chromatin accessibility map to previously identified enhancer regions at these loci (Fig. 5f)[40, 41]. Consistent with results above there was no noticeable impact on chromatin accessibility at the SCL locus (Fig. 5f). These results demonstrate that Eomes regulates accessibility at SCL-bound *cis*-regulatory elements.

Sites co-occupied by Eomes, Tead4 and Smad2/3 are transiently marked by H3K27Ac during early stages of hematopoietic development

To facilitate identification of Eomes target genes we generated ESCs expressing C-terminally V5-tagged Eomes (Eo-V5) (Extended Data Fig. 5a-c,f). Intracellular flow cytometry demonstrated that Eo-V5 expression peaked at day 4 during hematovascular mesoderm development (Extended Data Fig. 5d). Eo-V5 is expressed broadly in primitive/cardiac mesoderm (Flk-1^{+}/PdgfRa^{+}) as well as a subset of developing hematovascular (Flk-1^{hi}/PdgfRa^{-}) mesodermal cells (Extended Data Fig. 5e). Homozygous Eo-V5 EB cultures generate Flk-1^{+}/PdgfRa^{+} primitive/cardiac mesoderm and c-Kit^{+}/CD41^{+} hematopoietic progenitors, confirming that Eomes-V5 functions normally (Extended Data Fig. 5g).

We used two independent Eo-V5 ESC clones (CL A and CL B) for ChIP-Seq analysis. V5-Eomes bound genomic regions common to both clones (Fig. 6a) were highly enriched for the Eomes binding motif[42] and were predominantly located >5 kb from transcriptional start sites (Fig. 6b). 30% of genes linked to ChIP peaks were found to be mis-regulated in day 4 Flk-1^{hi}/PdgfRa^{-} Eomes-null cells including transcriptional regulators (Runx1, Mixl1, Klf5, Pbx1, Tbx3, Foxf1, Meis2) and signaling molecules (Dkk1, Gli2, Fzd7, Lefty2) controlling hematovascular development[27, 43-48] (Fig. 6c).

Next, we examined published ChIP-Seq datasets[49, 50] to assess co-occupancy by transcriptional regulators, DNase hypersensitivity sites and local histone marks during hematopoietic differentiation (Fig. 6d). The majority of Eomes occupied sites were marked by H3K27Ac and display DNase hypersensitivity in hemangioblasts (T^{+}/Flk-1^{+}) but not hematopoietic progenitors (CD41^{+}) (Fig. 6d). Strikingly, many are also co-bound by Smad2/3 and the TF Tead4 (Fig. 6d). Overlapping Eomes, Smad2/3 and Tead4 peaks identified 72 sites corresponding to genes associated with hematopoiesis and mesoderm development (Fig. 6e). We observe co-occupancy at genes down-regulated in day 4 Flk-1^{hi}/PdgfRa^{-} Eomes-null EBs (Fig 6c) including the promoter region of Mixl1, previously shown to regulate the generation of Flk-1+ hematopoietic mesoderm[32, 42, 44, 51] and putative *cis*-regulatory elements controlling Dkk1 and Tbx3 expression (Fig. 6h). Eomes, Tead4 and Smad2/3 co-occupy a potential cis-regulatory region 181kb upstream of the Runx1 TSS locus marked transiently by

H3K27Ac (Fig. 6h). Recent ChIP-seq experiments[51] confirm Eomes occupancy at this -181kb region (Extended Data Fig. 6) as well as the Runx1 proximal promoter (P2) that is active in HE[52] and several Runx1 enhancers (+110, +171, +204, -327) known to regulate expression during hematopoiesis[40, 53] (Extended Data Fig. 6). Eomes induction also rescues Runx1 expression in this context[51] suggesting that Eomes directly regulates Runx1 expression.

Finally, we overlaid our day 4 Eomes ChIP-Seq peaks with the ATAC-Seq peaks with reduced accessibility in day 4 Flk-1^{hi}/PdgfRa^{-} Eomes-null mesoderm as well SCL ChIP-Seq peaks from day 4 wild-type Flk-1^{+} EBs[39]. Very few of the ATAC peaks (33/3629) or SCL ChIP Peaks (19/4393) are bound by Eomes at day 4 (Extended Data Fig. 7a). Interestingly, Eomes ChIP peaks are accessible at early mesodermal (T^{+}/Flk-1^{-}) stages of development and become marked by H3K27Ac after the onset of Flk-1 expression[49] (Extended Data Fig. 7b). By contrast, Eomes-dependent ATAC peaks normally bound by SCL only become accessible in the hemangioblast (T^{+}/Flk-1^{+}) population[49] (Extended Data Fig. 7b). These results suggest that Eomes-dependent SCL bound *cis*-regulatory regions become accessible only subsequent to Eomes functional activity at earlier stages in the hematopoietic differentiation pathway.

Single-cell RNA-Seq reveals the stage at which hematopoietic development is blocked in Eomes loss-of-function cultures

To characterize the stage when hematopoietic development is blocked in Eomes loss-of-function cultures we performed scRNA-seq on Eomes-null and wildtype Flk-1^{hi}/PdgfRa^{-} populations at day 4 and day 5 (Extended Data Fig. 8a). An integrated analysis[54] was performed that allowed uniform manifold approximation and projection (UMAP), and the identification of 13 clusters (Extended Data Fig. 8). Cluster identities were determined by comparing marker genes conserved across genotypes (Supplementary Table 1) to those previously used to document discrete cell populations present in E6.5 to E8.5 mouse gastrulation atlas[15]. Additionally, we were able to map the *in vitro* derived cells onto the mouse gastrulation atlas[15], allowing us to transfer cell identities and embryonic stages onto our scRNA-seq dataset (Fig. 7a-d).

Cells from day 4 EBs were found mainly in clusters 2-6 (Extended Data Fig. 8b,c) and resembled *in vivo* mixed mesoderm and hematoendothelial progenitors (Fig. 7a) that express T, Mixl1, ER71 and SCL (Fig. 7b, Extended Data Fig. 8e). By contrast, day 5 cells mainly contributed to clusters 7-13 (Extended Data Fig. 8b,c) that resembled *in vivo* hematoendothelial progenitors, endothelium, allantois and blood progenitors 1 and 2 (Fig. 7a) and expressed varying levels of Runx1, Gata1, Cdh5, Pecam1 and Spin2c (Fig. 7b, Extended Data Fig. 8e). Day 4 Eomes-null and wild-type cells contributed relatively equally to mesodermal/hematoendothelial progenitor clusters 2-6 (Extended Data Fig. 8c). By contrast, day 5 Eomes-null cells predominately contributed to the hematoendothelial progenitor, endothelial and allantoic clusters (9-13) at the expense of blood progenitor clusters (7 and 8; Extended Data Fig. 8c). The exceptional Eomes-null cells contributing to clusters 7 and 8

expressed hematovascular genes SCL, ER71, Cdh5 and CD31 but had reduced expression of EHT regulators Runx1/Gfi1b (Extended Data Fig. 8e,f). Interestingly, many Eomes-null Flk-1^{hi}/PdgfRa^{-} cells display transcriptional profiles similar to endothelial cells and hematoendothelial progenitors from E7.75-E8.5 mouse embryos (Fig. 7d). Mapping cells onto the *in vivo* hematoendothelial differentiation trajectory of the mouse gastrulation atlas[15] (cf. Fig. 2f) suggests that the developmental block in Eomes-null cultures reflects the failure of hematoendothelial progenitors to transition into blood progenitors 1/2 (Fig. 7e).

Runx1 re-expression in Eomes-/- EHT cultures rescues the production of definitive hematopoietic progenitors

Day 5 Eomes-null Flk-1^{hi}/PdgfRa^{-} cultures contain endothelial cells (Fig. 7a,e, Extended Data Fig. 8c) but could not form Runx1^{+} HE (Fig. 4d). Both Runx1-null and Eomes-null ESCs generate a Cdh5^{+}/cKit^{+}/CD41^{lo} population (Extended Data Fig. 9a,b). However, this population was absent from equivalent SCL-null cultures (Extended Data Fig. 9a,b). To further characterize Eomes functional contributions in relation to Runx1 we deleted Eomes in the context of a Runx1 inducible ESC line[14, 52] (iRunx1; Runx1-null with a doxycycline (dox) inducible Runx1b cDNA inserted into the ROSA26 locus) (Extended Data Fig. 4d,e). This strategy enabled us to drive Runx1 expression in Eomes-null EHT cultures and perform rescue experiments.

As expected, day 5 iRunx1 Eomes-null EBs generate a Flk-1^{hi}/PdgfRa$^{lo/-}$ population (Fig. 8,a) but lack primitive erythrocyte progenitors (Fig. 8b), highlighting differences in requirements for Runx1 and Eomes during primitive erythropoiesis. As expected[52], rescuing EHT and generation of functional hematopoietic progenitors via enforced Runx1 expression is highly dose-dependent (Fig. 8c,d). Titration experiments establish that the addition of 90 ng/mL of dox from day 6-8 in iRunx1 Eomes +/+ EHT cultures efficiently rescues generation of definitive erythro-myeloid clonogenic progenitors and Cdh5^{+}/CD41^{+} and Cdh5^{+}/CD45^{+} cells (Fig. 8c,d and Extended Data Fig. 9c). Strikingly, these conditions also rescue, albeit less efficiently, the generation of Cdh5^{+}/CD41^{+} and Cdh5^{+}/CD45^{+} cells and restore hematopoietic colony formation in iRunx1 Eomes-null cultures (Fig. 8c,d and Extended Data Fig. 8c,d). These findings demonstrate that Eomes acts upstream of Runx1 expression during definitive hematopoiesis.

Discussion

Here we show in the absence of Eomes function Flk-1^{+} hematoendothelial progenitors are correctly specified. However, upon further differentiation these progenitors cannot transition into primitive erythrocytes or HE capable of expressing Runx1 and undergoing EHT (Fig. 8e). As judged by scRNA-seq analyses these *in vitro* cells closely resemble those formed *in vivo* when hematopoiesis predominates in the murine YS (E7.5-E8.5). These results highlight the validity of using ESC

differentiation cultures as a model of YS hematopoiesis and have allowed us to uncover an essential role for Eomes in this process.

Our ATAC-Seq analysis of Eomes-mutant hematoendothelial progenitors suggests that the block in primitive erythrocyte development occurs because SCL can no longer access the enhancer network through which it normally specifies this lineage. SCL itself is not responsible for governing accessibility of key enhancers that guide this process[39]. These enhancers only become accessible during normal hematopoietic differentiation after the onset of Flk-1 expression. Eomes expression precedes Flk-1/SCL expression during hematoendothelial development. Thus, Eomes potentially functions as a pioneer factor opening SCL enhancers to direct primitive erythrocyte development. Our ChIP-Seq results, however, argue against this idea since the majority of SCL-bound enhancers are not occupied by Eomes.

Recent experiments demonstrate that hemogenic competency of YS endothelial progenitors is actively restrained via BMI1-dependent silencing of Runx1 expression[55]. Additionally, re-expression of Runx1 in non-HE cells is sufficient for their conversion into HE[56, 57]. Therefore, Runx1 is sufficient to promote conversion of YS endothelium towards a hemogenic fate. Here we demonstrate that Eomes acts upstream of Runx1 expression in the HE lineage. Moreover, Runx1 re-expression in Eomes-null cultures rescues the formation of definitive hematopoietic progenitors. ChIP-seq in day 4/5 EBs reveals Eomes occupancy at the Runx1 proximal promoter P2 as well as previously described[40, 53] (+110, +171, +204, -327) and potentially novel (-171/-181) Runx1 enhancers. Furthermore, ATAC-seq demonstrates that hematoendothelial progenitors formed in the absence of Eomes lack chromatin accessibility at enhancers known to drive Runx1 expression in the HE lineage/sites of definitive hematopoiesis[40, 58] (+3, +23, +110, -322, -327). Considering that YS endothelial cells are derived from Eomes expressing precursors, Eomes likely endows hemogenic competence via its ability to allow Runx1 induction at later developmental stages within the endothelial lineage. Thus, Eomes directs the emergence of an epigenetic landscape that primes HE specification.

The majority of Eomes ChIP-Seq peaks are located at *cis*-regulatory regions active transiently during mesodermal stages of development. Strikingly, many of these Eomes bound sites are co-occupied in similar stage EBs by Tead4 and Smad2/3, TFs that act downstream of Hippo/YAP and Activin/Nodal signalling respectively and have been shown previously to regulate hematopoietic development[27, 28, 31, 49, 59]. Computational analysis shows that sites co-bound by this triad of TFs are associated with genes regulating both mesoderm and blood cell development. Interestingly, disruption of Tead-YAP complex formation profoundly disrupts EHT and the generation of $CD41^{+}$ cells[49]. Additionally, Tead signalling is essential during mesodermal stages of development, coincident with the onset of Eomes functional activity[49]. It therefore seems likely that Eomes guides hematopoietic mesoderm development in the context of active Activin/Nodal and Tead/YAP signalling.

Fate mapping studies previously suggested that YS hematopoietic and endothelial lineages become segregated within the proximal epiblast, prior to ingression through the PS[2, 60]. The first cells to ingress through the streak predominantly generate primitive hematopoietic cells whilst the second

wave generates endothelial precursors[2] that subsequently acquire HE or non-HE fates. Conditional inactivation of Eomes in the PS using a T.Cre deleter strain has no noticeable impact on embryonic development[23]. Therefore, Eomes is likely only required for YS hematopoiesis within a narrow developmental time window at the very outset of gastrulation in the proximal epiblast/PS. The present study makes Eomes the earliest known transcriptional regulator of specifically hematopoietic but not endothelial development, placing it at the top of a transcriptional hierarchy that governs hemogenic competence in the developing mouse gastrula.

Main Figure Legends

Figure 1. Eomes is expressed in extraembryonic mesodermal progenitors that give rise to yolk-sac hematopoietic and vascular cells.

a, Schematic representation of mouse gastrulation. Extra-embryonic mesoderm (ExM) progenitors migrate proximally from the primitive streak (PS, dotted line) and give rise to the blood islands (BI) of the developing yolk-sac (YS). ExE, extraembryonic ectoderm; Epi, epiblast; VE, visceral endoderm. **b, c,** Early/mid streak stage embryos (E6.5) stained for Brachyury (red) and Eomes (green) and counterstained with DAPI (blue); n = 19 embryos (E6.5) and n = 19 embryos (E7.5). The length of the PS is denoted by the dotted line. **d – f,** Immunofluorescence staining of E7.5 Eomes $^{GFP/+}$[21] embryos for Flk-1(**d**, red; n = 11 embryos), Runx1(**e**, red; n = 11 embryos), Eomes (**f**, red n = 6 embryos) and Eomes-GFP (**d-f**, green). Nuclei are stained with DAPI (blue). Dotted white lines indicate the extraembryonic/embryonic boundary. White boxes denote the zoomed in areas displayed in the lower panels. **g,** Descendants of Eomes^{iCre} expressing cells give rise to hematopoietic and endothelial cells of the YS BI. Mice carrying an improved Cre recombinase (iCre) inserted into the ATG start site at the Eomes locus were crossed to ROSA26^{R} reporter mice that express LacZ upon Cre induced recombination. Wholemount X-gal staining was performed on E8.5 and E9.5 embryos and sections were counterstained with nuclear fast-red to highlight non-labelled cells; n ≥ 3 embryos. Scale bars, 100 μM.

Figure 2. Eomes, SCL and Runx1 expression during hematopoietic development *in vitro* and *in vivo*.

a, Schematic representation of the ESC differentiation protocol. **b, c,** Representative phase contrast photomicrographs at day 0 **(b)** and day 4 **(c)** of the differentiation protocol; n ≥ 3 independent differentiations. Scale bars, 100 μM. Embryoid body, EB. **d,** Flow cytometric analysis of EB cultures generated from Eomes, SCL and Runx1 reporter ESC lines. Cells expressing the indicated

fluorescent reporters are shown by coloured dots. Eomes-GFP, yellow; SCL-mCherry, red; Runx1-Venus, green. The percentages of reporter positive cells within the circled Flk-1^{hi}/PdgfRa^{-} cell population are indicated (n=1 differentiation). **e,** Analysis of day 5 EBs showing fluorescent reporter activity and expression of the hematopoietic marker CD41 (n=1 differentiation). **f,** Force-directed graph layout of cells isolated from E6.5 to E8.5 embryos associated with the blood/endothelial lineage (adapted from Pijuan-Sala et al. 2019, Ref 15)[15]. Left plot highlights various cell-types that are generated along the hematovascular lineage trajectory as mesoderm differentiates into endothelial and hematopoietic cells. Right plots are overlaid with Log_2 normalized gene expression levels. HE, hematoendothelial.

Figure 3. Eomes functional loss disrupts primitive and definitive hematopoiesis but not endothelial development

a, ESC differentiation protocols modelling yolk-sac hematopoiesis differ from day 5 onwards (EB suspension culture, red and EHT culture, blue). **b,** Representative flow cytometric analysis of Flk-1/PdgfRa expression in wild-type (WT) and Eomes$^{-/-}$ EBs at day 4/5. Graphical data indicate the mean +/- SEM; n = 5 (WT D4), n = 7 (Eomes$^{-/-}$ D4), n = 8 (WT D5) amd n = 10 (Eomes$^{-/-}$ D5) independent differentiations. **c**, Heatmap showing Log2(FPKM) expression of hematovascular genes in day 4 WT and Eomes$^{-/-}$ Flk-1^{hi}/PdgfRa^{-} cells from n = 3 independent differentiations. **d**, Hematopoietic potential of cells isolated from day5/6 WT and Eomes$^{-/-}$ EBs plated in hematopoietic colony-forming assays. Graphical data indicate mean +/- SEM; n = 2 (day 5) and n = 3 (day 6) biologically independent samples. Ery-P, primitive erythrocyte; Ery-D, definitive erythrocyte; GM, granulocyte-macrophage; GEMM, granulocyte-erythro-myeloid. Scale bar, 100 μM. **e**, Representative flow cytometric analysis of cKit/CD41 and cKit/CD45 expression in day 7 WT and Eomes$^{-/-}$ EBs. Graphical data indicate mean +/- SEM; n = 3 biologically independent samples. **f,** Representative flow cytometric analysis of Cdh5/CD31 expression in day 6 WT and Eomes$^{-/-}$ EBs. Graphical data indicate mean +/- SEM; n = 3 biologically independent samples. **g,** Log_2Fold Change (Eomes$^{-/-}$ versus WT) of hematovascular marker gene expression in day 6 EB cultures determined using reverse transcription quantitative PCR (RT-qPCR); mean +/- SEM; n = 3 biologically independent samples. GAPDH was used as a housekeeping gene. **h,** Representative phase contrast images of day 8 WT and Eomes$^{-/-}$ EHT cultures; n = 3 independent differentiations. Scale bars, 100 μM **i,** Representative flow cytometric analysis of Cdh5 expression and cKit/CD41 or cKit/CD45 expression within the Cdh5+ compartment in day 8 WT and Eomes$^{-/-}$ EHT cultures. Graphical data indicate mean +/- SEM; n = 3 independent differentiations. For all graphical representations of flow cytometry/colony-forming data individual replicates are shown as coloured dots (WT = grey, Eomes$^{-/-}$ = pink). Statistical analyses were performed using two-tailed unpaired Student's t-tests. Statistical source data are provided in Source Data Fig. 3.

Figure 4. Eomes-null cultures lack Runx1+ hemogenic endothelial cells

a,c, Representative flow cytometric analysis of Flk-1/PdgfRa and SCL-mCherry (**a**) or Runx1-Venus (**c**) expression in day 5 WT and Eomes$^{-/-}$ EBs. Coloured dots indicate cells positive for the expression of fluorescent reporters. SCL-mCherry,red; Runx1-Venus, green. Histograms display SCL-mCherry (**a**) and Runx1-Venus (**c**) expression levels in the Flk-1^{hi}/PdgfRa^{-} compartment; grey peaks depict expression in a control cell line. Graphical data indicate mean +/- SEM; n = 3 (WT and Eomes$^{-/-}$ SCL-mCherry), n = 4 (WT Runx1-Venus) and n = 5 (Eomes$^{-/-}$ Runx1-Venus) independent differentiations. **b**, Representative flow cytometric analysis of CD41/SCL-mCherry expression within the Cdh5^{+}/c-Kit^{+} compartment in day 6 WT SCL-mCherry and Eomes-/- SCL-mCherry EBs. Graphical representations display mean +/- SEM; n = 3 independent differentiations. **d,** Representative flow cytometric analysis of Cdh5/cKit expression (left) and Runx1-Venus/CD41 expression within the Cdh5^{+}/cKit^{+} (middle) and Cdh5^{-} (right) compartments in day 8 WT and Eomes$^{-/-}$ EHT cultures. Graphical representations indicate mean +/- SEM; n = 3 independent differentiations. **e**, Hematopoietic colony-forming potential of cells isolated from day 5 bulk EBs and day 8 EHT cultures plated in hematopoietic colony assays. Each dot displays the number of colonies formed in each technical replicate from n=2 independent differentiations; 2 technical replicates/independent differentiation. Ery-P, primitive erythrocyte; Ery-D, definitive erythrocyte; GM, granulocyte-macrophage; GEMM, granulocyte-erythro-myeloid. **f,** Representative phase contrast images of Runx1-Venus Eomes$^{+/+}$ and Runx1-Venus Eomes$^{-/-}$ EHT cultures at day 8; n = 3 independent differentiations. Scale bars, 100 μM. For all graphical representations of flow cytometry individual replicates are shown as coloured dots (Eomes$^{+/+}$ = grey

and Eomes$^{-/-}$ = pink). Statistical analyses were performed using unpaired two-tailed Student's t-tests. Statistical source data are provided in Source Data Fig. 4.

Figure 5. Eomes regulates chromatin accessibility at SCL bound cis-regulatory regions

a, Pie chart depicting the proportion of ATAC peaks that lose (blue) or gain (red) chromatin accessibility in Eomes$^{-/-}$ day 4 Flk-1^{hi}/PdgfRa^{-} cells. Bar chart depicting the distribution of ATAC peaks located nearby transcriptional start sites (TSS) with unchanged (grey), reduced (blue) or increased (red) chromatin accessibility in day 4 Eomes$^{-/-}$ vs. WT Flk-1^{hi}/PdgfRa^{-} cells; n = 3 independent differentiations. **b,** Sites of reduced chromatin accessibility in Eomes$^{-/-}$ cells are enriched for hematopoietic TF binding motifs. Statistical analyses were performed using *AME* (Analysis of Motif Enrichment). **c,** Heatmaps showing ATAC signals from WT (blue, left) or Eomes$^{-/-}$ (blue, right) day 4 Flk-1^{hi}/PdgfRa^{-} cells and ChIP signal for H3K4Me1 (orange), H3K27Ac (red) and SCL (green) occupancy from day 4 WT Flk-1^{+} cells[39]. Heatmaps show a 4kb flanking region surrounding sites of reduced chromatin accessibility in day 4 Eomes$^{-/-}$ Flk-1^{hi}/PdgfRa^{-}cells. **d,** Venn diagram depicting the overlap of SCL bound regions[39] and sites of reduced chromatin accessibility. Enriched GO Terms in the Mouse Phenotype category for the 949 shared genomic regions (purple). Statistical analyses were performed using *GREAT* (Genomic Regions Enrichment Analysis Tool). **e,** MA plot highlighting genes that are differentially expressed in Eomes$^{-/-}$ and WT hematovascular mesoderm (Flk-1^{hi}/PdgfRa^{-}) that have nearby sites of reduced chromatin accessibility (red and blue squares) that are also bound by SCL in WT Flk-1^{+} mesoderm[39] (orange and green squares). **f**, IGV snapshots of ATAC-Seq (blue) and ChIP-Seq (green) tracks highlighting hematopoietic regulators that have nearby genomic regions with reduced chromatin accessibility in Eomes$^{-/-}$ Flk-1^{hi}/PdgfRa^{-}cells that are also bound by SCL[39] in WT Flk-1^{+} mesoderm are highlighted by purple bars. Numbers above the purple bars indicate the relative location of these sites in kilobases to the TSS of the indicated genes. (*the -3.5 enhancer at the Gata1 locus was called as a peak by MACS2 ($p<0.05$) in only the WT Flk-1^{hi}/PdgfRa^{-} samples)

Figure 6. Genomic regions transiently marked by H3K27Ac are bound by Eomes, Tead4 and Smad2/3 during early stages of hematopoietic mesoderm development.

a, Heatmaps of ChIP peaks in a 4kb region from day 4 EBs from two independent Eomes$^{V5/V5}$ clones. **b,** An Eomes consensus binding motif[42] identified using HOMER is enriched under ChIP-Seq peaks (top). Bar graph (below) depicts the distribution of ChIP-Seq peaks relative to nearby transcriptional start sites. **c,** Venn diagram showing the overlap between ChIP-Seq peak associated genes and those differentially expressed (fold change >1.5X) in the Eomes$^{-/-}$ Flk-1^{hi}/PdgfRa^{-} hematovascular mesoderm population. The top 24 genes having associated ChIP-Seq peaks significantly upregulated (green, left) or downregulated (red, right) in Eomes$^{-/-}$ versus WT day 4 Flk-1^{hi}/PdgfRa^{-} hematovascular mesoderm are listed. Numbers indicate the fold change (FC). Orange genes have nearby Smad2/3/Eomes overlapping peaks, purple genes have nearby Tead4/Eomes overlapping peaks and blue genes have nearby Tead4/Eomes/Smad2/3 overlapping peaks. **d**, Heatmaps showing ChIP-Seq signal for Tead4 (purple)[49] and Smad2/3 (orange)[50] occupancy in day 3 or day 4 Flk-1^{+} EB cultures, respectively. Heatmaps showing ChIP-Seq signal for H3K27Ac (green) histone modifications in hemangioblast (HB) and hematopoietic (HP) cells[49]. Heatmaps showing DNaseI hypersensitivity signal in hemangioblast (HB) and hematopoietic (HP) cells (Goode et al., 2016 Ref 50). All heatmaps show a 4kb region flanking peak centres of the 338 Eomes bound sites. **e,** Venn diagram depicting the overlap of the Eomes, Smad2/3 and Tead4 bound regions. **f,** Tead2 and Tbox:Smad motifs identified using *HOMER* that are significantly enriched under the Eomes bound ChIP-Seq peaks. **g,** Enriched GO Terms in the Mouse Phenotype category for the 72 Eomes, Smad2/3 and Tead4 overlapping genomic regions (blue). Statistical analyses were performed using *GREAT* (Genomic Regions Enrichment Analysis Tool) **h**, IGV snapshots of Eomes, Tead4, Smad2/3 and H3K27Ac ChIP-Seq peaks overlapping with DNase1 hypersensitivity (DN1 HS). Blue bars highlight Eomes bound sites and the numbers above indicate the relative location of these sites in kilobases to the TSS of the gene indicated. HB, hemangioblast (T^{+}/Flk-1^{+}); HP, hematopoietic progenitor (CD41^{+}).

Figure 7. Comparison of scRNA-Seq profiles of wildtype and Eomes-null Flk1^{hi}/PdgfRa^{-} cells generated *in vitro* to wildtype cells from E6.5 – E8.5 mouse embryos.

a, Mapped cell types in uniform manifold approximation and projection (UMAP) plots. Top panel shows WT and Eo-/- Flk-1^{hi}/PdgfRa^{-} cells from either day 4 (left) or day 5 (right). Bottom panel shows Flk-1^{hi}/PdgfRa^{-} cells from WT (left) or Eomes$^{-/-}$ (right). Cells are colored by their cell type annotation, based on their 35 nearest neighbors in the mouse gastrulation atlas[15] denoted in the legend. The black box (bottom panel) highlights blood progenitors that are diminished in the Eomes$^{-/-}$cultures.

PGC, primordial germ cell; WT, wildtype; Eo -/-, Eomes-null **b,** Normalized expression levels of the indicated genes overlaid on UMAPs for all cells. **c,** Mapped probability mapping scores in UMAP embeddings for all wildtype (left) and Eomes-/- (right) cells. A probability score >0.5 indicates high mapping quality. **d,** Mapped embryo stages in UMAP embeddings. Cells are coloured by the nearest mapped embryo stage from the mouse atlas as indicated in the legend below. Bar chart shows the number of wildtype (black) or Eomes-/- (grey) cells from each mapped embryo stage. E, embryonic stage. **e,** Mapping day 4/5 Flk-1^{hi}/PdgfRa^{-} wildtype (top) and Eomes-/- (bottom) cells onto the blood-related differentiation trajectory[15]. The black arrowhead denotes the point at which hematopoietic development seems to be blocked in Eomes-/- cultures.

Figure 8. Runx1 re-expression in Eomes-null/Runx1-null EHT cultures rescues definitive hematopoiesis.

a, Flow cytometric analysis of Flk-1/PdgfRa expression in day 5 iRunx1 Eomes$^{+/+}$ and iRunx1 Eomes$^{-/-}$ EBs. **b,** Hematopoietic colony-forming potential of cells isolated from day 5 iRunx1 Eomes $^{+/+}$ and iRunx1 Eomes$^{-/-}$ EBs. Graphical representation displays mean +/- SEM; n=3 independent differentiations and representative photomicrographs are shown on the right. Ery-P, primitive erythrocyte. Scale bar, 100 μM. Statistical analysis was performed using a two-tailed unpaired Student's t-test. **c,** Hematopoietic colony-forming potential of day 8 EHT cultures in which Runx1 expression was uninduced/induced via addition of 0, 90 and 300 ng/mL of dox from day 6-8. Graphical representations display mean +/- SEM; n = 2 (iRunx1 Eomes+/+) and n = 3 (iRunx1 Eomes -/-) independent differentiations. Ery-D, definitive erythrocyte; GM, granulocyte-macrophage; GEMM, granulocyte-erythrocyte-myeloid. H&E stained hematopoietic cells (bottom right) from a representative GEMM colony (brightfield, bottom left) from a dox induced iRunx1 Eomes$^{-/-}$ EHT culture. Mac, macrophage; n, neutrophil; e, erythrocyte. Scale bars: brightfield,100 μM; H&E, 20 μM. **d,** Representative flow cytometric analyses of cKit/CD41 and cKit/CD45 expression within the Cdh5+ compartment of day 8 EHT cultures in which Runx1 expression was uninduced or induced via addition of 0, 90 and 300 ng/mL of dox from day 6-8. Graphical representations indicate mean +/- SEM; n ≥ 3 independent differentiations. Statistical analyses were performed using a 2-way ANOVA and Tukey's multiple comparison test. Statistical source data are provided in Source Data Fig. 8. **e,** Model summarizing the effects of Eomes-loss-of-function on the two waves of YS hematopoiesis. Primitive erythrocyte formation depends on SCL and Eomes functional activity. The generation of hemogenic endothelium (HE) depends on SCL functional activity. EHT and the generation of definitive hematopoietic cells depends on the functional activity of Runx1 and Eomes. Eomes-/- hematoendothelial progenitors (HEPs) lack chromatin accessibility at numerous enhancers that are normally bound by SCL and are therefore unable to transition into primitive erythrocytes. Eomes$^{-/-}$ hematoendothelial progenitors generate Cdh5+/cKit+/CD41^{lo} "hemogenic" endothelial cells that fail to upregulate Runx1 expression (green) and this in part explains the block in definitive hematopoiesis in Eomes$^{-/-}$ EHT cultures.

Acknowledgements

We would like to acknowledge Michal Maj and Line Ericsen, and Kevin Clark in the flow cytometry facilities at the Dunn School and WIMM respectively for providing cell sorting services. The WIMM facility is supported by the MRC HIU; MRC MHU (MC_UU_12009); NIHR Oxford BRC and John Fell Fund (131/030 and 101/517), the EPA fund (CF182 and CF170) and by the WIMM Strategic Alliance awards G0902418 and MC_UU_12025. We thank Neil Ashley for his help on 10x sample preparation and sequencing. The WIMM Single Cell Core Facility was supported by the MRC MHU (MC_UU_12009), the Oxford Single Cell Biology Consortium (MR/M00919X/1) and the WT-ISSF (097813/Z/11/B#) funding. The facility was supported by WIMM Strategic Alliance awards G0902418 and MC_UU_12025. We also thank the High-Throughput Genomics Group (Wellcome Trust (WT) Centre for Human Genetics, funded by WT 090532/Z/09/Z), for generating sequencing data. We thank Valerie Kouskoff for providing the iRunx1 ES cell line, Supat Thongjuea and Guanlin Wang for advice with the scRNA-Seq analysis, Joey Riepsaame for advice with CRISP-R experiments, and Doug Higgs, Hedia Chagraoui, Dominic Owens, Andrew Nelson and Arne Mould for

helpful discussions. M.D.B and C.P are supported by programmes in the MRC Molecular Hematology Unit Core award (Grant number: MC_UU_12009/2 M.D.B. and MC_UU_12009/9 C.P.). L.G. was supported by a Clarendon PhD studentship and the MRC Molecular Haematology Unit. The work was supported by grants from the Wellcome Trust (214175/Z/18/Z E.J.R, 10281/Z/13/Z L.T.G.H). L.T.G.H was supported by a Clarendon Fund Scholarship and Trinity College Titley Scholarship. E.J.R. is a Wellcome Trust Principal Fellow.

Author Contributions

L.T.G.H, E.K.B, C.P, M.D.B and E.J.R designed the study. L.T.G.H, C.S, I.C, A.D.S performed the experiments. L.T.G.H, I.I.R, J.M and B.G performed scRNA-seq analyses. L.G generated the Runx1-Venus reporter line. L.T.G.H, E.K.B, M.D.B and E.J.R wrote the manuscript with input from all the authors.

Competing Financial Interests

The authors have no competing Financial interests

References

1. Arnold, S.J. & Robertson, E.J. Making a commitment: cell lineage allocation and axis patterning in the early mouse embryo. *Nature reviews Molecular cell biology* **10**, 91-103 (2009).
2. Kinder, S.J. *et al.* The orderly allocation of mesodermal cells to the extraembryonic structures and the anteroposterior axis during gastrulation of the mouse embryo. *Development* **126**, 4691-4701 (1999).
3. Ferkowicz, M.J. & Yoder, M.C. Blood island formation: longstanding observations and modern interpretations. *Exp Hematol* **33**, 1041-1047 (2005).
4. McGrath, K.E., Frame, J.M. & Palis, J. Early hematopoiesis and macrophage development. *Semin Immunol* **27**, 379-387 (2015).
5. Frame, J.M., Fegan, K.H., Conway, S.J., McGrath, K.E. & Palis, J. Definitive Hematopoiesis in the Yolk Sac Emerges from Wnt-Responsive Hemogenic Endothelium Independently of Circulation and Arterial Identity. *Stem Cells* **34**, 431-444 (2016).
6. Kissa, K. & Herbomel, P. Blood stem cells emerge from aortic endothelium by a novel type of cell transition. *Nature* **464**, 112-115 (2010).
7. Boisset, J.C. *et al.* In vivo imaging of haematopoietic cells emerging from the mouse aortic endothelium. *Nature* **464**, 116-120 (2010).
8. Bertrand, J.Y. *et al.* Haematopoietic stem cells derive directly from aortic endothelium during development. *Nature* **464**, 108-111 (2010).
9. McGrath, K.E. *et al.* Distinct sources of hematopoietic progenitors emerge before HSCs and provide functional blood cells in the mammalian embryo. *Cell reports* **11**, 1892-1904 (2015).
10. de Bruijn, M.F., Speck, N.A., Peeters, M.C. & Dzierzak, E. Definitive hematopoietic stem cells first develop within the major arterial regions of the mouse embryo. *EMBO J* **19**, 2465-2474 (2000).
11. Keller, G. Embryonic stem cell differentiation: emergence of a new era in biology and medicine. *Genes & development* **19**, 1129-1155 (2005).
12. Murry, C.E. & Keller, G. Differentiation of embryonic stem cells to clinically relevant populations: lessons from embryonic development. *Cell* **132**, 661-680 (2008).
13. Porcher, C., Chagraoui, H. & Kristiansen, M.S. SCL/TAL1: a multifaceted regulator from blood development to disease. *Blood* **129**, 2051-2060 (2017).
14. Lancrin, C. *et al.* The haemangioblast generates haematopoietic cells through a haemogenic endothelium stage. *Nature* **457**, 892-895 (2009).
15. Pijuan-Sala, B. *et al.* A single-cell molecular map of mouse gastrulation and early organogenesis. *Nature* **566**, 490-495 (2019).

16. Porcher, C. *et al.* The T cell leukemia oncoprotein SCL/tal-1 is essential for development of all hematopoietic lineages. *Cell* **86**, 47-57 (1996).
17. Shivdasani, R.A., Mayer, E.L. & Orkin, S.H. Absence of blood formation in mice lacking the T-cell leukaemia oncoprotein tal-1/SCL. *Nature* **373**, 432-434 (1995).
18. de Bruijn, M. & Dzierzak, E. Runx transcription factors in the development and function of the definitive hematopoietic system. *Blood* **129**, 2061-2069 (2017).
19. Huber, T.L., Kouskoff, V., Fehling, H.J., Palis, J. & Keller, G. Haemangioblast commitment is initiated in the primitive streak of the mouse embryo. *Nature* **432**, 625-630 (2004).
20. Lugus, J.J., Park, C., Ma, Y.D. & Choi, K. Both primitive and definitive blood cells are derived from Flk-1+ mesoderm. *Blood* **113**, 563-566 (2009).
21. Arnold, S.J., Sugnaseelan, J., Groszer, M., Srinivas, S. & Robertson, E.J. Generation and analysis of a mouse line harboring GFP in the Eomes/Tbr2 locus. *Genesis* **47**, 775-781 (2009).
22. Soriano, P. Generalized lacZ expression with the ROSA26 Cre reporter strain. *Nature genetics* **21**, 70 (1999).
23. Arnold, S.J., Hofmann, U.K., Bikoff, E.K. & Robertson, E.J. Pivotal roles for eomesodermin during axis formation, epithelium-to-mesenchyme transition and endoderm specification in the mouse. *Development* **135**, 501-511 (2008).
24. Shalaby, F. *et al.* Failure of blood-island formation and vasculogenesis in Flk-1-deficient mice. *Nature* **376**, 62-66 (1995).
25. Lee, D. *et al.* ER71 acts downstream of BMP, Notch, and Wnt signaling in blood and vessel progenitor specification. *Cell Stem Cell* **2**, 497-507 (2008).
26. Koyano-Nakagawa, N. & Garry, D.J. Etv2 as an essential regulator of mesodermal lineage development. *Cardiovasc Res* **113**, 1294-1306 (2017).
27. Nostro, M.C., Cheng, X., Keller, G.M. & Gadue, P. Wnt, activin, and BMP signaling regulate distinct stages in the developmental pathway from embryonic stem cells to blood. *Cell stem cell* **2**, 60-71 (2008).
28. Irion, S. *et al.* Temporal specification of blood progenitors from mouse embryonic stem cells and induced pluripotent stem cells. *Development* **137**, 2829-2839 (2010).
29. Chagraoui, H. *et al.* SCL/TAL1 cooperates with Polycomb RYBP-PRC1 to suppress alternative lineages in blood-fated cells. *Nat Commun* **9**, 5375 (2018).
30. Mikkola, H.K., Fujiwara, Y., Schlaeger, T.M., Traver, D. & Orkin, S.H. Expression of CD41 marks the initiation of definitive hematopoiesis in the mouse embryo. *Blood* **101**, 508-516 (2003).
31. Kattman, S.J. *et al.* Stage-specific optimization of activin/nodal and BMP signaling promotes cardiac differentiation of mouse and human pluripotent stem cell lines. *Cell stem cell* **8**, 228-240 (2011).
32. Izumi, N., Era, T., Akimaru, H., Yasunaga, M. & Nishikawa, S. Dissecting the molecular hierarchy for mesendoderm differentiation through a combination of embryonic stem cell culture and RNA interference. *Stem Cells* **25**, 1664-1674 (2007).
33. Mitjavila-Garcia, M.T. *et al.* Expression of CD41 on hematopoietic progenitors derived from embryonic hematopoietic cells. *Development* **129**, 2003-2013 (2002).
34. Ferkowicz, M.J. *et al.* CD41 expression defines the onset of primitive and definitive hematopoiesis in the murine embryo. *Development* **130**, 4393-4403 (2003).
35. Costello, I. *et al.* The T-box transcription factor Eomesodermin acts upstream of Mesp1 to specify cardiac mesoderm during mouse gastrulation. *Nature cell biology* **13**, 1084-1091 (2011).
36. Van Den Ameele, J. *et al.* Eomesodermin induces Mesp1 expression and cardiac differentiation from embryonic stem cells in the absence of Activin. *EMBO reports* **13**, 355-362 (2012).
37. Clarke, R.L. *et al.* The expression of Sox17 identifies and regulates hemogenic endothelium. *Nature cell biology* **15**, 502 (2013).
38. Buenrostro, J.D., Giresi, P.G., Zaba, L.C., Chang, H.Y. & Greenleaf, W.J. Transposition of native chromatin for fast and sensitive epigenomic profiling of open chromatin, DNA-binding proteins and nucleosome position. *Nat Methods* **10**, 1213-1218 (2013).
39. Org, T. *et al.* Scl binds to primed enhancers in mesoderm to regulate hematopoietic and cardiac fate divergence. *EMBO J* **34**, 759-777 (2015).
40. Schutte, J. *et al.* An experimentally validated network of nine haematopoietic transcription factors reveals mechanisms of cell state stability. *Elife* **5**, e11469 (2016).
41. Onodera, K. *et al.* GATA-1 transcription is controlled by distinct regulatory mechanisms during primitive and definitive erythropoiesis. *Proc Natl Acad Sci U S A* **94**, 4487-4492 (1997).

42. Teo, A.K.K. *et al.* Pluripotency factors regulate definitive endoderm specification through eomesodermin. *Genes & development* **25**, 238-250 (2011).
43. Vijayaragavan, K. *et al.* Noncanonical Wnt signaling orchestrates early developmental events toward hematopoietic cell fate from human embryonic stem cells. *Cell Stem Cell* **4**, 248-262 (2009).
44. Ng, E.S. *et al.* The primitive streak gene Mixl1 is required for efficient haematopoiesis and BMP4-induced ventral mesoderm patterning in differentiating ES cells. *Development* **132**, 873-884 (2005).
45. DiMartino, J.F. *et al.* The Hox cofactor and proto-oncogene Pbx1 is required for maintenance of definitive hematopoiesis in the fetal liver. *Blood* **98**, 618-626 (2001).
46. Fleury, M., Eliades, A., Carlsson, P., Lacaud, G. & Kouskoff, V. FOXF1 inhibits hematopoietic lineage commitment during early mesoderm specification. *Development* **142**, 3307-3320 (2015).
47. Wang, M. *et al.* MEIS2 regulates endothelial to hematopoietic transition of human embryonic stem cells by targeting TAL1. *Stem Cell Res Ther* **9**, 340 (2018).
48. Davenport, T.G., Jerome-Majewska, L.A. & Papaioannou, V.E. Mammary gland, limb and yolk sac defects in mice lacking Tbx3, the gene mutated in human ulnar mammary syndrome. *Development* **130**, 2263-2273 (2003).
49. Goode, D.K. *et al.* Dynamic Gene Regulatory Networks Drive Hematopoietic Specification and Differentiation. *Dev Cell* **36**, 572-587 (2016).
50. Wang, Q. *et al.* The p53 Family Coordinates Wnt and Nodal Inputs in Mesendodermal Differentiation of Embryonic Stem Cells. *Cell Stem Cell* **20**, 70-86 (2017).
51. Tosic, J. *et al.* Eomes and Brachyury control pluripotency exit and germ-layer segregation by changing the chromatin state. *Nat Cell Biol* **21**, 1518-1531 (2019).
52. Lie, A.L.M. *et al.* Regulation of RUNX1 dosage is crucial for efficient blood formation from hemogenic endothelium. *Development* **145** (2018).
53. Fitch, S.R. *et al.* Gata3 targets Runx1 in the embryonic haematopoietic stem cell niche. *IUBMB Life* **72**, 45-52 (2020).
54. Butler, A., Hoffman, P., Smibert, P., Papalexi, E. & Satija, R. Integrating single-cell transcriptomic data across different conditions, technologies, and species. *Nat Biotechnol* **36**, 411-420 (2018).
55. Eliades, A. *et al.* The Hemogenic Competence of Endothelial Progenitors Is Restricted by Runx1 Silencing during Embryonic Development. *Cell Rep* **15**, 2185-2199 (2016).
56. Tober, J., Yzaguirre, A.D., Piwarzyk, E. & Speck, N.A. Distinct temporal requirements for Runx1 in hematopoietic progenitors and stem cells. *Development* **140**, 3765-3776 (2013).
57. Yzaguirre, A.D., Howell, E.D., Li, Y., Liu, Z. & Speck, N.A. Runx1 is sufficient for blood cell formation from non-hemogenic endothelial cells in vivo only during early embryogenesis. *Development* **145** (2018).
58. Swiers, G. *et al.* Early dynamic fate changes in haemogenic endothelium characterized at the single-cell level. *Nat Commun* **4**, 2924 (2013).
59. Obier, N. *et al.* Cooperative binding of AP-1 and TEAD4 modulates the balance between vascular smooth muscle and hemogenic cell fate. *Development* **143**, 4324-4340 (2016).
60. Padron-Barthe, L. *et al.* Clonal analysis identifies hemogenic endothelium as the source of the blood-endothelial common lineage in the mouse embryo. *Blood* **124**, 2523-2532 (2014).

Methods

Mouse strains

Animal procedures were performed in accordance with Home Office (UK) regulations and approved by the Oxford Local Animal Welfare and Ethical Committee. $Eomes^{GFP}$, Rosa26R, $Eomes^{CA/N}$;$Sox2^{Cre}$ and Flk-1^{LacZ} strains were genotyped as previously described[21-24]. The $Eomes^{iCre}$ allele was generated using the same strategy as previously described[35]. The iCre coding sequence followed by a polyA cassette and a loxP-flanked neomycin-resistance cassette was introduced into exon 1 between the SphI (translational start) and EagI sites, resulting in removal of ~500bp of the endogenous 5′ coding region of Exon 1. Drug-resistant ESC colonies screened by Southern blot using a 5' external probe[21] were transfected with pMC1.Cre, to remove the selection cassette. Two independent excised ESC clones were used to generate germline chimeras. Offspring were genotyped by PCR using iCre specific primers (Supplementary Table 2).

Immunostaining.

E6.5 embryos were fixed in 4% PFA at room temperature (RT) for 30 min. E7.5 embryos and day 4 EBs were fixed in 1% PFA overnight at 4ºC. Samples were washed with 0.1% Triton-X, permeabilized with 0.5% Triton-X in PBS for 15 min, washed with 0.1% Triton-X, blocked in 5% donkey serum, 0.2% BSA and 0.1% Triton-X in PBS, incubated with primary antibodies in block solution, washed with 0.1% Triton-X, incubated with fluorophore-conjugated secondary antibodies for 2 hrs at RT, washed with 0.1% Triton-X and counterstained with DAPI. Images were captured with an Olympus FV1000 and collected using Olympus FluoView (version 4.2). Antibodies used are listed in Supplementary Table 3.

Whole-mount in situ hybridization and LacZ staining.

E6.5-E7.5 embryos were subject to whole-mount *in situ* hybridization (WISH) using standard protocols[61] with probes against ER71[62], Eomes[23] and iCre (Supplementary Table 4). LacZ staining was performed according to standard protocols[61]. For histology, paraffin-embedded embryos were sectioned (8.0 μm) and counterstained with Nuclear FastRed.

ESC maintenance and differentiation.

WT (CCE), Runx1-Venus (E14), SCL-mCherry (J1)[29], Eomes-null (CCE, Runx1-Venus, SCL-mCherry, iRunx1), SCL-null (J1)[17], Runx1-null (J1)[63] and iRunx1[14] ESC lines were maintained in feeder free culture conditions as previously described[35]. 48-72 hrs prior to induction of hematopoietic differentiation cells were cultured in serum free ES media containing 50% Neurobasal Media (Gibco, Cat # 21103049), 50% DMEM/F12 (Gibco, Cat # 11320033), supplemented with 0.5X of both N2 (Gibco, Cat#17502048) and B27 (Gibco, Cat# 17504044), 1%Pen/Strep, 1% glutamine, 0.05% BSA (Gibco, Cat# 15260037), 1 μM PD0325091, 3 μM CHIR99021 and 1000 U/ml LIF. At D0 cells were

seeded at a density of 1×10^5 ml^{-1} in serum-free differentiation (SF-D) media[27] and cultured on an orbital shaker at 70 rpm for ~18 hrs in the absence of growth factors to form EBs. At D2, EBs were split 1:3 in SF-D media containing recombinant human (rh) VEGF (5 ng ml^{-1}; R&D Systems), rhBMP4 (10 ng ml^{-1}; R&D Systems) and Activin A (5 ng ml^{-1}; R&D Systems) for 48 hr. At D4, EBs were split 1:1 or 1:2 in SF-D media containing rhVEGF (5 ng ml^{-1}; R&D Systems), rhBMP4 (10 ng ml^{-1}; R&D Systems) and Activin A (5 ng ml^{-1}; R&D Systems) for 24 hr. For bulk cultures, EBs were washed at D5 and D6 and cultured in SF-D media containing rhVEGF (5 ng ml^{-1}; R&D Systems) and SCF (50 ng ml^{-1}; BioLegend). From D4 onwards EBs were grown in petri dishes coated with 5% (v/v) Poly-heme solution (Sigma, Cat# P3932-10G). For EHT cultures, D5 EBs were dissociated with Trypsin-LE (Gibco), stained with anti-Flk-1 (APC) antibody (Supplementary Table 3) for 30 min on ice and Flk-1^+ cells isolated by MACS using anti-APC microbeads (Miltenyi, Cat# 130-090-855) were plated on Matrigel (Corning, Cat# 354230) coated 96 or 12 well plates at a concentration of 5×10^4 cells/200 µl in SF-D containing rhVEGF (5 ng ml^{-1}; R&D Systems), rhbFGF (10 ng ml^{-1}; R&D Systems) and SCF (50 ng ml^{-1};BioLegend) to form HE for 72 hours. Media was changed on D6 and D7. For Runx1 induction 90 ng/mL and 300 ng/mL of doxycycline, dissolved in water, was added to the culture media from day 6-8.

Hematopoietic progenitor colony assays.

EBs/EHT monolayers were dissociated at D5, D6 or D8 and $5x10^4$, $2x10^4$ or $1x10^5$/2.5 $x10^4$ cells, respectively, were plated in Methylcellulose-Based Medium (MethoCult GF M3434; Stem Cell Technologies). Primitive erythroid colonies were counted at day 5 and definitive erythroid, granulocyte/macrophage and mixed colonies counted at 7-8 days post-plating. For all statistical analyses unpaired two-tailed Student's t-tests were performed in GraphPad Prism 8 (version 8.1.0).

Flow cytometry, cell sorting and MACS.

EBs were dissociated using Trypsin-LE. For EHT cultures floating and adherent cells were pooled, washed 3x with FACS buffer (PBS + 2% FCS), stained with antibodies for 30 min (4ºC), washed and resuspended in FACS buffer containing DAPI (1:5000, BD Pharmigen) and analysed on either a BD Fortessa X20 or a Cytek DxP8. Cell sorting for RNA-Seq and ATAC-Seq was completed on a MoFlo Astrios. For MACS, cells were stained at a concentration of 10^7 cells/150 uL FACS buffer containing 3.75 uL of anti-Flk-1(APC) antibody for 30 min (4ºC), washed with PBE (PBS + 2mM EDTA + 0.5% BSA) and incubated in 80 uL of PBE + 20 uL of anti-APC microbeads (Miltenyi, Cat# 130-090-855) for 30 min (4ºC), washed with PBE then passed over a LS magnetic column twice. For intracellular flow cytometry day 3-5 EoV5/V5 EBs were dissociated and stained for Flk-1 and PdgfRa prior to fixation. Cells were subsequently permeabilized and V5 staining was performed using the FoxP3 Staining Buffer Set (Invitrogen, Cat# 00-5523). Antibodies used are listed in Supplementary Table 3. The flow cytometry data was collected using BDFacsDiva (version 8), FlowJoCE (version 7.5) or Summit

(version 6.3.1) software. For all statistical analyses unpaired two-tailed Student's t-tests were performed in GraphPad Prism 8 (version 8.1.0).

RNA isolation and quantitative RT-PCR.

Total RNA was isolated using the RNeasy Mini Kit (QIAGEN, Cat#74104) using on-column DNase treatment. Complementary DNA was generated using the SuperScriptIII kit (Invitrogen) with oligo-dT primers. RT–qPCR was performed using the Quantitect SYBRGreen PCR kit and a Rotor-gene Q (Qiagen) and analysed using the delta-delta Ct method, as described previously[35]. Primer sequences are provided in Supplementary Table 2.

RNA-Seq.

RNA isolated from Flk-1^{hi}/PdgfRa^{-} single cell suspensions (1.5x10^{5} cells) from three independent hematopoietic differentiations of WT (CCE) and Eomes-null (clone 6A6, CCE) cells using the RNeasy Micro Kit (QIAGEN, Cat#74004) was normalized to 800ng per sample, depleted of cytoplasmic and mitochondrial ribosomal RNA sequences (Ribo-Zero Gold rRNA Removal Kit (H/M/R), Cat: #MRZG12324) and library preparation performed using the Illumina TruSeq Stranded Total RNA Library Prep (H/M/R) (Cat: #20020597), followed by sequencing (75-cycle paired end) on the Illumina HiSeq4000 platform.

RNA-Seq analysis.

Paired-end reads were aligned against the mm10 genome using the STAR RNA-seq aligner with default parameters outputting bam files using --outSAMtype BAM SortedByCoordinate[64]. BAM file primary alignments with a mapping quality of > 254 were treated as RNA-Seq data and imported into Seqmonk 1.45.4. (https://www.bioinformatics.babraham.ac.uk/projects/download.html#seqmonk). The RNA-Seq quantitation pipeline ($p<0.05$ and multiple testing correction applied) in SeqMonk utilizing DESeq2[65] was performed to identify significantly differentially expressed genes ($p<0.05$, fold change > 1.5 and FPKM >1).

scRNA-Seq.

10,000 Flk-1^{hi}/PdgfRa^{-} cells from D4/5 WT and Eomes-null EBs were sorted (BD FACSAria III) into 20 µL PBS/0.05% BSA (non-acetylated) and the volume topped up to 38 µL for loading onto the 10X Chromium Controller. Processing of samples was performed using the Chromium Single Cell 3' library & Gel Bead Kit v3 (10x Genomics). Barcoded cell cDNAs were pooled and converted to sequence ready libraries. Multiplexed libraries were then sequenced on Illumina Nextseq using a high output 150bp Nextseq V2.5 kit.

scRNA-Seq analysis.

Sequencing data was demultiplexed in the binary base call (BCL) format, FASTQ files were aligned to the mm10 genome using 10X Genomics Cell Ranger software (version 2.0.0) and unique molecular identifier (UMI) counts determined. The Seurat v3 software package[54, 66] was used in R Studio to perform scRNA-Seq analysis. Pre-processing was performed and cells with > 2000 RNA features and < 8 % mitochondrial RNA were used for downstream analysis. Each sample was randomly down sampled to include 3805 cells and WT and Eomes-null samples from days 4 and 5 were merged together, normalized and 2000 variable features were identified using the VST method. Integration anchors for WT and Eomes-null Seurat objects were identified and integration was performed using the first 20 principle component (PC) dimensions. Clusters were identified and UMAPs generated using the first 16 PC and a resolution of 0.8. Cell type identities were assigned by comparing the conserved markers from each of the 13 clusters to cell type markers previously published for cell types identified in E6.5 to E8.5 mouse embryos[15]. Supplementary Table 1 lists the conserved markers.

In vitro cell type annotation was performed by mapping against the mouse gastrulation atlas[15]. Raw counts from both experiments were merged and normalised using the scater (1.14.6) package[67]. Then, highly variable genes were extracted from the joint data using scran's (1.14.6) decomposeVar function[68]. Genes with an FDR lower than 0.05 were considered as highly variable and used to compute the top fifty principal components along the joint dataset. Batch correction was performed on the gastrulation atlas principal components using the fastMNN's algorithm following the exact procedure from the original publication[15]. Integrated datasets were also corrected using fastMNN. *In vitro* cells were annotated by looking at the top 35 nearest neighbours from the atlas and selecting the most frequent cell type. A mapping score was assigned to reflect the mapped cell type frequency, where a higher score indicates a more consistent annotation. *In vitro* cells were additionally mapped back onto the force directed graph of hematoendothelial cells (hematoendothelial differentiation trajectory) from the original publication[15] by identifying the single nearest neighbour.

ATAC-seq.

Tagmentation and indexing of single cell suspensions ($6x10^4$ cells) from three independent differentiations of WT (CCE) and Eomes-null (clone 6A6, CCE) day 4 Flk-1^{hi}/PdgfRa$^-$ cells was performed as previously described[38]. To control for sequence bias of the Tn5 transposase, 100ng genomic DNA of WT (CCE) ESCs was also tagmented and indexed. Libraries were purified with two rounds of Agencourt AMPure XP bead cleanup (Agencourt, 1.5× bead:sample ratio). Library size and concentration were determined using the 2100 Bioanalyzer High Sensitivity DNA Kit (Agilent). Samples were sequenced using a 75-cycle paired end Nextera kit with custom Nextera index primers taken from Table S1 in Buenrostro et al. 2013[38] on the Illumina HiSeq4000 platform.

ATAC-seq analysis.

Paired-end reads were aligned to the mouse genome assembly mm10 using Bowtie2[69] with the very-sensitive option, sorted and mitochondrial reads discarded using Samtools[70] and duplicates removed using Picard (https://broadinstitute.github.io/picard/). Bigwig files were generated using deepTools2[71]. Biological replicates were randomly downsampled to contain the same number of reads for each individual sample and peaks in each sample called using MACS2[72] using the Tn5 control as a control. MACS2 called peaks with a p-value < 10^{-3} were used in downstream analyses. Significant changes in ATAC-Seq datasets were identified using the DiffBind package (version 2.2.12) (http://bioconductor.org/packages/release/bioc/html/DiffBind.html) using bam files and an integrative bed file of all identified peaks in each sample with the following filters: FDR < 0.05, fold change > 1.5. GREAT 4.0.4 analysis[73] was performed using default basal plus extension parameters with whole genome as a background to identify peak-gene associations. Enrichment of TF motifs in differentially accessible ATAC-seq peaks was performed using the Analysis of Motif Enrichment (AME 4.12.0) feature in the MEME suite[74] with a background control of all ATAC-seq peaks.

Bigwig files were downloaded from GSE47085 and genomic coordinates were converted from mm9 to mm10 using Crossmap 0.2.9[75]. An SCL peak file was downloaded from Supplementary Table S1A from Van Handel et al. 2015[39] and genomic coordinates were converted from mm9 to mm10 using UCSC LiftOver. Bedtools was used to intersect peak files and identify overlapping genomic regions[76]. GREAT 4.0.4 analysis[73] was performed using default basal plus extension parameters with whole genome as a background to identify peak-gene association. Identified genes were annotated in Seqmonk 1.45.4 for comparison of ATAC-Seq and gene expression changes from RNA-Seq. Changes in ATAC-Seq signal were assessed using heatmaps generated in deepTools2[71], and genomic snapshots visualized in IGV[77] generated from bigwig files creates using deepTools2[71].

CRISPR modification of ESCs.

Custom synthetic crRNA (using the CC-Top CRISPR design tool[78]) and ssODNs (Integrated DNA Technologies, USA) were resuspended in IDT duplex buffer. Sequences are provided in Supplementary Table 5. Cas9 ribonucleoprotein (RNP) complexes were assembled immediately prior to electroporation following the manufacturer's protocol (Alt-R CRISPR-Cas9 System:Delivery of ribonucleoprotein complexes into Jurkat T cells using the Neon® Transfection System). ESC were electroporated using the Neon transfection system (Voltage = 1600V, pulse width = 10 ms, number of pulses = 3) with the appropriate ssODN (50 pmol) and RNP. If two crRNAs were used then RNPs were produced separately and mixed 1:1 prior to electroporation.

For generation of Eomes-null Runx1-Venus and Eomes-null SCL-Cherry reporter and Eomes-null iRunx1 ESCs two custom crRNAs (Supplementary Table 6) were designed to recapitulate the

previously described Eomes loss of function allele[23]. ssODNs were designed that contained a 5' homology arm upstream of the intron 1 DNA DS break site, followed by insertion of a new EcoRV, Sph1 or Spe1 restriction site and a 3' homology arm located downstream of the intron 5 DNA break site (Supplementary Table 6). 10 uL of $2x10^4$ ESCs in Buffer R were electroporated with 1 uL of a 1:1 mix of the RNPs and 2 uL of the ssODN. Low density plating was performed after 72 hrs, and after 7-10 days clones were picked and screened using a three primer PCR strategy that simultaneously amplified the WT allele and the null allele (Supplementary Table 2). Genotypes of clones were verified using Southern blotting or PCR followed by restriction enzyme digests.

For generation of the $Eomes^{V5/V5}$ ESC lines a custom crRNA was designed to target the UAG translational stop site in exon 6 of Eomes and a ssODN was designed to insert a triple glycine V5 epitope tag (3XGly-V5) directly upstream of the UAG translational stop site of Eomes (Supplementary Table 6). Homozygous insertion of the 3XGly-V5 tag at the C-terminus of the Eomes locus was assessed by PCR across the C-terminus of Eomes with primers listed in Supplementary Table 2. In frame insertion with the correct 3XGly-V5 sequence was confirmed via Sanger sequencing of a 971 bp PCR product (Supplementary Table 2) that spanned the C-terminus of Eomes. Western blotting and immunofluorescence staining were performed on day 4 EBs to confirm successful V5 tagging of the endogenous Eomes protein.

Generation of the Runx1-Venus ESC reporter line.

For generation of the Runx1-Venus mouse ESC reporter line a 3xFlag-P2A-Venus was inserted in the last exon of Runx1 (exon 6), before the stop codon. Briefly, a 4kb 5' homology arm and a 4.2 3' homology arm were amplified from E14 gDNA by PCR and cloned into pUC19 (Invitrogen). A GeneARt (Invitrogen) synthetic construct consisting of Runx1_ex6-3xFlag-P2A-Venus was cloned into the pUC19 vector containing the homology arms using Gibson assembly (pUC19-Runx1-Venus_GA_FP: ccaacatgccccccgCGCGCCTGGAGGAGGCCG, pUC19-Runx1-Venus_GA_RP: cggcaggcccagtccCTCGATGGCGATGGCGCTC). The resulting pUC19-Runx1_Ex6-P2A-Venus-Long HAconstruct was used for transfection into undifferentiated E14 ESCs with a CRISPR/Cas9 vector expressing a gRNA (Supplementary Table 5) that cut immediately preceding the RUNX1 stop codon. The guide RNA (gRNA) was designed using the MIT CRISPR design tool (http://crispr.mit.edu/)[79]. The double stranded gRNA was constructed by annealing oligos (Integrated DNA Technologies; IDT) consisting of the gRNA sequence (forward) and reverse complement sequences (reverse) (Supplementary Table 5). The gRNA was cloned into the BbsI site of pX458 (Addgene plasmid 48138); BbsI restriction sites were added to the oligos for this purpose. All constructs were verified by Sanger sequencing. E14 ESCs were transfected using TransIT LT1 (Mirus) and a pX458:pUC19 ratio of 1:2. Integration was checked by long-range PCR with a forward primer outside of the 5' HA and a reverse primer 3' of the Runx1 endogenous stop codon, generating a 5.8kb amplicon for the correctly targeted allele and a 4.4kb amplicon for the wild type allele

(Supplementary Table 2). A clone with the Venus reporter integrated in both alleles (RV11) was used for all experiments.

ChIP-Seq.

Day 4 Eomes$^{V5/V5}$ (CCE) and WT (CCE) D4 EBs were dissociated and ~3-4x10^{7} cells were cross-linked for 10 min at RT with 1% (v/v) formaldehyde, and quenched with 125mM glycine. Nuclei were recovered and lysed to obtain chromatin, which was then sonicated to 200–500 bp, pre-cleared with protein G Dynabeads (Thermofisher Scientific) and ~175 ug of chromatin was immunoprecipitated with 10µg of anti-V5 (Abcam cat# ab9116, lot# GR: 322448-4) bound to protein G Dynabeads overnight on a rotator at 4ºC. Dynabeads were washed and immune complexes were eluted in IP elution buffer (1% SDS, 0.1M NaHCO3), reverse crosslinked overnight at 65ºC, RNaseA treated for 1.5hrs at 42ºC, proteinase K treated for 2hrs at 45ºC and DNA was recovered using a Zymo column kit. DNA was multiplexed and paired end sequencing was performed on a single lane of an Illumina HiSeq4000 platform.

ChIP-Seq analysis.

Paired-end reads were aligned to the mouse genome assembly mm10 using Bowtie2[69] with default parameters. PCR duplicates were removed using Samtools 1.9[70]. Peaks were called against input DNA using MACS 2.1.2[72] and were considered significant if they had a fold enrichment > 2 and FDR < 0.05. Bedtools 2.27.1[76] was used to intersect the peak files from both Eomes$^{V5/V5}$ clones and subtract peaks called in the WT control and genomic intervals located in mm10 blacklist regions (https://www.encodeproject.org/files/ENCFF547MET/@@download/ENCFF547MET.bed.gz), generating a peak file containing 338 genomic intervals used for downstream analyses (Supplementary Table 6). The HOMER (v4.10.4) software package[80] was used to perform motif enrichment analysis. GREAT 4.0.4 analysis[73] was performed using default basal plus extension parameters with the whole genome used as a control to identify peak-gene associations. Heatmaps and bigwig files were generated using Deeptools 3.1.3[71]. Bigwig files and peak files were downloaded from GSE69101[49]. Data from GSE110164[50] were downloaded and used to generate peak files and bigwig files as previously described[81]. Bigwig files and peak files were downloaded from GSE128466[51].

Statistics and Reproducibility.

Statistical analyses for flow cytometry and colony forming assays were performed using GraphPad Prism (8.1.0).

Data availability statement.

The RNA-Seq, scRNA-Seq, ChIP-seq and ATAC-seq data have been deposited in the Gene Expression Omnibus (GEO) GSE140005. Previously published sequencing data that were re-

analysed here are available under accession code GSE110164, GSE128466 and GSE47085. All other data supporting the findings of this study and biological materials presented in this study are available on reasonable request. Source data are available for this paper.

References

1. Arnold, S.J. & Robertson, E.J. Making a commitment: cell lineage allocation and axis patterning in the early mouse embryo. *Nature reviews Molecular cell biology* **10**, 91-103 (2009).
2. Kinder, S.J. *et al.* The orderly allocation of mesodermal cells to the extraembryonic structures and the anteroposterior axis during gastrulation of the mouse embryo. *Development* **126**, 4691-4701 (1999).
3. Ferkowicz, M.J. & Yoder, M.C. Blood island formation: longstanding observations and modern interpretations. *Exp Hematol* **33**, 1041-1047 (2005).

4. McGrath, K.E., Frame, J.M. & Palis, J. Early hematopoiesis and macrophage development. *Semin Immunol* **27**, 379-387 (2015).
5. Frame, J.M., Fegan, K.H., Conway, S.J., McGrath, K.E. & Palis, J. Definitive Hematopoiesis in the Yolk Sac Emerges from Wnt-Responsive Hemogenic Endothelium Independently of Circulation and Arterial Identity. *Stem Cells* **34**, 431-444 (2016).
6. Kissa, K. & Herbomel, P. Blood stem cells emerge from aortic endothelium by a novel type of cell transition. *Nature* **464**, 112-115 (2010).
7. Boisset, J.C. *et al.* In vivo imaging of haematopoietic cells emerging from the mouse aortic endothelium. *Nature* **464**, 116-120 (2010).
8. Bertrand, J.Y. *et al.* Haematopoietic stem cells derive directly from aortic endothelium during development. *Nature* **464**, 108-111 (2010).
9. McGrath, K.E. *et al.* Distinct sources of hematopoietic progenitors emerge before HSCs and provide functional blood cells in the mammalian embryo. *Cell reports* **11**, 1892-1904 (2015).
10. de Bruijn, M.F., Speck, N.A., Peeters, M.C. & Dzierzak, E. Definitive hematopoietic stem cells first develop within the major arterial regions of the mouse embryo. *EMBO J* **19**, 2465-2474 (2000).
11. Keller, G. Embryonic stem cell differentiation: emergence of a new era in biology and medicine. *Genes & development* **19**, 1129-1155 (2005).
12. Murry, C.E. & Keller, G. Differentiation of embryonic stem cells to clinically relevant populations: lessons from embryonic development. *Cell* **132**, 661-680 (2008).
13. Porcher, C., Chagraoui, H. & Kristiansen, M.S. SCL/TAL1: a multifaceted regulator from blood development to disease. *Blood* **129**, 2051-2060 (2017).
14. Lancrin, C. *et al.* The haemangioblast generates haematopoietic cells through a haemogenic endothelium stage. *Nature* **457**, 892-895 (2009).
15. Pijuan-Sala, B. *et al.* A single-cell molecular map of mouse gastrulation and early organogenesis. *Nature* **566**, 490-495 (2019).
16. Porcher, C. *et al.* The T cell leukemia oncoprotein SCL/tal-1 is essential for development of all hematopoietic lineages. *Cell* **86**, 47-57 (1996).
17. Shivdasani, R.A., Mayer, E.L. & Orkin, S.H. Absence of blood formation in mice lacking the T-cell leukaemia oncoprotein tal-1/SCL. *Nature* **373**, 432-434 (1995).
18. de Bruijn, M. & Dzierzak, E. Runx transcription factors in the development and function of the definitive hematopoietic system. *Blood* **129**, 2061-2069 (2017).
19. Huber, T.L., Kouskoff, V., Fehling, H.J., Palis, J. & Keller, G. Haemangioblast commitment is initiated in the primitive streak of the mouse embryo. *Nature* **432**, 625-630 (2004).
20. Lugus, J.J., Park, C., Ma, Y.D. & Choi, K. Both primitive and definitive blood cells are derived from Flk-1+ mesoderm. *Blood* **113**, 563-566 (2009).
21. Arnold, S.J., Sugnaseelan, J., Groszer, M., Srinivas, S. & Robertson, E.J. Generation and analysis of a mouse line harboring GFP in the Eomes/Tbr2 locus. *Genesis* **47**, 775-781 (2009).
22. Soriano, P. Generalized lacZ expression with the ROSA26 Cre reporter strain. *Nature genetics* **21**, 70 (1999).
23. Arnold, S.J., Hofmann, U.K., Bikoff, E.K. & Robertson, E.J. Pivotal roles for eomesodermin during axis formation, epithelium-to-mesenchyme transition and endoderm specification in the mouse. *Development* **135**, 501-511 (2008).
24. Shalaby, F. *et al.* Failure of blood-island formation and vasculogenesis in Flk-1-deficient mice. *Nature* **376**, 62-66 (1995).
25. Lee, D. *et al.* ER71 acts downstream of BMP, Notch, and Wnt signaling in blood and vessel progenitor specification. *Cell Stem Cell* **2**, 497-507 (2008).
26. Koyano-Nakagawa, N. & Garry, D.J. Etv2 as an essential regulator of mesodermal lineage development. *Cardiovasc Res* **113**, 1294-1306 (2017).
27. Nostro, M.C., Cheng, X., Keller, G.M. & Gadue, P. Wnt, activin, and BMP signaling regulate distinct stages in the developmental pathway from embryonic stem cells to blood. *Cell stem cell* **2**, 60-71 (2008).
28. Irion, S. *et al.* Temporal specification of blood progenitors from mouse embryonic stem cells and induced pluripotent stem cells. *Development* **137**, 2829-2839 (2010).
29. Chagraoui, H. *et al.* SCL/TAL1 cooperates with Polycomb RYBP-PRC1 to suppress alternative lineages in blood-fated cells. *Nat Commun* **9**, 5375 (2018).
30. Mikkola, H.K., Fujiwara, Y., Schlaeger, T.M., Traver, D. & Orkin, S.H. Expression of CD41 marks the initiation of definitive hematopoiesis in the mouse embryo. *Blood* **101**, 508-516 (2003).

31. Kattman, S.J. *et al.* Stage-specific optimization of activin/nodal and BMP signaling promotes cardiac differentiation of mouse and human pluripotent stem cell lines. *Cell stem cell* **8**, 228-240 (2011).
32. Izumi, N., Era, T., Akimaru, H., Yasunaga, M. & Nishikawa, S. Dissecting the molecular hierarchy for mesendoderm differentiation through a combination of embryonic stem cell culture and RNA interference. *Stem Cells* **25**, 1664-1674 (2007).
33. Mitjavila-Garcia, M.T. *et al.* Expression of CD41 on hematopoietic progenitors derived from embryonic hematopoietic cells. *Development* **129**, 2003-2013 (2002).
34. Ferkowicz, M.J. *et al.* CD41 expression defines the onset of primitive and definitive hematopoiesis in the murine embryo. *Development* **130**, 4393-4403 (2003).
35. Costello, I. *et al.* The T-box transcription factor Eomesodermin acts upstream of Mesp1 to specify cardiac mesoderm during mouse gastrulation. *Nature cell biology* **13**, 1084-1091 (2011).
36. Van Den Ameele, J. *et al.* Eomesodermin induces Mesp1 expression and cardiac differentiation from embryonic stem cells in the absence of Activin. *EMBO reports* **13**, 355-362 (2012).
37. Clarke, R.L. *et al.* The expression of Sox17 identifies and regulates hemogenic endothelium. *Nature cell biology* **15**, 502 (2013).
38. Buenrostro, J.D., Giresi, P.G., Zaba, L.C., Chang, H.Y. & Greenleaf, W.J. Transposition of native chromatin for fast and sensitive epigenomic profiling of open chromatin, DNA-binding proteins and nucleosome position. *Nat Methods* **10**, 1213-1218 (2013).
39. Org, T. *et al.* Scl binds to primed enhancers in mesoderm to regulate hematopoietic and cardiac fate divergence. *EMBO J* **34**, 759-777 (2015).
40. Schutte, J. *et al.* An experimentally validated network of nine haematopoietic transcription factors reveals mechanisms of cell state stability. *Elife* **5**, e11469 (2016).
41. Onodera, K. *et al.* GATA-1 transcription is controlled by distinct regulatory mechanisms during primitive and definitive erythropoiesis. *Proc Natl Acad Sci U S A* **94**, 4487-4492 (1997).
42. Teo, A.K.K. *et al.* Pluripotency factors regulate definitive endoderm specification through eomesodermin. *Genes & development* **25**, 238-250 (2011).
43. Vijayaragavan, K. *et al.* Noncanonical Wnt signaling orchestrates early developmental events toward hematopoietic cell fate from human embryonic stem cells. *Cell Stem Cell* **4**, 248-262 (2009).
44. Ng, E.S. *et al.* The primitive streak gene Mixl1 is required for efficient haematopoiesis and BMP4-induced ventral mesoderm patterning in differentiating ES cells. *Development* **132**, 873-884 (2005).
45. DiMartino, J.F. *et al.* The Hox cofactor and proto-oncogene Pbx1 is required for maintenance of definitive hematopoiesis in the fetal liver. *Blood* **98**, 618-626 (2001).
46. Fleury, M., Eliades, A., Carlsson, P., Lacaud, G. & Kouskoff, V. FOXF1 inhibits hematopoietic lineage commitment during early mesoderm specification. *Development* **142**, 3307-3320 (2015).
47. Wang, M. *et al.* MEIS2 regulates endothelial to hematopoietic transition of human embryonic stem cells by targeting TAL1. *Stem Cell Res Ther* **9**, 340 (2018).
48. Davenport, T.G., Jerome-Majewska, L.A. & Papaioannou, V.E. Mammary gland, limb and yolk sac defects in mice lacking Tbx3, the gene mutated in human ulnar mammary syndrome. *Development* **130**, 2263-2273 (2003).
49. Goode, D.K. *et al.* Dynamic Gene Regulatory Networks Drive Hematopoietic Specification and Differentiation. *Dev Cell* **36**, 572-587 (2016).
50. Wang, Q. *et al.* The p53 Family Coordinates Wnt and Nodal Inputs in Mesendodermal Differentiation of Embryonic Stem Cells. *Cell Stem Cell* **20**, 70-86 (2017).
51. Tosic, J. *et al.* Eomes and Brachyury control pluripotency exit and germ-layer segregation by changing the chromatin state. *Nat Cell Biol* **21**, 1518-1531 (2019).
52. Lie, A.L.M. *et al.* Regulation of RUNX1 dosage is crucial for efficient blood formation from hemogenic endothelium. *Development* **145** (2018).
53. Fitch, S.R. *et al.* Gata3 targets Runx1 in the embryonic haematopoietic stem cell niche. *IUBMB Life* **72**, 45-52 (2020).
54. Butler, A., Hoffman, P., Smibert, P., Papalexi, E. & Satija, R. Integrating single-cell transcriptomic data across different conditions, technologies, and species. *Nat Biotechnol* **36**, 411-420 (2018).
55. Eliades, A. *et al.* The Hemogenic Competence of Endothelial Progenitors Is Restricted by Runx1 Silencing during Embryonic Development. *Cell Rep* **15**, 2185-2199 (2016).
56. Tober, J., Yzaguirre, A.D., Piwarzyk, E. & Speck, N.A. Distinct temporal requirements for Runx1 in hematopoietic progenitors and stem cells. *Development* **140**, 3765-3776 (2013).

57. Yzaguirre, A.D., Howell, E.D., Li, Y., Liu, Z. & Speck, N.A. Runx1 is sufficient for blood cell formation from non-hemogenic endothelial cells in vivo only during early embryogenesis. *Development* **145** (2018).
58. Swiers, G. *et al.* Early dynamic fate changes in haemogenic endothelium characterized at the single-cell level. *Nat Commun* **4**, 2924 (2013).
59. Obier, N. *et al.* Cooperative binding of AP-1 and TEAD4 modulates the balance between vascular smooth muscle and hemogenic cell fate. *Development* **143**, 4324-4340 (2016).
60. Padron-Barthe, L. *et al.* Clonal analysis identifies hemogenic endothelium as the source of the blood-endothelial common lineage in the mouse embryo. *Blood* **124**, 2523-2532 (2014).
61. Behringer, R., Gertsenstein, M., Nagy, K.V. & Nagy, A. *Manipulating the Mouse Embryo: A Laboratory Manual*. (Cold Spring Harbor Laboratory Press, 2014).
62. DiTacchio, L. *et al.* Transcription factors ER71/ETV2 and SOX9 participate in a positive feedback loop in fetal and adult mouse testis. *J Biol Chem* **287**, 23657-23666 (2012).
63. Wang, Q. *et al.* Disruption of the Cbfa2 gene causes necrosis and hemorrhaging in the central nervous system and blocks definitive hematopoiesis. *Proc Natl Acad Sci U S A* **93**, 3444-3449 (1996).
64. Dobin, A. *et al.* STAR: ultrafast universal RNA-seq aligner. *Bioinformatics* **29**, 15-21 (2013).
65. Love, M.I., Huber, W. & Anders, S. Moderated estimation of fold change and dispersion for RNA-seq data with DESeq2. *Genome biology* **15**, 550 (2014).
66. Stuart, T. *et al.* Comprehensive Integration of Single-Cell Data. *Cell* **177**, 1888-1902 e1821 (2019).
67. McCarthy, D.J., Campbell, K.R., Lun, A.T. & Wills, Q.F. Scater: pre-processing, quality control, normalization and visualization of single-cell RNA-seq data in R. *Bioinformatics* **33**, 1179-1186 (2017).
68. Lun, A.T., McCarthy, D.J. & Marioni, J.C. A step-by-step workflow for low-level analysis of single-cell RNA-seq data with Bioconductor. *F1000Res* **5**, 2122 (2016).
69. Langmead, B. & Salzberg, S.L. Fast gapped-read alignment with Bowtie 2. *Nat Methods* **9**, 357-359 (2012).
70. Li, H. *et al.* The Sequence Alignment/Map format and SAMtools. *Bioinformatics* **25**, 2078-2079 (2009).
71. Ramirez, F. *et al.* deepTools2: a next generation web server for deep-sequencing data analysis. *Nucleic Acids Res* **44**, W160-165 (2016).
72. Zhang, Y. *et al.* Model-based analysis of ChIP-Seq (MACS). *Genome Biol* **9**, R137 (2008).
73. McLean, C.Y. *et al.* GREAT improves functional interpretation of cis-regulatory regions. *Nat Biotechnol* **28**, 495-501 (2010).
74. McLeay, R.C. & Bailey, T.L. Motif Enrichment Analysis: a unified framework and an evaluation on ChIP data. *BMC Bioinformatics* **11**, 165 (2010).
75. Zhao, H. *et al.* CrossMap: a versatile tool for coordinate conversion between genome assemblies. *Bioinformatics* **30**, 1006-1007 (2014).
76. Quinlan, A.R. & Hall, I.M. BEDTools: a flexible suite of utilities for comparing genomic features. *Bioinformatics* **26**, 841-842 (2010).
77. Robinson, J.T. *et al.* Integrative genomics viewer. *Nat Biotechnol* **29**, 24-26 (2011).
78. Stemmer, M., Thumberger, T., Del Sol Keyer, M., Wittbrodt, J. & Mateo, J.L. CCTop: An Intuitive, Flexible and Reliable CRISPR/Cas9 Target Prediction Tool. *PLoS One* **10**, e0124633 (2015).
79. Hsu, P.D. *et al.* DNA targeting specificity of RNA-guided Cas9 nucleases. *Nat Biotechnol* **31**, 827-832 (2013).
80. Heinz, S. *et al.* Simple combinations of lineage-determining transcription factors prime cis-regulatory elements required for macrophage and B cell identities. *Mol Cell* **38**, 576-589 (2010).
81. Senft, A.D. *et al.* Combinatorial Smad2/3 Activities Downstream of Nodal Signaling Maintain Embryonic/Extra-Embryonic Cell Identities during Lineage Priming. *Cell Rep* **24**, 1977-1985 e1977 (2018).

475

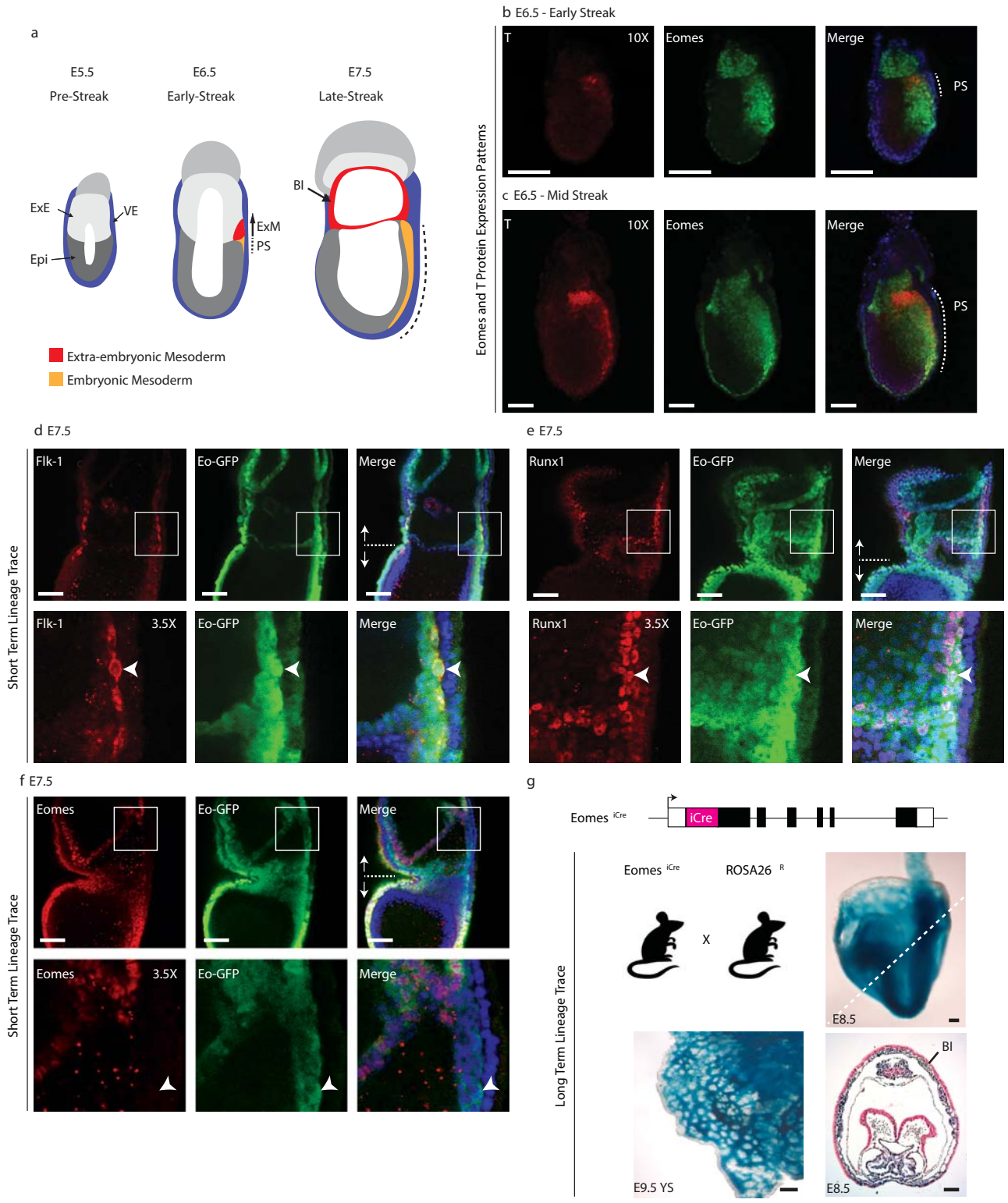
a
E5.5
Pre-Streak
E6.5
Early-Streak
E7.5
Late-Streak
ExE
VE
Epi
ExM
PS
Bl
Extra-embryonic Mesoderm
Embryonic Mesoderm
b E6.5 - Early Streak
c E6.5 - Mid Streak
Eomes and T Protein Expression Patterns
T
10X
Eomes
Merge
PS
d E7.5
e E7.5
Short Term Lineage Trace
Flk-1
Eo-GFP
Merge
Runx1
3.5X
f E7.5
g
Eomes iCre
iCre
ROSA26 R
X
Long Term Lineage Trace
E8.5
E9.5 YS
Bl

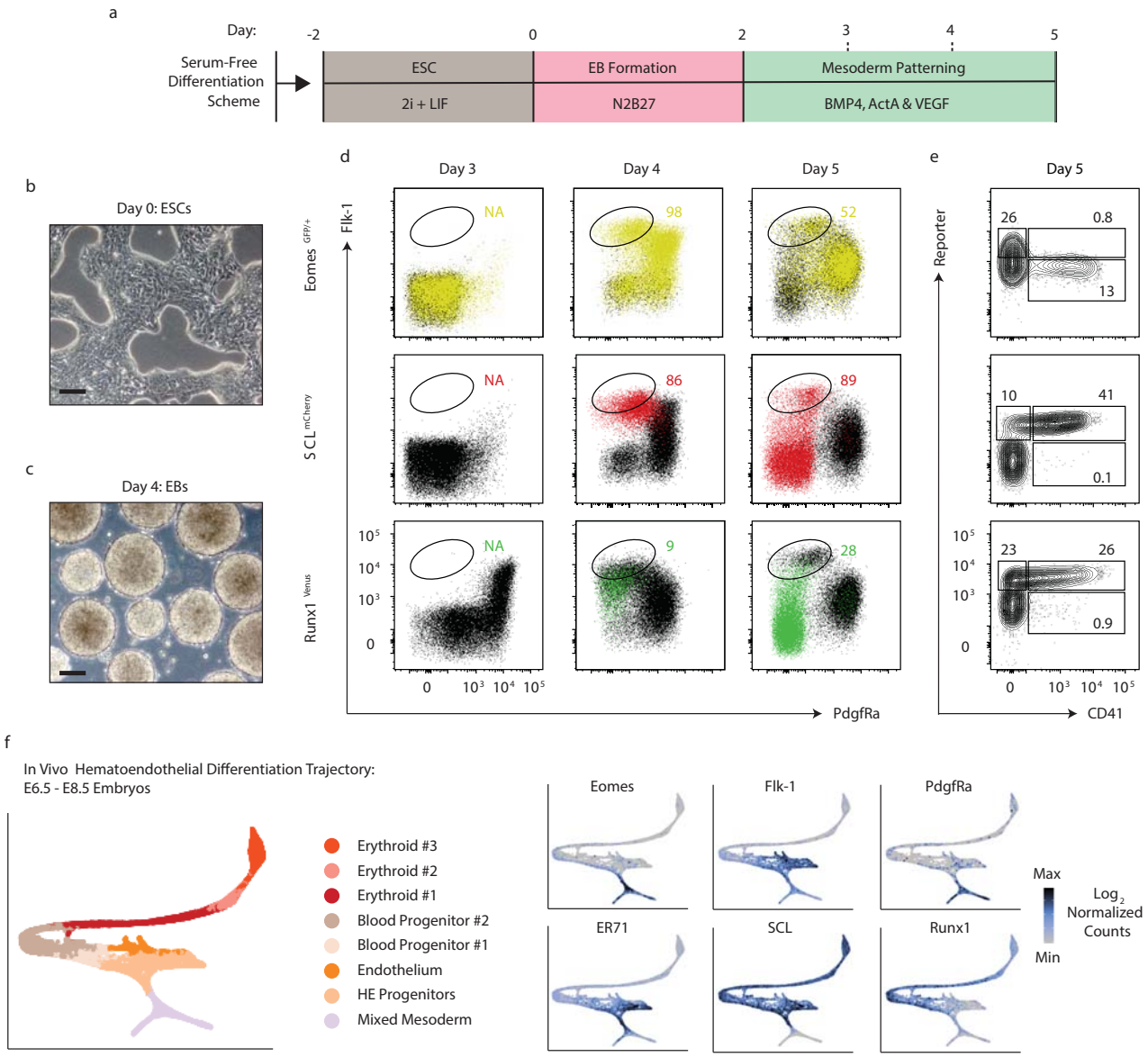
a
Day:
-2
0
2
3
4
5
Serum-Free Differentiation Scheme
ESC
EB Formation
Mesoderm Patterning
2i + LIF
N2B27
BMP4, ActA & VEGF
b
Day 0: ESCs
c
Day 4: EBs
d
Day 3
Day 4
Day 5
Flk-1
Eomes GFP/+
SCL mCherry
Runx1 Venus
NA
98
52
86
89
9
28
PdgfRa
e
Day 5
Reporter
26
0.8
13
10
41
0.1
23
26
0.9
CD41
f
In Vivo Hematoendothelial Differentiation Trajectory:
E6.5 - E8.5 Embryos
Erythroid #3
Erythroid #2
Erythroid #1
Blood Progenitor #2
Blood Progenitor #1
Endothelium
HE Progenitors
Mixed Mesoderm
Eomes
Flk-1
PdgfRa
ER71
SCL
Runx1
Max
Min
Log2 Normalized Counts

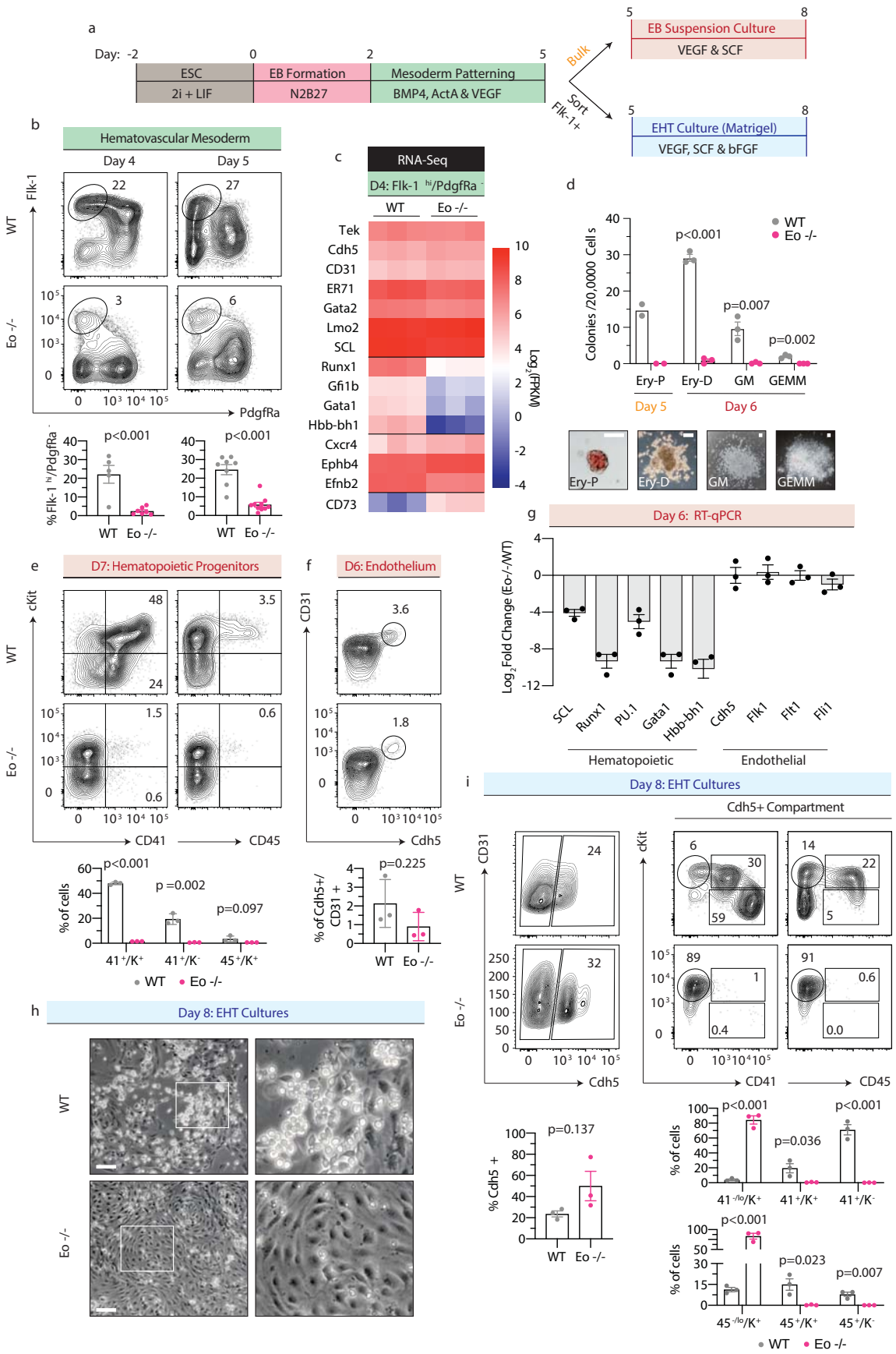
a
Day: -2
0
2
5
ESC
2i + LIF
EB Formation
N2B27
Mesoderm Patterning
BMP4, ActA & VEGF
Bulk
Sort Flk-1+
5
8
EB Suspension Culture
VEGF & SCF
EHT Culture (Matrigel)
VEGF, SCF & bFGF
b
Hematovascular Mesoderm
Day 4
Day 5
Flk-1
PdgfRa
WT
Eo -/-
22
27
3
6
% Flk-1 hi/PdgfRa -
p<0.001
c
RNA-Seq
D4: Flk-1 hi/PdgfRa -
Tek
Cdh5
CD31
ER71
Gata2
Lmo2
SCL
Runx1
Gfi1b
Gata1
Hbb-bh1
Cxcr4
Ephb4
Efnb2
CD73
Log2(FPKM)
d
Colonies /20,0000 Cells
p<0.001
p=0.007
p=0.002
Ery-P
Ery-D
GM
GEMM
Day 5
Day 6
e
D7: Hematopoietic Progenitors
cKit
CD41
CD45
48
24
3.5
1.5
0.6
% of cells
p=0.002
p=0.097
41+/K+
41+/K-
45+/K+
f
D6: Endothelium
CD31
Cdh5
3.6
1.8
% of Cdh5+/ CD31 +
p=0.225
g
Day 6: RT-qPCR
Log2 Fold Change (Eo-/-/WT)
SCL
Runx1
PU.1
Gata1
Hbb-bh1
Cdh5
Flk1
Flt1
Fli1
Hematopoietic
Endothelial
h
Day 8: EHT Cultures
i
Day 8: EHT Cultures
Cdh5+ Compartment
24
32
6
30
59
14
22
5
89
1
0.4
91
0.6
0.0
% Cdh5 +
p=0.137
% of cells
p<0.001
p=0.036
41-/lo/K+
41+/K+
41+/K-
p=0.023
p=0.007
45-/lo/K+
45+/K+
45+/K-

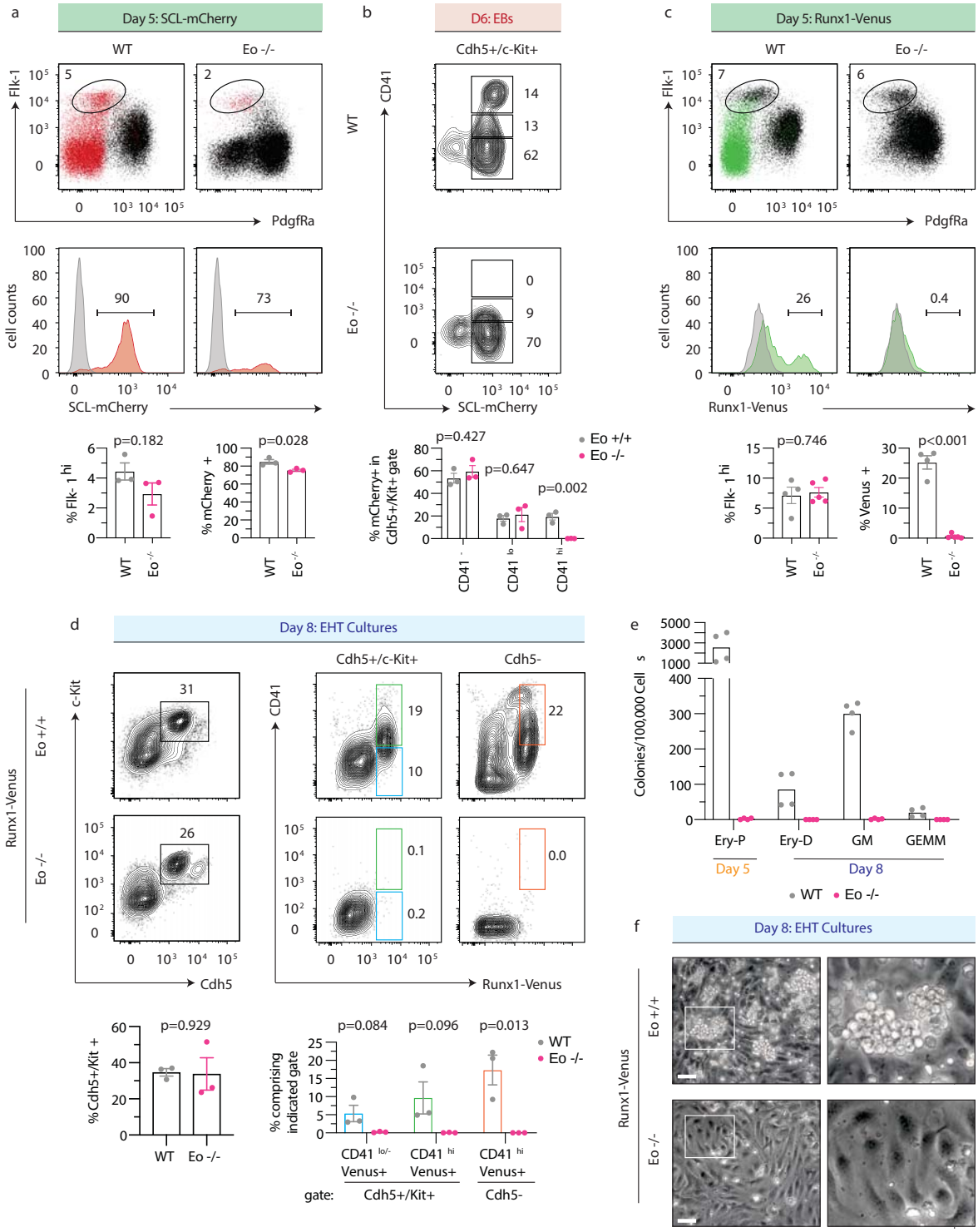

Harland_Figure. 4

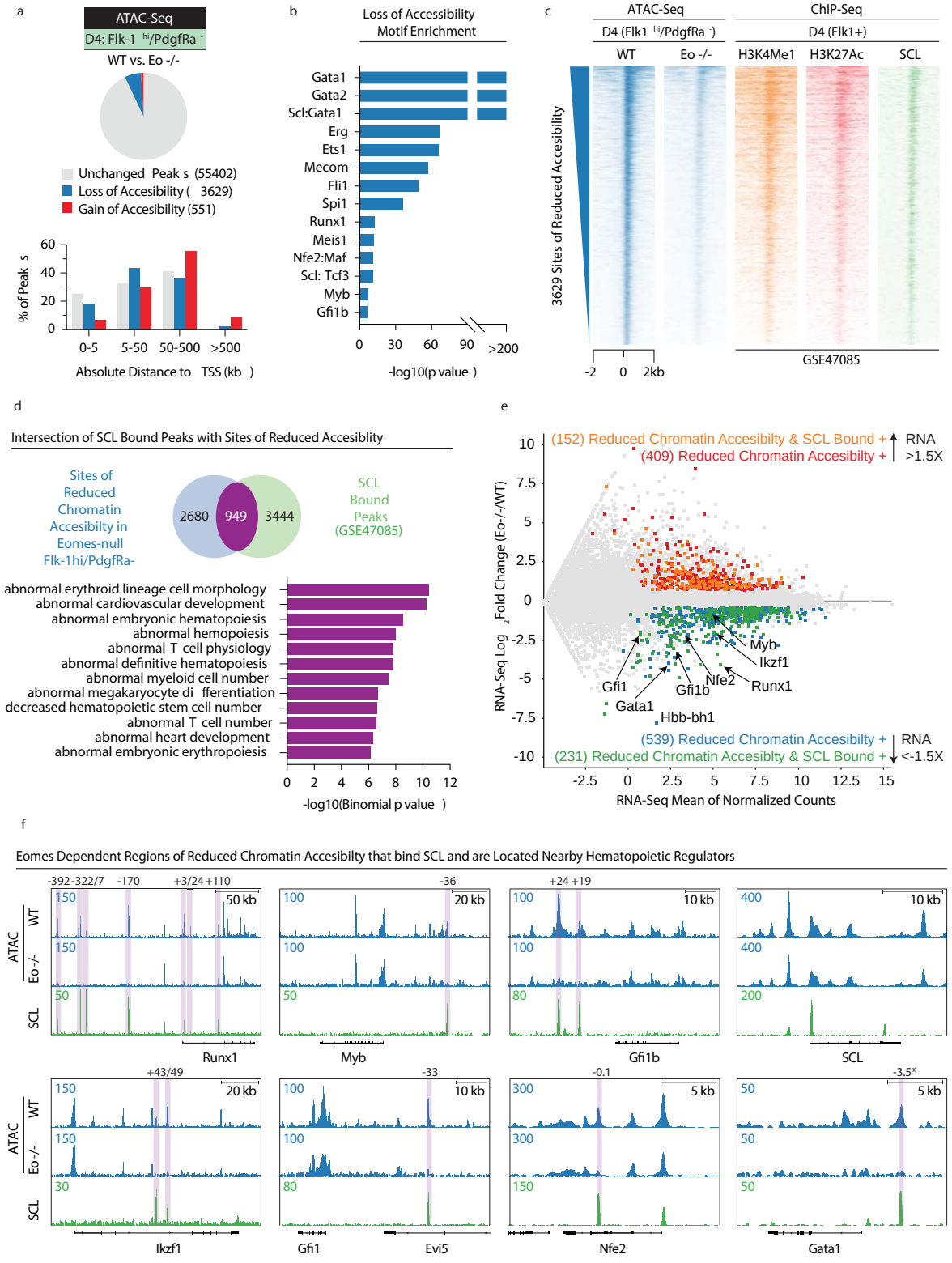
a
ATAC-Seq
D4: Flk-1 hi/PdgfRa -
WT vs. Eo -/-
Unchanged Peak s (55402)
Loss of Accesibility (3629)
Gain of Accesibility (551)
% of Peak s
0-5
5-50
50-500
>500
Absolute Distance to TSS (kb)
b
Loss of Accessibility
Motif Enrichment
Gata1
Gata2
Scl:Gata1
Erg
Ets1
Mecom
Fli1
Spi1
Runx1
Meis1
Nfe2:Maf
Scl: Tcf3
Myb
Gfi1b
-log10(p value)
c
ATAC-Seq
D4 (Flk1 hi/PdgfRa -)
WT
Eo -/-
ChIP-Seq
D4 (Flk1+)
H3K4Me1
H3K27Ac
SCL
3629 Sites of Reduced Accesibility
GSE47085
d
Intersection of SCL Bound Peaks with Sites of Reduced Accesiblity
Sites of Reduced Chromatin Accesibilty in Eomes-null Flk-1hi/PdgfRa-
2680
949
3444
SCL Bound Peaks (GSE47085)
abnormal erythroid lineage cell morphology
abnormal cardiovascular development
abnormal embryonic hematopoiesis
abnormal hemopoiesis
abnormal T cell physiology
abnormal definitive hematopoiesis
abnormal myeloid cell number
abnormal megakaryocyte di fferentiation
decreased hematopoietic stem cell number
abnormal T cell number
abnormal heart development
abnormal embryonic erythropoiesis
-log10(Binomial p value)
e
(152) Reduced Chromatin Accesibilty & SCL Bound +
(409) Reduced Chromatin Accesibilty +
RNA >1.5X
RNA-Seq Log 2 Fold Change (Eo-/-/WT)
Myb
Ikzf1
Gfi1
Nfe2
Gfi1b
Runx1
Gata1
Hbb-bh1
(539) Reduced Chromatin Accesibilty +
(231) Reduced Chromatin Accesiblty & SCL Bound +
RNA <-1.5X
RNA-Seq Mean of Normalized Counts
f
Eomes Dependent Regions of Reduced Chromatin Accesibilty that bind SCL and are Located Nearby Hematopoietic Regulators
ATAC
WT
Eo -/-
SCL
Runx1
Myb
Gfi1b
SCL
Ikzf1
Gfi1
Evi5
Nfe2
Gata1

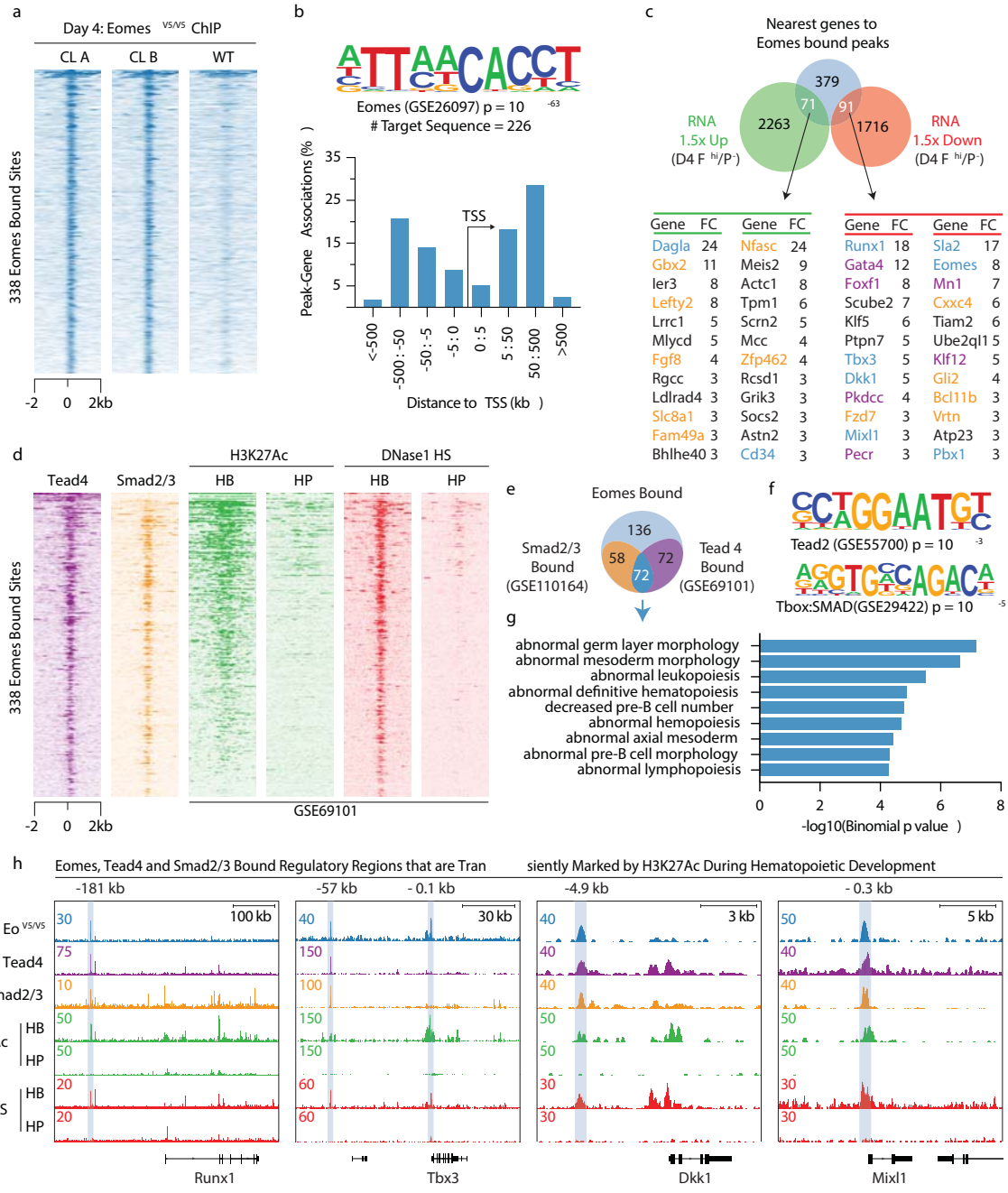
a
Day 4: Eomes V5/V5 ChIP
CL A
CL B
WT
338 Eomes Bound Sites
-2
0
2kb
b
Eomes (GSE26097) p = 10 -63
Target Sequence = 226
Peak-Gene Associations (%)
35
25
15
5
TSS
<-500
-500 : -50
-50 : -5
-5 : 0
0 : 5
5 : 50
50 : 500
>500
Distance to TSS (kb)
c
Nearest genes to
Eomes bound peaks
379
71
91
2263
1716
RNA
1.5x Up
(D4 F hi/P-)
RNA
1.5x Down
(D4 F hi/P-)
Gene FC Gene FC
Dagla 24 Nfasc 24
Gbx2 11 Meis2 9
Ier3 8 Actc1 8
Lefty2 8 Tpm1 6
Lrrc1 5 Scrn2 5
Mlycd 5 Mcc 4
Fgf8 4 Zfp462 4
Rgcc 3 Rcsd1 3
Ldlrad4 3 Grik3 3
Slc8a1 3 Socs2 3
Fam49a 3 Astn2 3
Bhlhe40 3 Cd34 3
Gene FC Gene FC
Runx1 18 Sla2 17
Gata4 12 Eomes 8
Foxf1 8 Mn1 7
Scube2 7 Cxxc4 6
Klf5 6 Tiam2 6
Ptpn7 5 Ube2ql1 5
Tbx3 5 Klf12 5
Dkk1 5 Gli2 4
Pkdcc 4 Bcl11b 3
Fzd7 3 Vrtn 3
Mixl1 3 Atp23 3
Pecr 3 Pbx1 3
d
Tead4
Smad2/3
H3K27Ac
HB
HP
DNase1 HS
HB
HP
338 Eomes Bound Sites
-2
0
2kb
GSE69101
e
Eomes Bound
136
58
72
72
Smad2/3
Bound
(GSE110164)
Tead 4
Bound
(GSE69101)
f
Tead2 (GSE55700) p = 10 -3
Tbox:SMAD(GSE29422) p = 10 -5
g
abnormal germ layer morphology
abnormal mesoderm morphology
abnormal leukopoiesis
abnormal definitive hematopoiesis
decreased pre-B cell number
abnormal hemopoiesis
abnormal axial mesoderm
abnormal pre-B cell morphology
abnormal lymphopoiesis
0
2
4
6
8
-log10(Binomial p value)
h
Eomes, Tead4 and Smad2/3 Bound Regulatory Regions that are Tran siently Marked by H3K27Ac During Hematopoietic Development
-181 kb
-57 kb
- 0.1 kb
-4.9 kb
- 0.3 kb
Eo V5/V5
Tead4
Smad2/3
H3K27Ac
HB
HP
DNI HS
HB
HP
100 kb
30 kb
3 kb
5 kb
Runx1
Tbx3
Dkk1
Mixl1

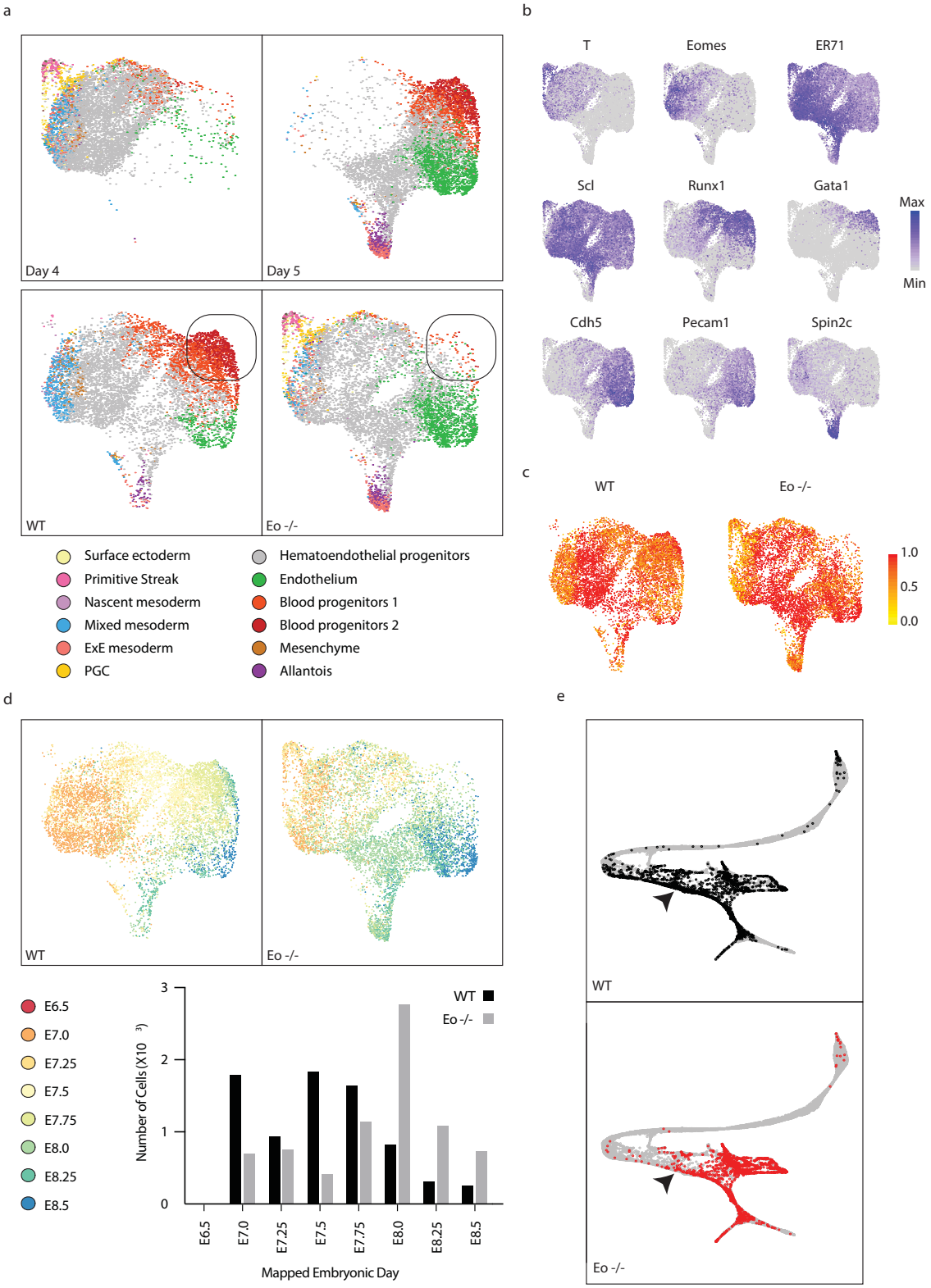
a
Day 4
Day 5
WT
Eo -/-
Surface ectoderm
Primitive Streak
Nascent mesoderm
Mixed mesoderm
ExE mesoderm
PGC
Hematoendothelial progenitors
Endothelium
Blood progenitors 1
Blood progenitors 2
Mesenchyme
Allantois
b
T
Eomes
ER71
Scl
Runx1
Gata1
Cdh5
Pecam1
Spin2c
Max
Min
c
WT
Eo -/-
1.0
0.5
0.0
d
WT
Eo -/-
E6.5
E7.0
E7.25
E7.5
E7.75
E8.0
E8.25
E8.5
Number of Cells (X10 3)
WT
Eo -/-
Mapped Embryonic Day
e
WT
Eo -/-

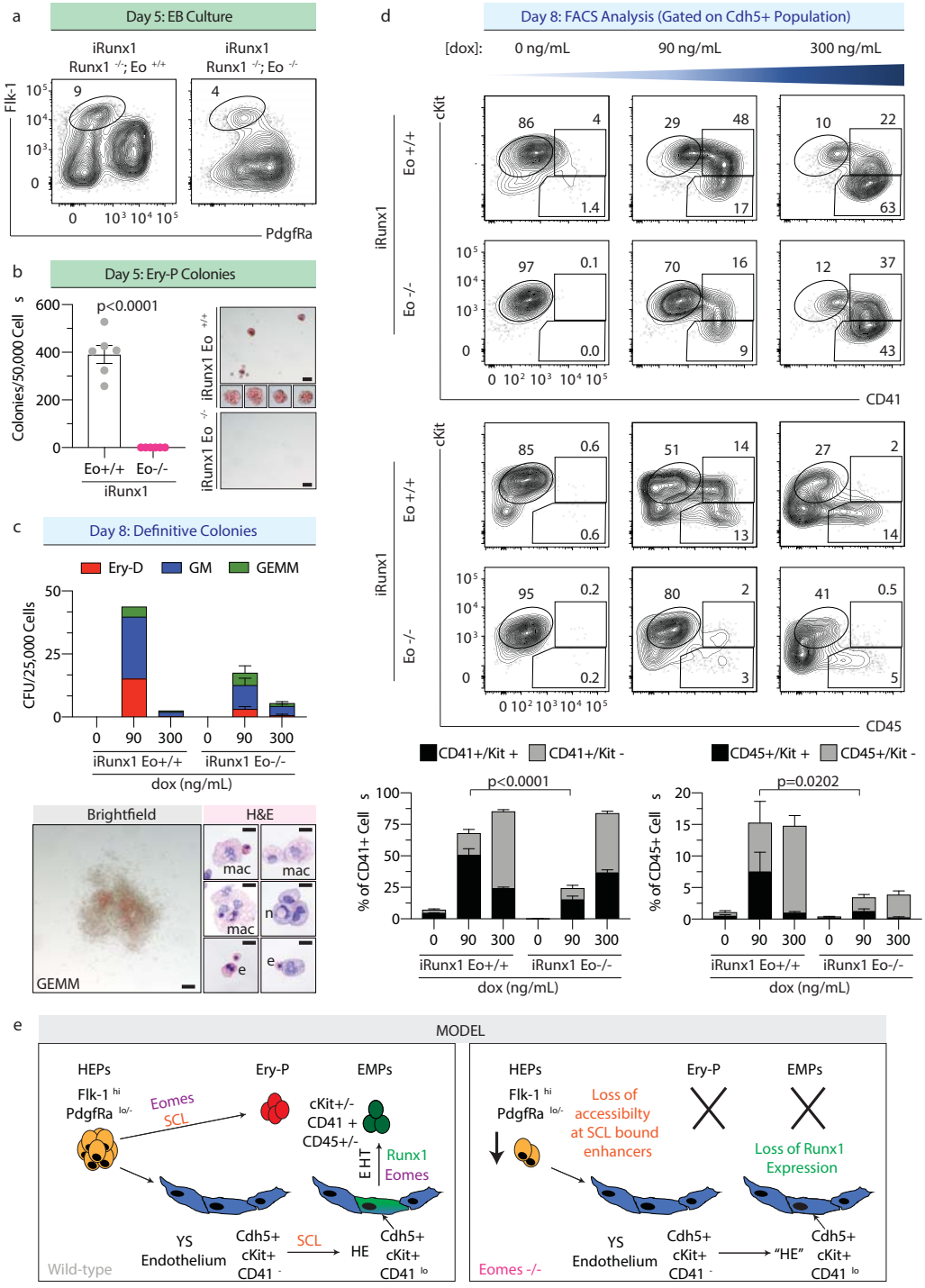

Harland_Figure. 8

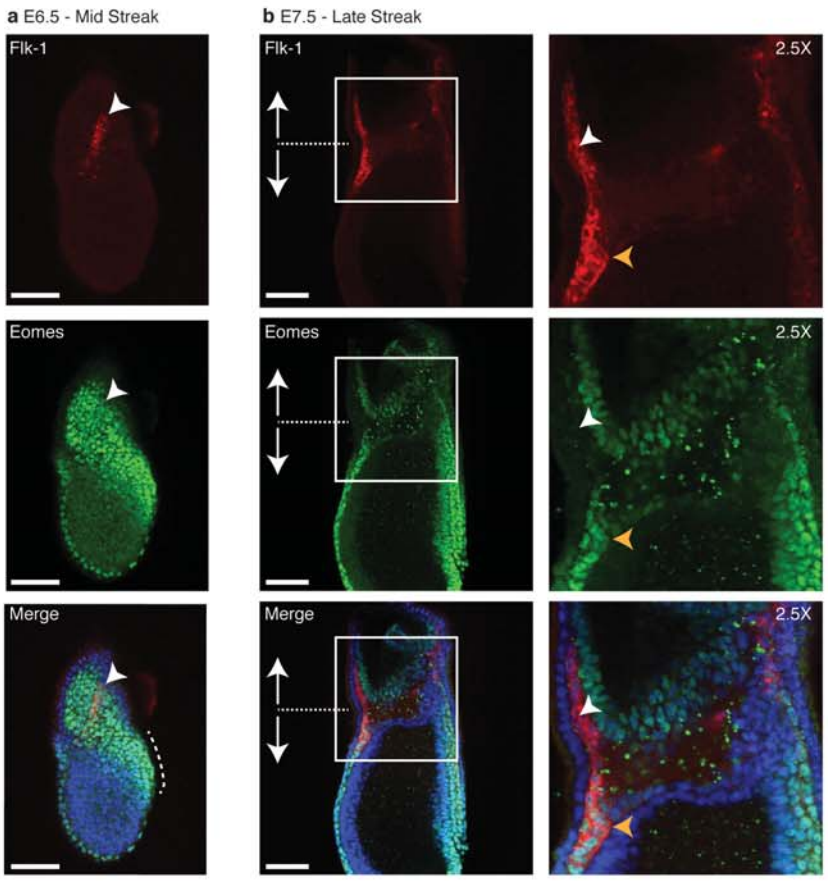
a E6.5 - Mid Streak
b E7.5 - Late Streak
Flk-1
Flk-1
2.5X
Eomes
Eomes
2.5X
Merge
Merge
2.5X

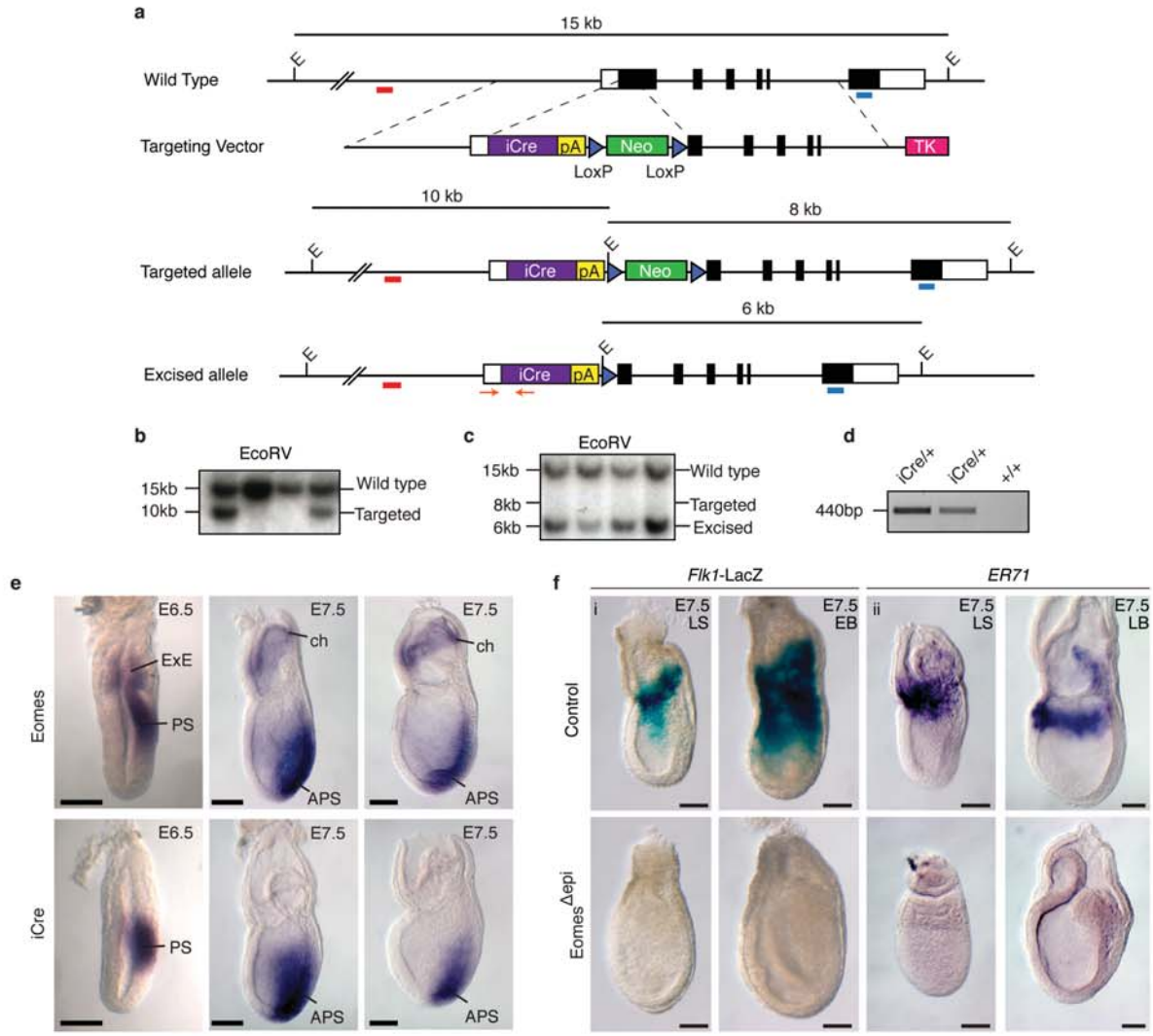
a
15 kb
Wild Type
E
E
Targeting Vector
iCre
pA
Neo
TK
LoxP
LoxP
10 kb
8 kb
Targeted allele
6 kb
Excised allele
b
EcoRV
15kb
10kb
Wild type
Targeted
c
EcoRV
15kb
8kb
6kb
Wild type
Targeted
Excised
d
iCre/+
iCre/+
+/+
440bp
e
Eomes
iCre
E6.5
E7.5
ExE
PS
ch
APS
f
Flk1-LacZ
ER71
Control
Eomes Δepi
i
ii
E7.5 LS
E7.5 EB
E7.5 LB

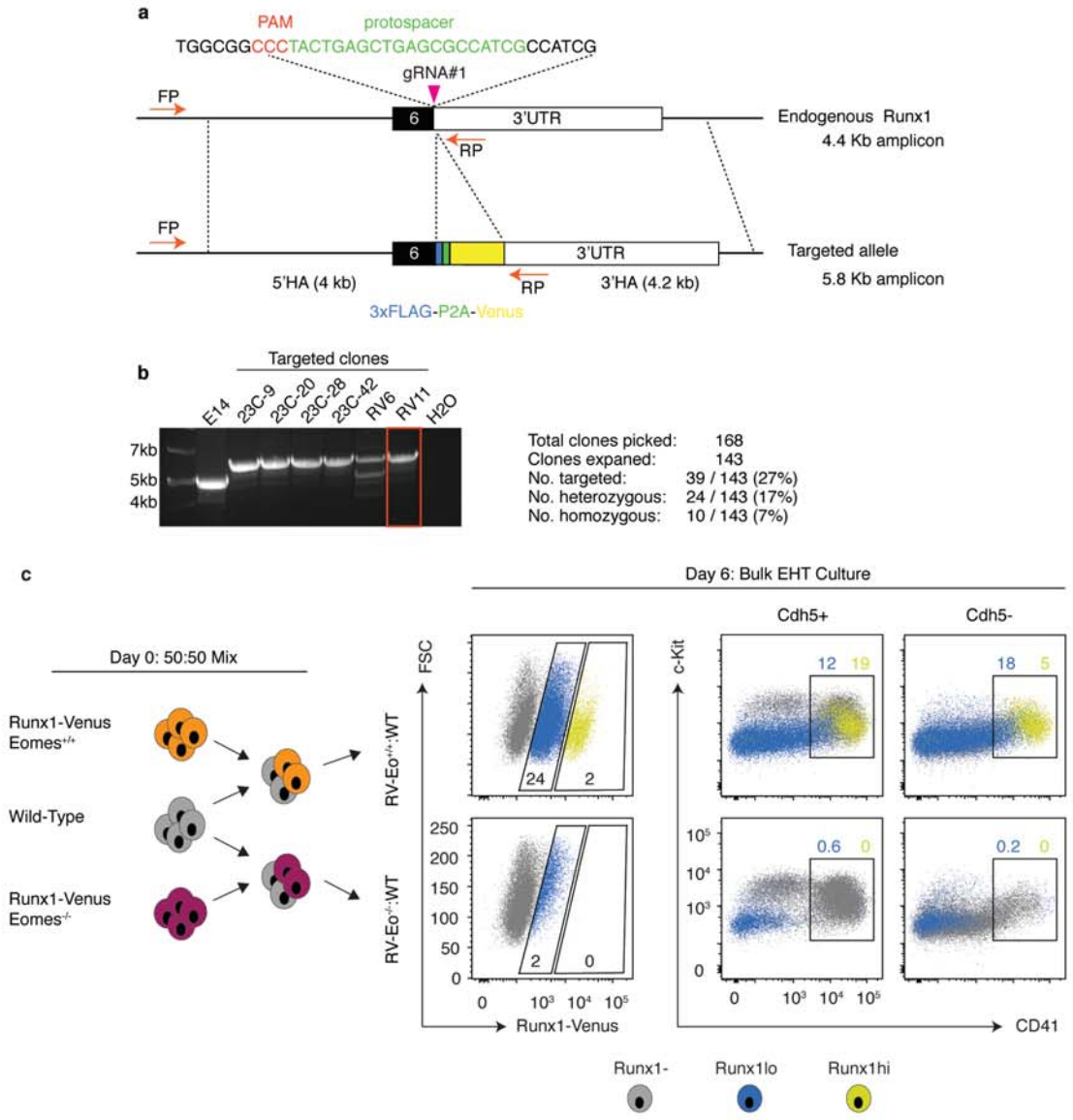
a
PAM
protospacer
TGGCGGCCCTACTGAGCTGAGCGCCATCGCCATCG
gRNA#1
FP
6
3'UTR
RP
Endogenous Runx1
4.4 Kb amplicon
FP
6
3'UTR
Targeted allele
5.8 Kb amplicon
5'HA (4 kb)
RP
3'HA (4.2 kb)
3xFLAG-P2A-Venus
b
Targeted clones
E14
23C-9
23C-20
23C-28
23C-42
RV6
RV11
H2O
7kb
5kb
4kb
Total clones picked: 168
Clones expaned: 143
No. targeted: 39 / 143 (27%)
No. heterozygous: 24 / 143 (17%)
No. homozygous: 10 / 143 (7%)
c
Day 0: 50:50 Mix
Runx1-Venus
Eomes+/+
Wild-Type
Runx1-Venus
Eomes-/-
Day 6: Bulk EHT Culture
Cdh5+
Cdh5-
FSC
c-Kit
RV-Eo+/+:WT
RV-Eo-/-:WT
24
2
12
19
18
5
2
0
0.6
0
0.2
0
Runx1-Venus
CD41
Runx1-
Runx1lo
Runx1hi

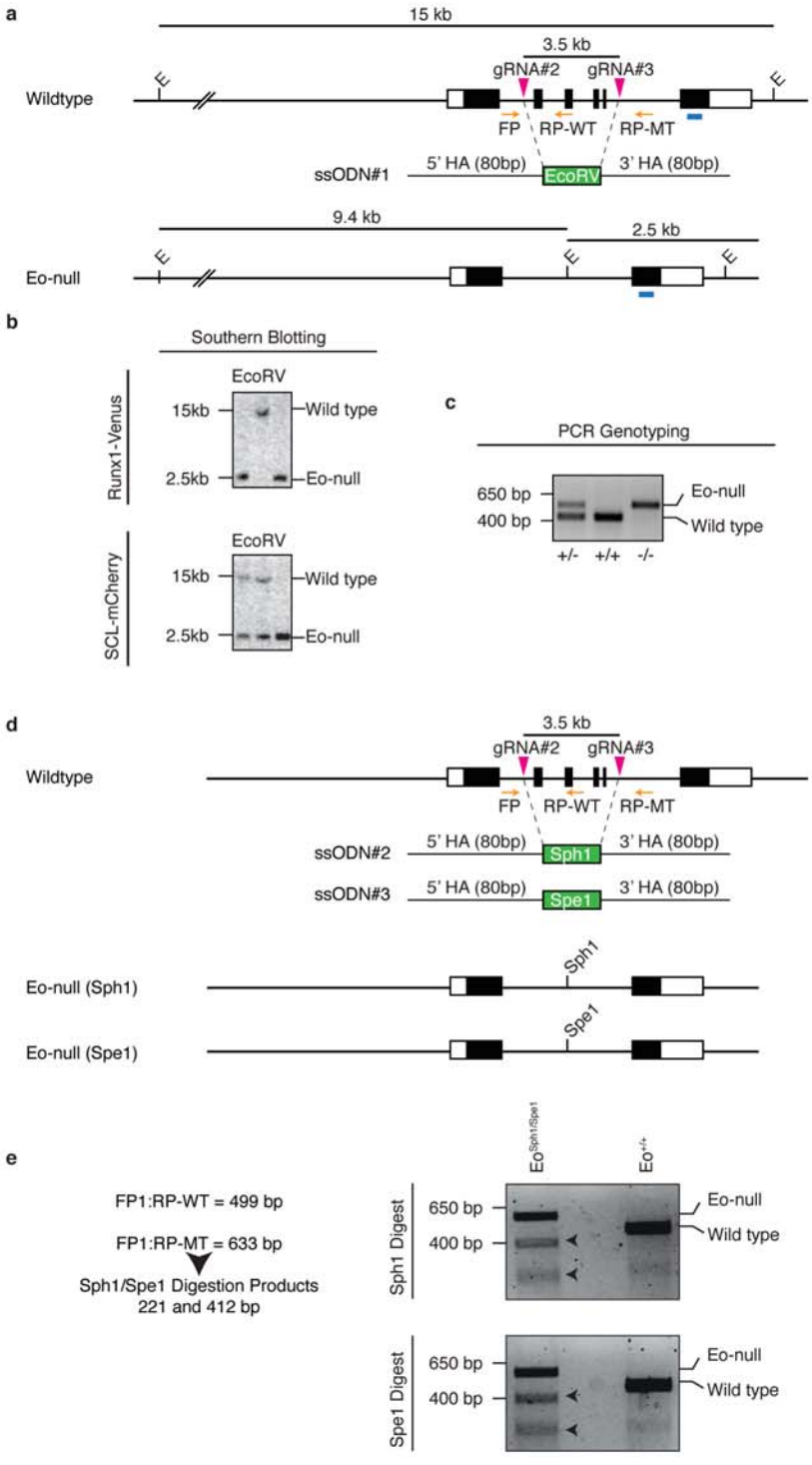
a
15 kb
3.5 kb
gRNA#2
gRNA#3
Wildtype
E
E
E
FP
RP-WT
RP-MT
ssODN#1
5' HA (80bp)
EcoRV
3' HA (80bp)
9.4 kb
2.5 kb
Eo-null
b
Southern Blotting
EcoRV
Runx1-Venus
15kb
Wild type
2.5kb
Eo-null
EcoRV
SCL-mCherry
15kb
Wild type
2.5kb
Eo-null
c
PCR Genotyping
650 bp
400 bp
Eo-null
Wild type
+/-
+/+
-/-
d
3.5 kb
gRNA#2
gRNA#3
Wildtype
FP
RP-WT
RP-MT
ssODN#2
5' HA (80bp)
Sph1
3' HA (80bp)
ssODN#3
5' HA (80bp)
Spe1
3' HA (80bp)
Sph1
Eo-null (Sph1)
Spe1
Eo-null (Spe1)
e
FP1:RP-WT = 499 bp
FP1:RP-MT = 633 bp
Sph1/Spe1 Digestion Products
221 and 412 bp
Eo Sph1/Spe1
Eo +/+
Sph1 Digest
650 bp
400 bp
Eo-null
Wild type
Spe1 Digest
650 bp
400 bp
Eo-null
Wild type

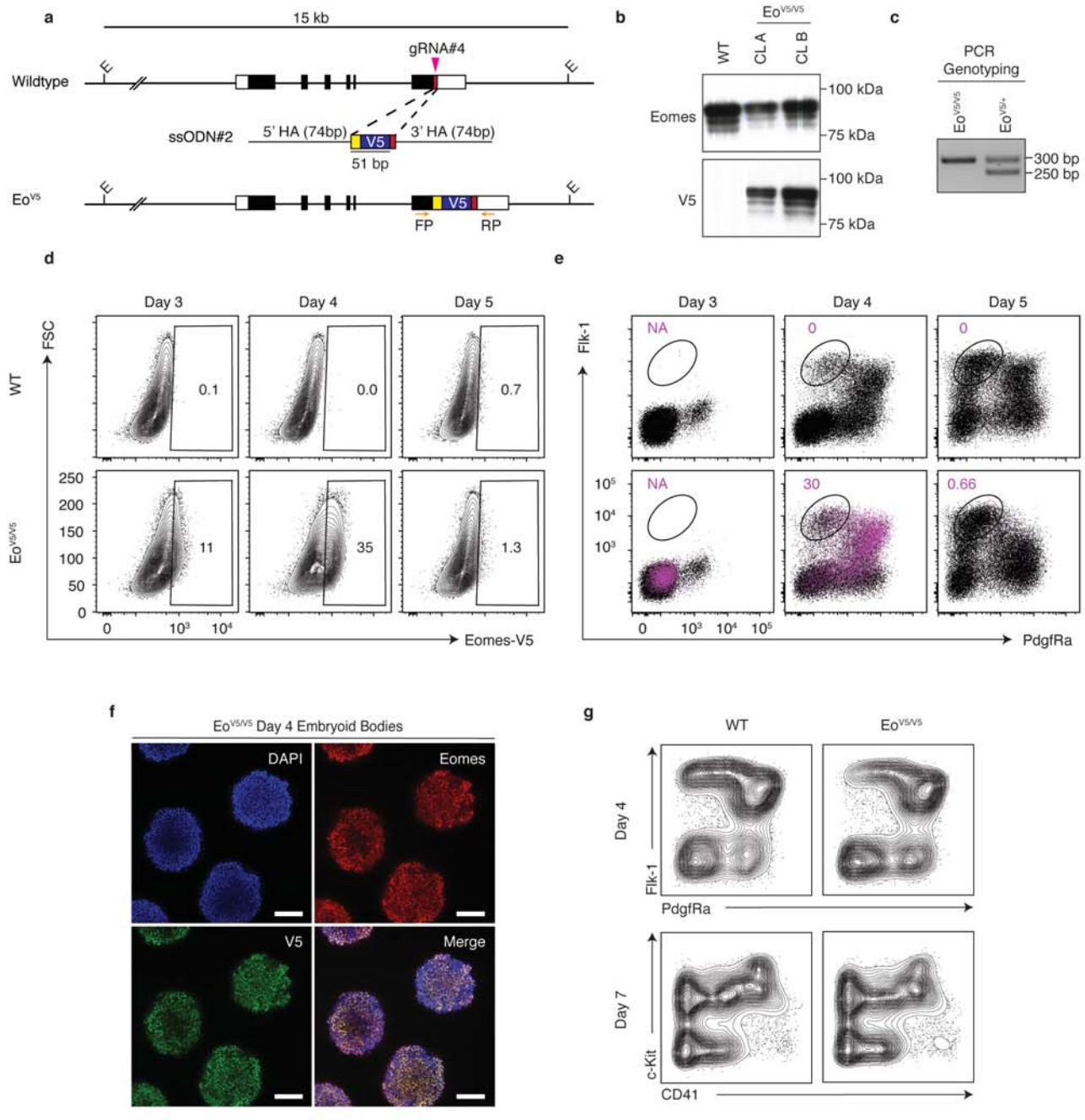
a
15 kb
gRNA#4
Wildtype
E
E
ssODN#2
5' HA (74bp)
V5
3' HA (74bp)
51 bp
Eo^V5
E
E
V5
FP
RP
b
Eo^V5/V5
WT
CL A
CL B
Eomes
100 kDa
75 kDa
V5
100 kDa
75 kDa
c
PCR Genotyping
Eo^V5/V5
Eo^V5/+
300 bp
250 bp
d
Day 3
Day 4
Day 5
WT
FSC
0.1
0.0
0.7
Eo^V5/V5
250
200
150
100
50
0
11
35
1.3
0
10^3
10^4
Eomes-V5
e
Day 3
Day 4
Day 5
Flk-1
NA
0
0
NA
30
0.66
10^5
10^4
10^3
0
10^3
10^4
10^5
PdgfRa
f
Eo^V5/V5 Day 4 Embryoid Bodies
DAPI
Eomes
V5
Merge
g
WT
Eo^V5/V5
Day 4
Flk-1
PdgfRa
Day 7
c-Kit
CD41

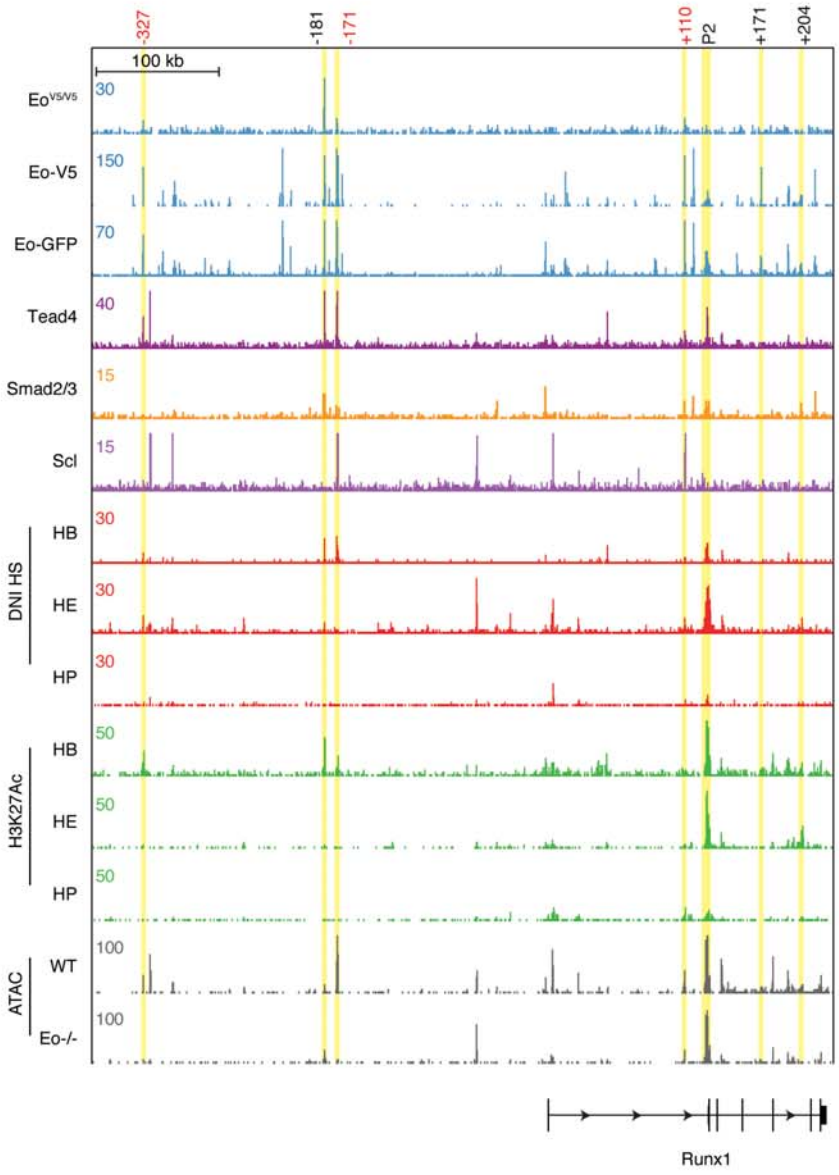
-327
-181
-171
+110
P2
+171
+204
100 kb
Eo^V5/V5
30
Eo-V5
150
Eo-GFP
70
Tead4
40
Smad2/3
15
Scl
15
DNI HS
HB
30
HE
30
HP
30
H3K27Ac
HB
50
HE
50
HP
50
ATAC
WT
100
Eo-/-
100
Runx1

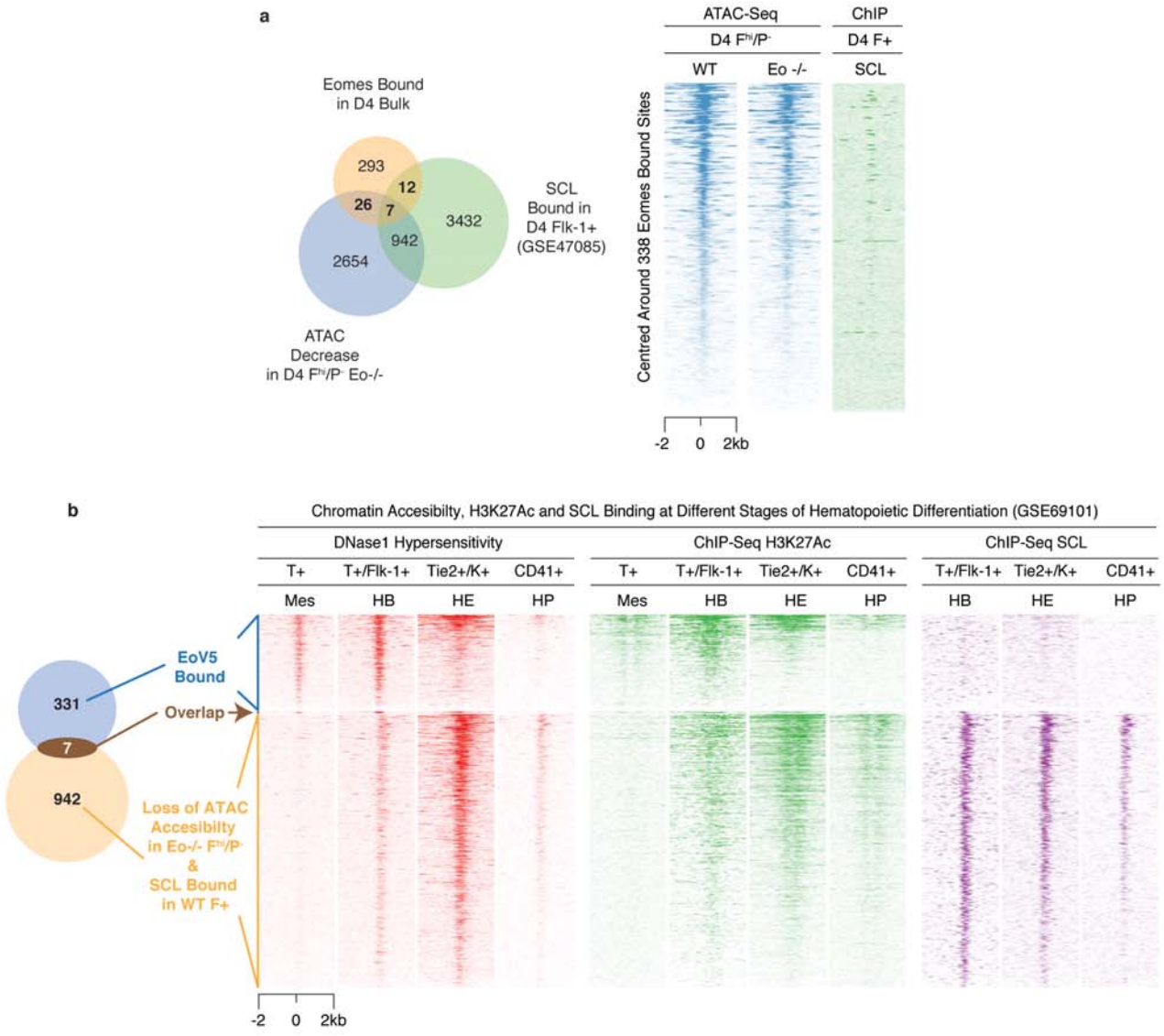
a
Eomes Bound
in D4 Bulk
293
12
26
7
3432
942
2654
SCL
Bound in
D4 Flk-1+
(GSE47085)
ATAC
Decrease
in D4 Fhi/P- Eo-/-
ATAC-Seq
D4 Fhi/P-
WT
Eo -/-
ChIP
D4 F+
SCL
Centred Around 338 Eomes Bound Sites
-2
0
2kb
b
Chromatin Accesibilty, H3K27Ac and SCL Binding at Different Stages of Hematopoietic Differentiation (GSE69101)
DNase1 Hypersensitivity
ChIP-Seq H3K27Ac
ChIP-Seq SCL
T+
T+/Flk-1+
Tie2+/K+
CD41+
Mes
HB
HE
HP
EoV5
Bound
331
Overlap
7
942
Loss of ATAC
Accesibilty
in Eo-/- Fhi/P-
&
SCL Bound
in WT F+
-2
0
2kb

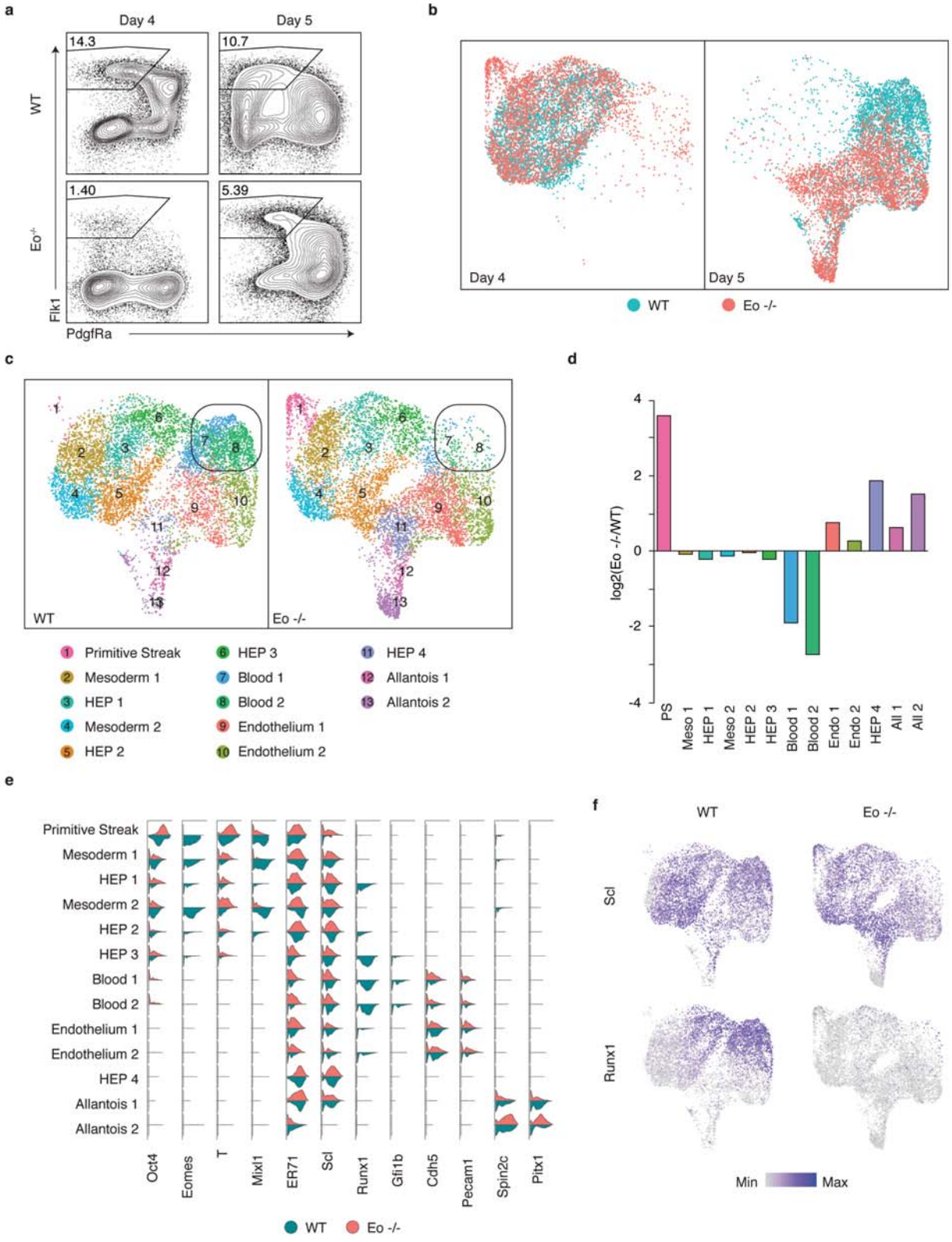
a
Day 4
Day 5
14.3
10.7
1.40
5.39
WT
Eo-/-
Flk1
PdgfRa
b
Day 4
Day 5
WT
Eo -/-
c
WT
Eo -/-
1 Primitive Streak
2 Mesoderm 1
3 HEP 1
4 Mesoderm 2
5 HEP 2
6 HEP 3
7 Blood 1
8 Blood 2
9 Endothelium 1
10 Endothelium 2
11 HEP 4
12 Allantois 1
13 Allantois 2
d
log2(Eo -/-/WT)
4
2
0
-2
-4
PS
Meso 1
HEP 1
Meso 2
HEP 2
HEP 3
Blood 1
Blood 2
Endo 1
Endo 2
HEP 4
All 1
All 2
e
Primitive Streak
Mesoderm 1
HEP 1
Mesoderm 2
HEP 2
HEP 3
Blood 1
Blood 2
Endothelium 1
Endothelium 2
HEP 4
Allantois 1
Allantois 2
Oct4
Eomes
T
Mixl1
ER71
Scl
Runx1
Gfi1b
Cdh5
Pecam1
Spin2c
Pitx1
WT
Eo -/-
f
WT
Eo -/-
Scl
Runx1
Min
Max

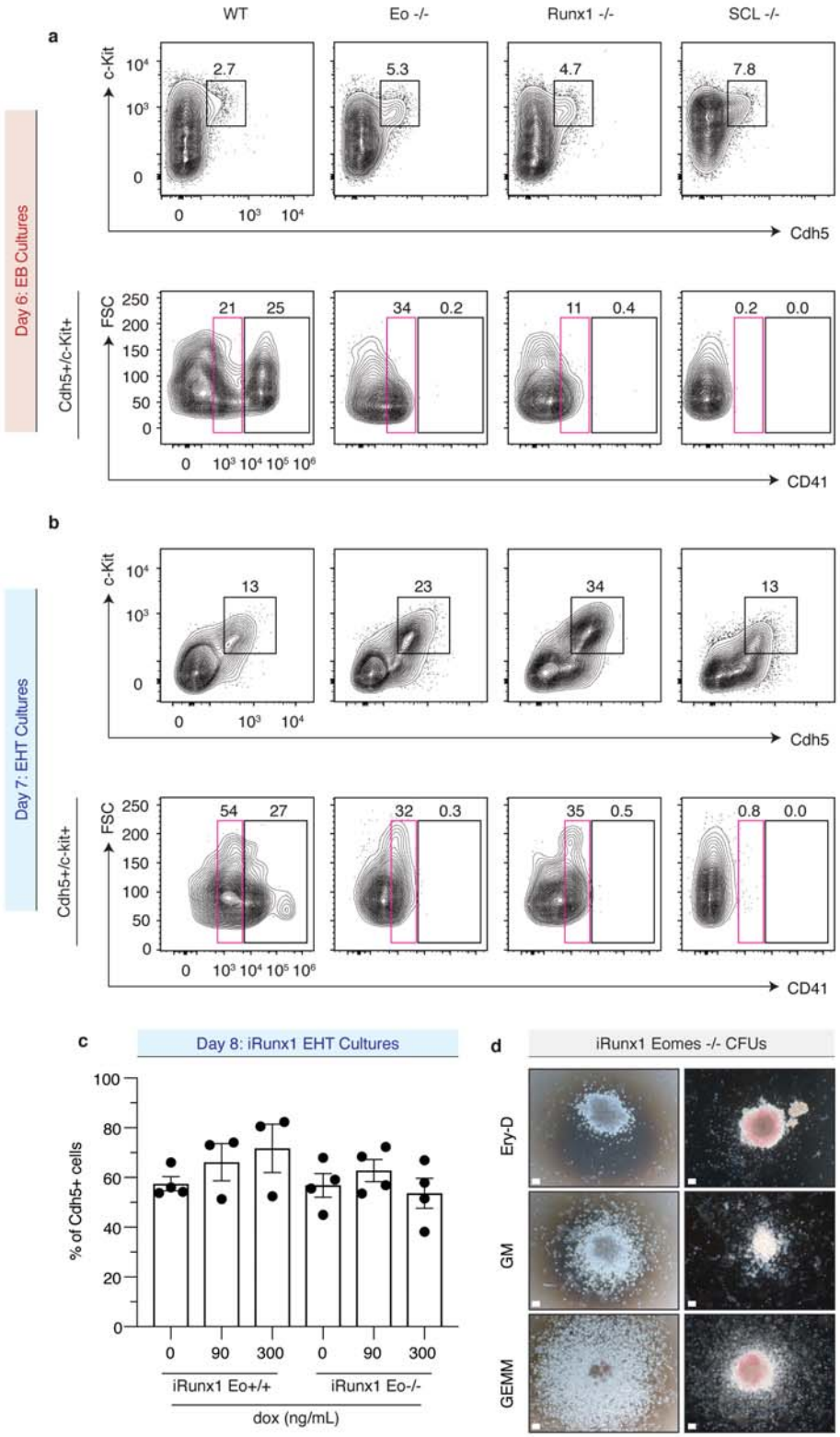
a
WT
Eo -/-
Runx1 -/-
SCL -/-
Day 6: EB Cultures
c-Kit
2.7
5.3
4.7
7.8
Cdh5
Cdh5+/c-Kit+
FSC
21
25
34
0.2
11
0.4
0.2
0.0
CD41
b
Day 7: EHT Cultures
c-kit
13
23
34
13
Cdh5
Cdh5+/c-kit+
54
27
32
0.3
35
0.5
0.8
0.0
CD41
c
Day 8: iRunx1 EHT Cultures
% of Cdh5+ cells
iRunx1 Eo+/+
iRunx1 Eo-/-
dox (ng/mL)
d
iRunx1 Eomes -/- CFUs
Ery-D
GM
GEMM

	Conserved Marker List (Positive Only)												
Cell Identity	Primitive Streak	Mesoderm 1	HE 1	Mesoderm 2	HE2	HE3	Blood 1	Blood 2	Endo 1	Endo 2	HE4	Allantois 1	Allantois 2
Figure Cluster	1	2	3	4	5	6	7	8	9	10	11	12	13
	Pou5f1	Mixl1	Lmo2	Mixl1	Lmo2	Fgf3	Ube2c	Gsta4	Ctla2a	Ctla2a	Csrp2	Cdkn1c	Hand1
	Fst	Krt8	Ifitm3	Tdgf1	Ube2c	Hand1	Gclm	Rnd2	Vim	Vim	Etv2	Csrp2	Spin2c
	Tdgf1	Tdgf1	Akap12	Cenpf	Nrp2	Zfpm1	Prc1	Gclm	Ecscr	Tmsb4x	Igfbp4	Twist1	Phlda2
	T	Hand1	Upp1	Tgfb2	Exoc3l	Hist1h1b	Cenpf	Fth1	Tmsb4x	Ramp2	Map1b	Cdx2	Pmp22
	Emb	Amot		Gpc3	Cenpf	Cbfa2t3	Rnd2	Prkar2b	Ramp2	Apoe	Mmp9	Dlk1	Cdkn1c
	Fgf8	Gpc3		Amot	Prc1		Top2a	Hist1h1b	Gja4	Cdh5	Dok4	Pitx1	Csrp2
	Mt1	Ifitm1		Ube2c	Arl6ip1		Zfpm1	Ftl1	Sparc	Mest	Hspa5	Spin2c	Pitx1
	Psme2	Tgfb2		Mesp1	Cdk1		Fth1	Zfpm1	Mest	Ecscr	Egfl7	Vcan	Cdx2
	Krt8	Mesp1		Ifitm1	Cenpe		Prkar2b	F2r	Col4a1	Gja4	Serpinh1	Tgfb2	Slc38a4
	Epcam	Wls		Arl6ip1	Etv2		Malat1	Srm	Egfl7	Ctsl	Hsp90b1	Sox4	Tgfb2
	Ifitm3	Dstn		Wls	Gadd45g		Jpt1	Col18a1	Cdh5	Sparc	Kdr	Map1b	Twist1
	Ldhb	T		Top2a	Top2a		Skap1	Fgf3	Crip2	Itm2a	Ifitm1	Slc38a4	Foxf1
	Mixl1	Ckb		Hand1	Plk1		Tacc1	Orc6	Ctsl	Col4a1	Gpc3	Swap70	Msx1
	Cyb5a	Prtg		Ccnb1	Tpx2		Tubb4b	Apoe	Itm2a	Gsta4	Cald1	Phlda2	Ccnd2
	Krt18	Ldhb		Tceal9	Ccnb1		Ccnb1		Igfbp4	Crip2	Tal1	Hspa5	Bambi
	Ckb	Actg1		Meg3	Bmp2		Hmmr		Hist1h1b	Igf1	Ssr2	Igf2r	Sfrp1
	L1td1	Tpm1		Gata6	Akap12		Aurka		Tmsb10	Col18a1	Slc16a3	Gpx3	Msx2
	Aldh2			Actg1	Smc4		Plk1		Col18a1	Tmsb10	Rbms1	Grb10	Crabp1
	Chchd10			Gja1	Cks2		Cks2		Col4a2	Ets1	Sox18	Hsp90b1	Morc4
	Cdkn1a			Ypel3	Kif20b		H2afx		Rasip1	Selenop	Pdia3	Etv2	Wnt5a
	S100a11			Cenpe	Kif11		Cdk1		Exoc3l4	Col4a2	Pdia6	Plac1	Peg10
	Sp5			Plk1	Mki67		Aurkb		Esam	Txnip	Lmo2	Plpp3	Plpp3
	Tagln			Prtg	Egfl7		Ddah2		Pecam1	F2r	Manf	Peg10	Sall4
	Psme1			Tpm1	Tal1		Cdca8		Abhd17a	Ets2	Dusp4	Afdn	Mllt3
	Ezr			Kif11	Incenp		Cenpe		Ets1	Ralb	Mdk	Kdr	Basp1
	Cldn7			Smc4	Mis18bp1		Nusap1		Tuba1a	Gngt2	Fam107b	Pdia3	Tceal9
	S100a10			Nusap1	Spc25		Mki67		Gngt2	Rasip1	Gcc2	Sept6	Hand2
	Sprr2a3			Sgo2a	Grrp1		Phlda1		Pgk1	Pecam1	Nrp1	Bambi	Rbpms2
	Tmem185a			Mki67	Aurka		Ftl1		Gng11	Tmem158		Vgll4	Rhou
	Spint2			Cdc42ep5	Hmmr		Incenp		Rasgrp3	Marc2		Parp1	Igf2r
	Npm3			Incenp	Bub3		Ccnf		H1f0	Pgk1		Hoxa7	Tbx4
	Stmn2			Cdk1	Nusap1		Tpx2		Myzap	Hapln1		Ccnjl	Suv39h1
	Psmb8			Rftn1	Kif23		Aspm		Hoxb2	Gng11		Capn6	Parp1
	Dppa5a			Mis18bp1	Dbf4		F2r		Icam2	Cmas		Amot	Tln2
	Terf1			Tpx2	Ier5l		Sgo2a		Creg1	Arpc3		Sfrp1	Fabp5
	Phlda2			Cks2			Ckap2l		Elk3	Abhd17a		Manf	Snai1
	Psmb10			T			Arl6ip1		Pdia6	Msn		Mdk	Rbbp7
	Meg3			Spc25			Cenpa		Afap1l1	Pdia3		Tbx4	Slc2a1
	Krt19			Kif20b			Cdc20		Sox17	Esam		Hoxa9	Efnb1
	Eno1			St3gal6			Racgap1		Clic1	Fstl1		Crabp1	Hoxa7
	Akap12			Ncapg			Kif11		Swap70	Cmtm8		Hoxc9	Amot
	Tgfb2			Prc1			Kif23		Ube2c	Afap1l1		Tceal9	Tbx3
	Plekhf2			Aurka			Klf13		Ets2	Sox17		Twist2	Hoxb6
	Acer2			S100a11			Smc4		Ndufa8	Cldn5		Dbn1	Bmp7
	Acadl						Ets2		Cd81	Gm45716		Basp1	Isl1
	Mt2						Anln		Cdk1	Gabarap		Sox11	Ugdh
	Ap1m2						Vat1		Fli1	Tek		Jag1	Plac1
	Irf1						Birc5		Tek	Tie1		H2afy2	Pdgfa
	Myl12b						Ccna2		Cgnl1	Gap43		Rdx	Capn6
	Wfdc2						Pimreg		Msn	Prcp		Slc2a1	Pja1
	Tspan13								N4bp3	Gmfg		Magi3	Arhgap29
	Dstn								Plvap	Anxa5		Mmp2	Dok4
	Dnmt3b								Arhgap29	Swap70		Rbpms2	Bex3
	Rbp1								BC028528			Hoxd9	Tbx2
	Actg1								Zfp711			Oat	Krt19
	Cited1								Ppp1r2			Cd24a	Rps6ka6
	Evx1os								Selenop			Tpd52l1	Peg3
	Car2								Arpc3			Nxn	Unc5c
	Tcea3								Cd34			Wnt5a	
	Gpc3											Isl1	
	Gldc											Akap12	
	Tapbp											Rasd1	
	Peg3											Dok4	
	Gja1											Hmgb1	
	Scly												
	Atp1b1												
	Tceal8												
	Mkrn1												
	Pdgfrl												
	Cdh1												
	Stx3												
	Cox7a2												
	Igfbp2												
	Dusp6												
	Tpd52												
	Rhoc												
	Ifitm1												
	Nub1												
	Ppp4r4												
	Bex1												
	Bex4												

Supplementary Table 1.

Gene	Forward Primer (5' -> 3')	Reverse Primer #1 (5' -> 3')	Reverse Primer #2 (5' -> 3')	Product Length #1 (WT)	Product Length #2 (Eo-null/V5/Runx1-Venus)	Application
GAPDH	CAATGACCCCTTCATTGACC	GATCTCGCTCCTGGAAGATG		145		qRT-PCR
SCL	ATAGCCTTAGCCAGCCGCTC	CGCCGCACTACTTTGGTGTG		154		
Runx1	CAGCCTCTCTGCAGAACTTT	ACGGCAGAGTAGGGAACT		89		
PU.1	AGCGATGGAGAAAGCCATAG	CAGCTCTGTGAAGTGGTTCT		102		
Gata1	CAACAGTATGGAGGGAATTCCT	GTGTCCAAGAACGTGTTGTTGC		162		
Hbb-bh1	GAAACCCCCGGATTAGAGCC	GAGCAAAGGTCTCCTTGAGGT		93		
Cdh5	AGGACAGCAACTTCACCCTCA	AACTGCCCATACTTGACCGTG		70		
Flk-1	CACCTGGCACTCTCCACCTTC	GATTTCATCCCACTACCGAAAG		240		
Flt-1	TGGCTCTACGACCTTAGACTG	CAGGTTTGACTTGTCTGAGGTT		247		
Fli1	ATGGACGGGACTATTAAGGAGG	GAAGCAGTCATATCTGCCTTGG		110		
iCre	AAGGAAAGGGGCACCTACAATC	TTTCCTGTTGTTCAGCTTGC		440		Genotyping
Eomes-null (Set#1)	TCTCCTCTCTAGTCACCTTCAC	CCCAATATCCACTCCTCACTTC	TCTACAGAGAGAGTTCCAGGAC	401	535	
Eomes-null (Set#2)	GCTCTGCTTAGGGTGTTTAAGTG	CCCAATATCCACTCCTCACTTC	TCTACAGAGAGAGTTCCAGGAC	499	633	
Eomes-V5 Sanger Sequencing Product	CCTGTGACCAACAAGCTAGAC	TTTAACCCTCTGGGCTGCTG			971	
Eomes-V5	GCAAGAGAAAGCGCCTGTC	AGGATACATCAAAGGTGGAAGG		250	301	
Runx1-Venus	CAAGAGGGATATGGGCAGA	TTCCCTCCGGGATTCTTCCT		5800	4400	

Supplementary Table 2.

Reagent or Resource	Source	Identifier	Lot #	RRID	Dilution	Application
Rabbit polyclonal anti-mouse Eomes	Abcam	Cat #ab23345	lot: GR306193-1	RRID:AB_778267	1 in 100/500	Immunofluorescence
Rabbit monoclonal anti-mouse Runx1	Abcam	Cat# ab92336	Lot: GR107772-16	RRID:AB_2049267	1 in 100	
Rabbit monoclonal anti-mouse VEGFR2 (Flk1)	Cell Signalling Technology	Cat# 2479	Lot: 18	RRID:AB_2212507	1 in 500	
Chicken polyclonal anti-GFP	Abcam	Cat# ab13970	Lot: GR3190550-4	RRID:AB_300798	1 in 1000	
Rat monoclonal anti-mouse Flk-1	Thermo Fisher Scientific	Cat# 14-5821-82		RRID:AB_467623	1 in 200	
Goat polyclonal anti-mouse T	SantaCruz Biotechnology	Cat# sc-17743	Lot: A1614	RRID:AB_634980	1 in 100	
Mouse monoclonal anti-V5 Tag	Thermo Fisher Scientific	Cat# R960-25		RRID:AB_2556564	1 in 200	
Donkey anti-rabbit IgG AlexaFluor 488 (#670)	Life Technologies	Cat# A-21206	Lot: 1480470	RRID:AB_141708	1 in 200	
Goat anti-Chicken AlexaFluor 488 (#722)	Life Technologies	Cat# A-11039	Lot: 1637891	RRID:AB_141708	1 in 200	
Donkey anti-Rabbit IgG AlexaFluor 594 (#714)	Life Technologies	Cat# A-21207	Lot: 1938375	RRID:AB_141637	1 in 200	
Donkey Anti-Mouse IgG AlexaFluor 488	Life Technologies	Cat# A-21202	Lot: 1975519	RRID:AB_141607	1 in 400	
Donkey anti-Rat AlexaFluor 594 (#680)	Life Technologies	Cat# A-21209		RRID:AB_2535795	1 in 400	
Donkey anti-goat IgG AlexaFluor 594 (#671)	Life Technologies	Cat# A-11058	Lot: 1445994	RRID:AB_142540	1 in 200	
DAPI	BIOTIUM	Cat# 40043	Lot: 1900122		1 in 5000	
Rat monoclonal anti-mouse Flk-1 APC	Thermo Fisher Scientific	Cat# 17-5821-81	Lot: 1998335	RRID:AB_657866	1 in 40	Flow Cytometry
Rat monoclonal anti-mouse PdgfRa PECy7	Thermo Fisher Scientific	Cat# 25-1401-82	Lot: 4334654	RRID:AB_2573400	1 in 160	
Rat monoclonal anti-mouse CD144 APC	Thermo Fisher Scientific	Cat# 17-1441-82	Lot: 4319919	RRID:AB_10598508	1 in 160	
Rat monoclonal anti-mouse CD144 PeCy7	Thermo Fisher Scientific	Cat# 25-1441-82	Lot: 4346553	RRID:AB_2573402	1 in 160	
Rat monoclonal anti-mouse CD117 BV605	BioLegend	Cat# 105847	Lot: B274670	RRID:AB_2783047	1 in 160	
Rat monoclonal anti-mouse CD117 APC	Thermo Fisher Scientific	Cat# 17-1172-82	Lot: 4277766	RRID:AB_469433	1 in 160	
Rat monoclonal anti-mouse CD41a PECy7	Thermo Fisher Scientific	Cat# 24-0411-82	Lot: 4293461	RRID:AB_1234970	1 in 200	
Rat monoclonal anti-mouse CD45 PECy7	Thermo Fisher Scientific	Cat# 25-0451-82	Lot: 4329704	RRID:AB_469625	1 in 160	
Rat monoclonal anti-mouse CD31 APC	BioLegend	Cat# 102510	Lot: 13233286	RRID:AB_312917	1 in 80	
Mouse monoclonal anti-V5 Tag, FITC	Invitrogen	Cat# R963-25		RRID:AB_2556567	1 in 400	
DAPI	BD Biosciences	Cat# 564907	Lot: 8012653		1 in 5000	
V5-tag antibody - ChIP Grade	Abcam	Cat# ab9116	Lot: GR: 322448-4	RRID:AB_307024		ChIP
Rabbit polyclonal anti-mouse Eomes	Abcam	Cat# ab23345	Lot: GR733208	RRID:AB_778267	1 in 2000	Western Blot
Mouse monoclonal anti-V5 Tag	Thermo Fisher Scientific	Cat# R960-25	Lot: 1923773	RRID:AB_2556564	1 in 1000	
Sheep anti-mouse HRP Conjugated (#160)	GE Healthcare	Cat # NA931V	Lot: 9621358	RRID: AB_772210	1 in 2000	
Donkey anti-rabbit HRP Conjugated (#159)	GE Healthcare	Cat# NA934V	Lot: 9761196	RRID: AB_772206	1 in 2000	
Anti-APC Microbeads	Miltenyi Biotec	Cat# 130090855	Lot: 5190123600		1 in 5	MACS

Supplementary Table 3.

Name	Sequence	Application
iCre	TCAGTCCCCATCCTCGAGCAGCCTCACCATGGCCCCAGTCTCAG AGTCCAGGTTTCTGATGTAGTTCATCACAATGTTCACATTGGTCCA GCCACCAGCCTGCATGATTTCAGGGATGGACACACCAGCCCTGG CCATGTCCCTGGCAGCACCCACTCTGGCAGAGTGGCCAGACCA GGCCAGGTATCTCTGCCCAGAGTCATCCTTGGCACCATAGATCA GGCGGTGGGTGGCCTCAAAGATCCCTTCCAGGGCCCGGGTGGA CAGTTGGGAGGTGGCAGAAGGGGCAGCCACACCATTCTTTCTGA CCCGGCAGAACAGGTAGTTGTTGGGGTCATCAGCCACACCAGAC ACAGAGATCCATCTCTCCACCAGCTTGGTAACCCCCAGGGACAG GGCCTTCTCCACACCAGCTGTGGACACCAGGGTCTTGGTCCTGC CAATGTGGATCAGCATTCTCCCACCATCGGTGCGGGAGATGTCCT TCACTCTGATTCTGGCAATTTCGGCAATGCGCAGCAGGGTGTTGT AGGCAATGCCCAGGAAGGCCAGGTTCCTGATGTCCTGGCATCTG TCAGAGTTCTCCATCAGGGATCTGACTTGGTCAAAGTCAGTGCGT TCAAAGGCCAGGGCCTGCTTGGCTCTCTCCCCAGCATCCACATT CTCCTTTCTGATTCTCCTCATCACCAGGGACACAGCATTGGAGTC AGAAGGGCGAGGCAGGCCAGATCTCCTGTGCAGCATGTTGAGCT GGCCCAGGTGCTGTTGGATGGTCTTCACAGCCAGGCCTCTGGCT TGCAGGTACAGGAGGTAGTCCCTCACATCCTCAGGTTCAGCAGG GAACCATTTCCTGTTGTTCAGCTTGCACCAGGCAGCCCAGGATCT GCACACAGACAGGAGCATCTTCCAGGTGTGTTCAGAGAAGG	WISH

Supplementary Table 4.

Figure ID	Company	Product #	Sequence	Application
gRNA#1(Protospacer)	N/A	N/A	CGATGGCGCTCAGCTCAGTAGGG	Generation of the Runx1-Venus ESC Reporter Line
gRNA#1Forward Oligo	N/A	N/A	caccgCGATGGCGCTCAGCTCAGTA	
gRNA#1Reverse Oligo	N/A	N/A	aaacCCCTACTGAGCTGAGCGCCATCGc	
gRNA #2	Integrated DNA Technologies	Alt-R® CRISPR-Cas9 crRNA	GGTTTGCAGCAGGCGATTTGTGG	Re-generation of Eomes-null ESC Line in Runx1-Venus and SCL-mCherry ESC lines (Figure S3.a-c)
gRNA #3	Integrated DNA Technologies	Alt-R® CRISPR-Cas9 crRNA	AGAGGCATCCCGGCACCCTGAGG	
ssODN #1	Integrated DNA Technologies	Ultramer® DNA Oligo	C*C*CTCTTAACCTCCCTCCCCATGCCCT AAATAAACTCTATTCTATACTATTCCATCT TGTGGCTGGTCCCTCAGGGATATCGCCT GCTGCAAACCCAGGAGCCAGCGGGTCAC GTAGATCTGCCCTCAAGGGTTCATTCCCA AATTTCCATC*T*C	
ssODN #2 (Sph1)	Integrated DNA Technologies	Ultramer® DNA Oligo	C*C*CTCTTAACCTCCCTCCCCATGCCCT AAATAAACTCTATTCTATACTATTCCATCT TGTGGCTGGTCCCTCAGGGCATGCGCCT GCTGCAAACCCAGGAGCCAGCGGGTCAC GTAGATCTGCCCTCAAGGGTTCATTCCCA AATTTCCATC*T*C	Re-generation of Eomes-null ESC Line in iRunx1 ESC lines (Figure S3.d,e)
ssODN #3 (Spe1)	Integrated DNA Technologies	Ultramer® DNA Oligo	C*C*CTCTTAACCTCCCTCCCCATGCCCT AAATAAACTCTATTCTATACTATTCCATCT TGTGGCTGGTCCCTCAGGACTAGTGCCT GCTGCAAACCCAGGAGCCAGCGGGTCAC GTAGATCTGCCCTCAAGGGTTCATTCCCA AATTTCCATC*T*C	
gRNA #4	Integrated DNA Technologies	Alt-R® CRISPR-Cas9 crRNA	AAGGTTAAAATAATGCTCTAGGG	Generation of Eomes-V5 ESC Line (Figure S5)
ssODN #4	Integrated DNA Technologies	Ultramer® DNA Oligo	G*T*AACCTAGGCAAAGAACACAACAAAA CACCACCAGGTCCATCTGGAAAGGTTAAA GGTTAAAATAATGCTCTACGTAGAATCGA GACCGAGGAGAGGGTTAGGGATAGGCTT ACCTCCTCCTCCGGGACTTGTGTAAAAAG CATAATAAGCCCCCATGCCTTTGGAGGTG TCTTTACTGTACTCTTCAGTGTTAAT*G*T	
*Phosphorothioated DNA bases				

Supplementary Table 5.

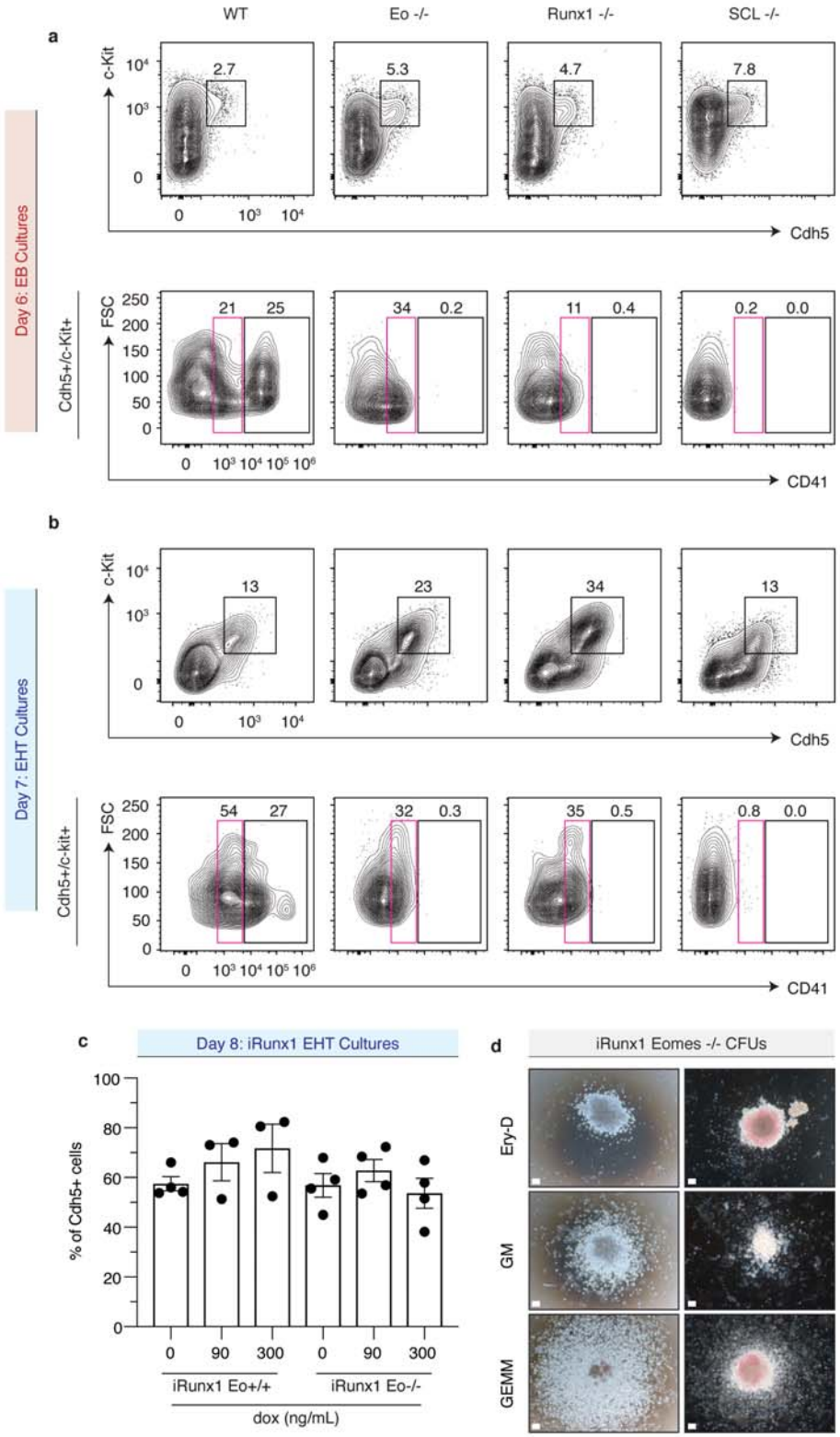
a
WT
Eo -/-
Runx1 -/-
SCL -/-
Day 6: EB Cultures
c-Kit
2.7
5.3
4.7
7.8
Cdh5
Cdh5+/c-Kit+
FSC
21
25
34
0.2
11
0.4
0.2
0.0
CD41
b
Day 7: EHT Cultures
c-kit
13
23
34
13
Cdh5
Cdh5+/c-kit+
54
27
32
0.3
35
0.5
0.8
0.0
CD41
c
Day 8: iRunx1 EHT Cultures
% of Cdh5+ cells
iRunx1 Eo+/+
iRunx1 Eo-/-
dox (ng/mL)
d
iRunx1 Eomes -/- CFUs
Ery-D
GM
GEMM

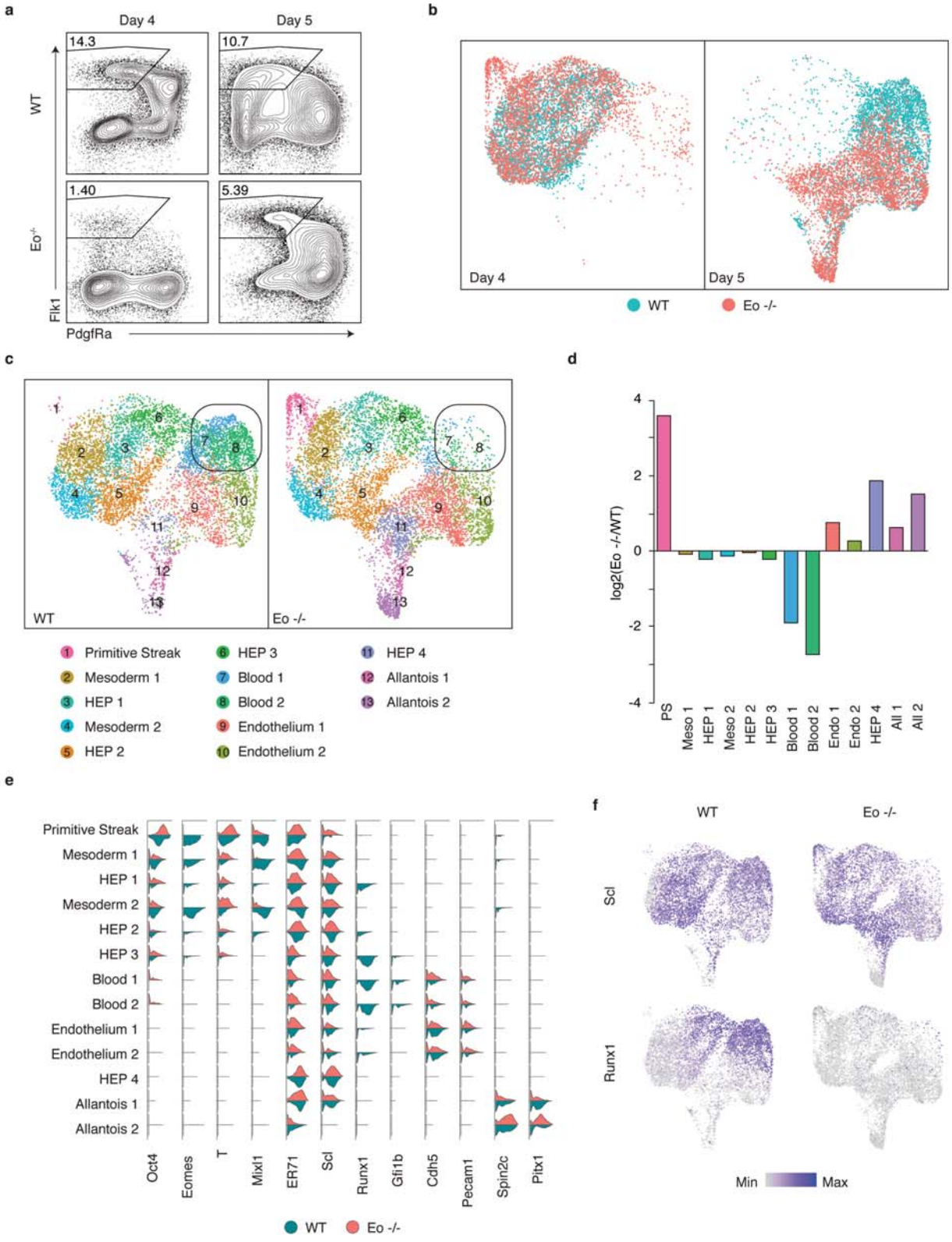
a
Day 4
Day 5
14.3
10.7
1.40
5.39
WT
Eo-/-
Flk1
PdgfRa
b
Day 4
Day 5
WT
Eo -/-
c
WT
Eo -/-
1 Primitive Streak
2 Mesoderm 1
3 HEP 1
4 Mesoderm 2
5 HEP 2
6 HEP 3
7 Blood 1
8 Blood 2
9 Endothelium 1
10 Endothelium 2
11 HEP 4
12 Allantois 1
13 Allantois 2
d
log2(Eo -/-/WT)
4
2
0
-2
-4
PS
Meso 1
HEP 1
Meso 2
HEP 2
HEP 3
Blood 1
Blood 2
Endo 1
Endo 2
HEP 4
All 1
All 2
e
Primitive Streak
Mesoderm 1
HEP 1
Mesoderm 2
HEP 2
HEP 3
Blood 1
Blood 2
Endothelium 1
Endothelium 2
HEP 4
Allantois 1
Allantois 2
Oct4
Eomes
T
Mixl1
ER71
Scl
Runx1
Gfi1b
Cdh5
Pecam1
Spin2c
Pitx1
WT
Eo -/-
f
WT
Eo -/-
Scl
Runx1
Min
Max

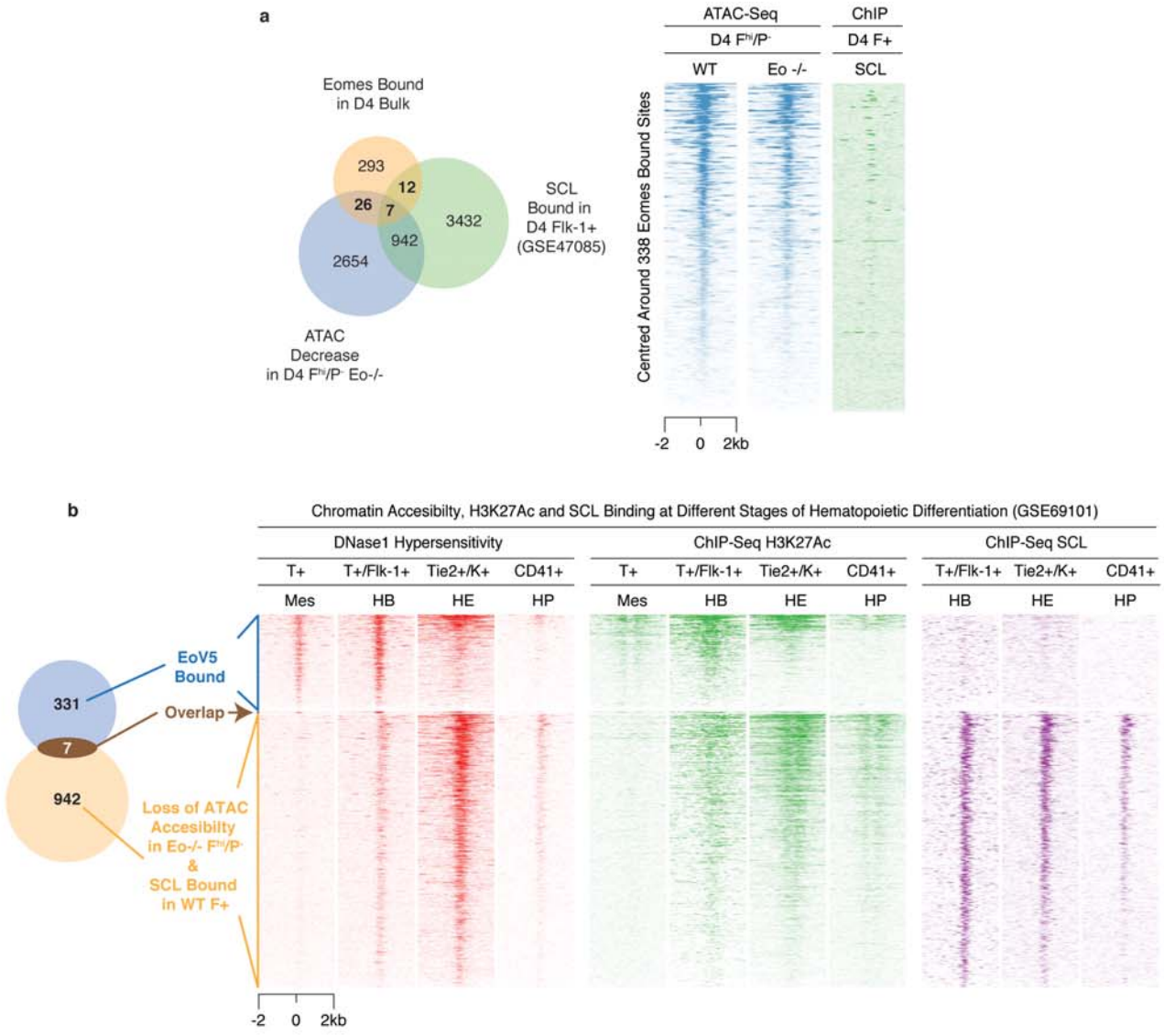
a
Eomes Bound
in D4 Bulk
293
12
26
7
3432
942
2654
SCL
Bound in
D4 Flk-1+
(GSE47085)
ATAC
Decrease
in D4 Fhi/P- Eo-/-
ATAC-Seq
D4 Fhi/P-
WT
Eo -/-
ChIP
D4 F+
SCL
Centred Around 338 Eomes Bound Sites
-2
0
2kb
b
Chromatin Accesibilty, H3K27Ac and SCL Binding at Different Stages of Hematopoietic Differentiation (GSE69101)
DNase1 Hypersensitivity
ChIP-Seq H3K27Ac
ChIP-Seq SCL
T+
T+/Flk-1+
Tie2+/K+
CD41+
Mes
HB
HE
HP
EoV5
Bound
331
Overlap
7
942
Loss of ATAC
Accesibilty
in Eo-/- Fhi/P-
&
SCL Bound
in WT F+
-2
0
2kb

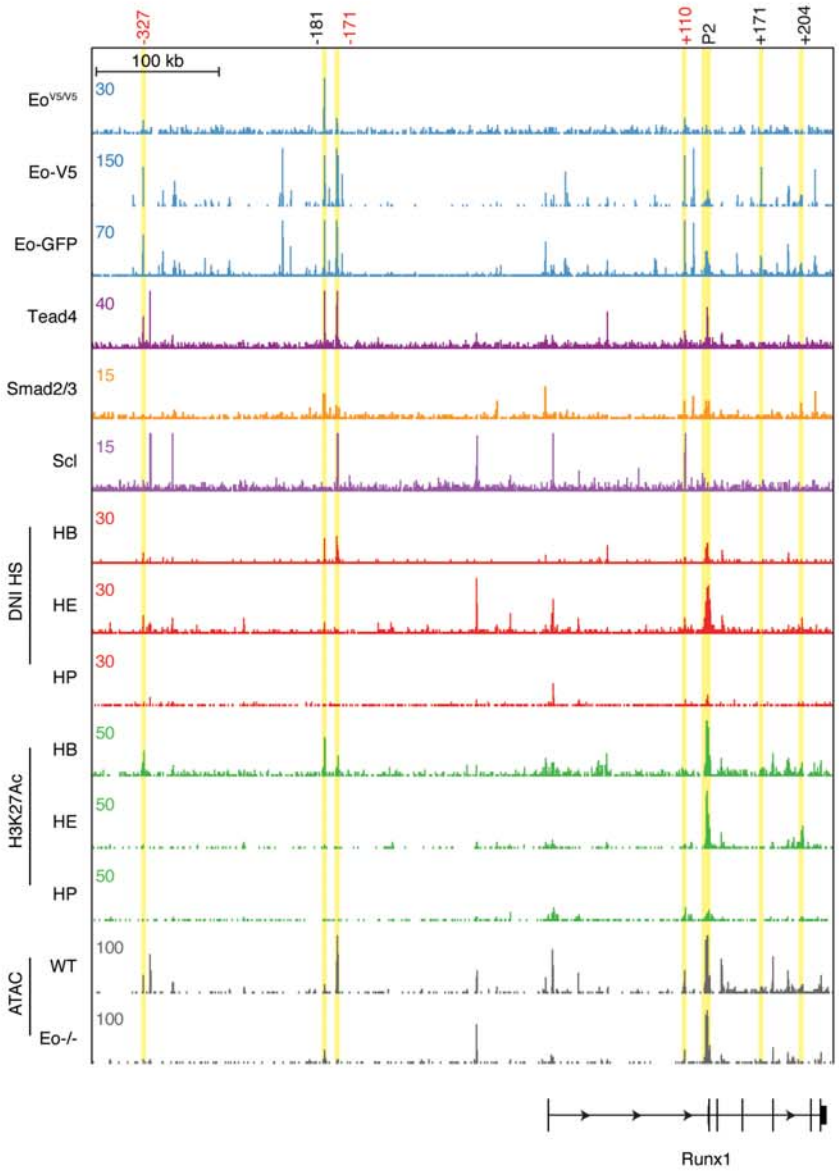
-327
-181
-171
+110
P2
+171
+204
100 kb
Eo^V5/V5
30
Eo-V5
150
Eo-GFP
70
Tead4
40
Smad2/3
15
Scl
15
DNI HS
HB
30
HE
30
HP
30
H3K27Ac
HB
50
HE
50
HP
50
ATAC
WT
100
Eo-/-
100
Runx1

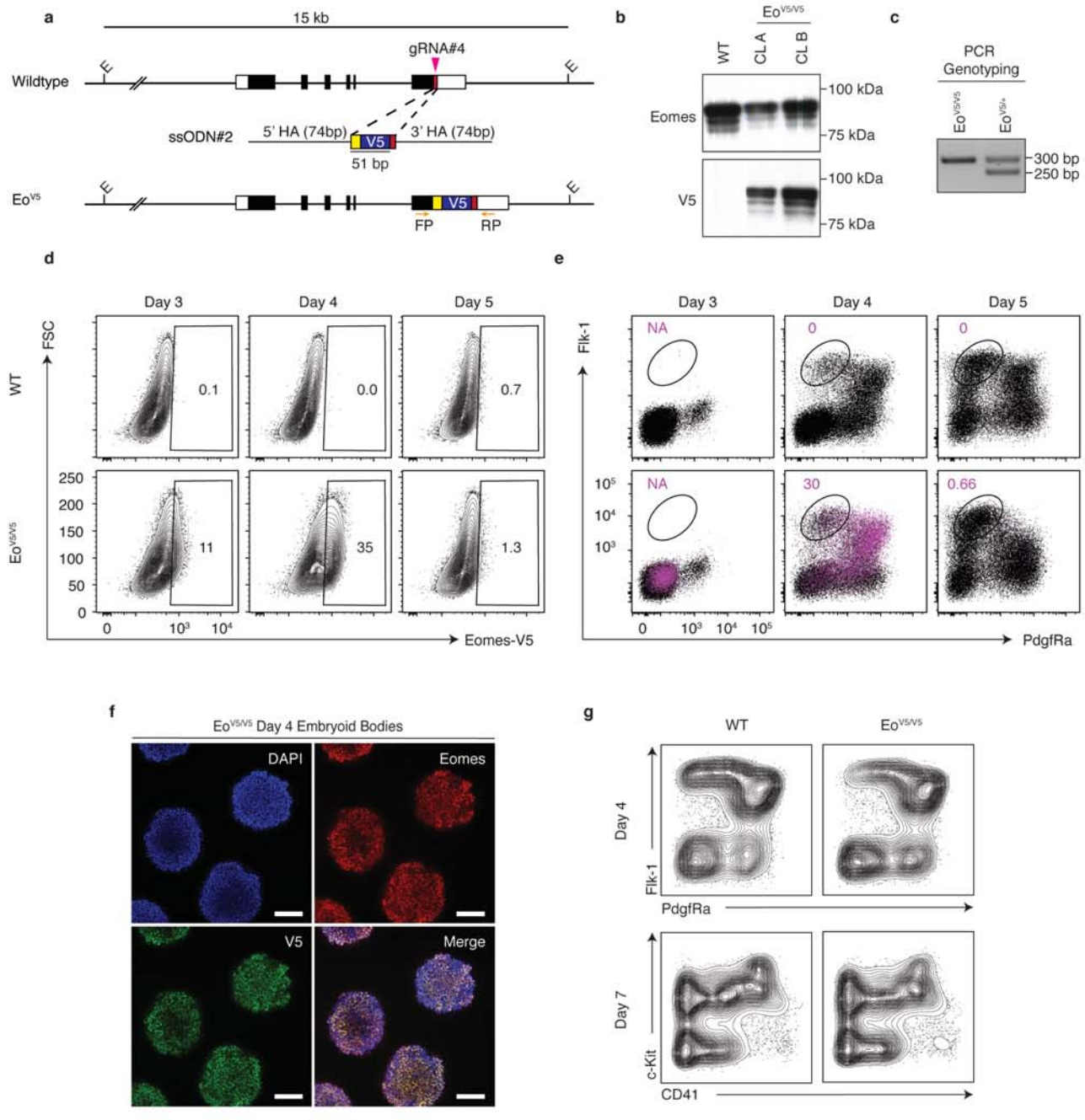
a
15 kb
gRNA#4
Wildtype
E
E
ssODN#2
5' HA (74bp)
V5
3' HA (74bp)
51 bp
Eo^V5
E
E
V5
FP
RP
b
Eo^V5/V5
WT
CL A
CL B
Eomes
100 kDa
75 kDa
V5
100 kDa
75 kDa
c
PCR Genotyping
Eo^V5/V5
Eo^V5/+
300 bp
250 bp
d
Day 3
Day 4
Day 5
WT
FSC
0.1
0.0
0.7
Eo^V5/V5
250
200
150
100
50
0
11
35
1.3
0
10^3
10^4
Eomes-V5
e
Day 3
Day 4
Day 5
Flk-1
NA
0
0
NA
30
0.66
10^5
10^4
10^3
0
10^3
10^4
10^5
PdgfRa
f
Eo^V5/V5 Day 4 Embryoid Bodies
DAPI
Eomes
V5
Merge
g
WT
Eo^V5/V5
Day 4
Flk-1
PdgfRa
Day 7
c-Kit
CD41

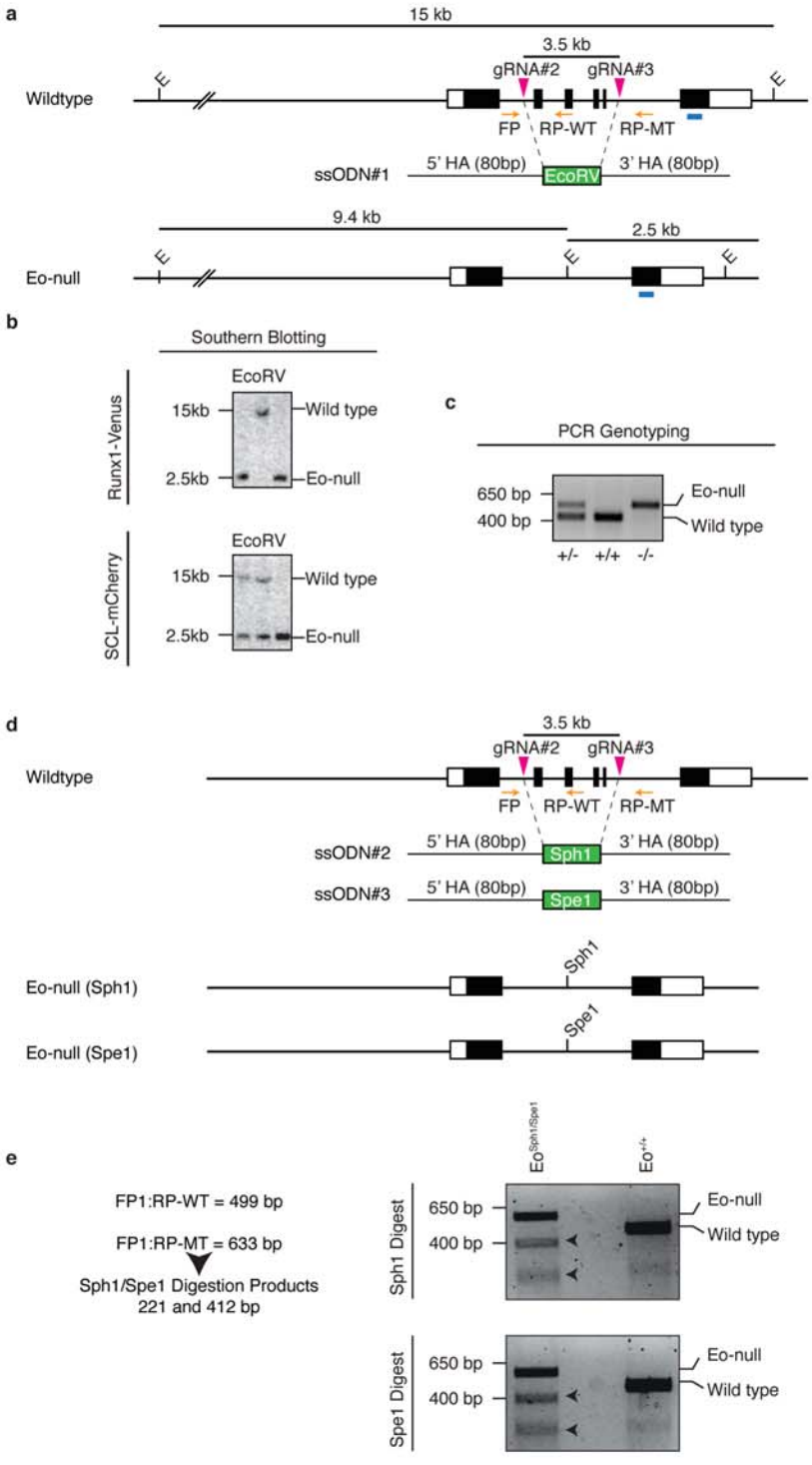
a
15 kb
3.5 kb
gRNA#2
gRNA#3
Wildtype
E
E
E
FP
RP-WT
RP-MT
ssODN#1
5' HA (80bp)
EcoRV
3' HA (80bp)
9.4 kb
2.5 kb
Eo-null
b
Southern Blotting
EcoRV
Runx1-Venus
15kb
Wild type
2.5kb
Eo-null
EcoRV
SCL-mCherry
15kb
Wild type
2.5kb
Eo-null
c
PCR Genotyping
650 bp
400 bp
Eo-null
Wild type
+/-
+/+
-/-
d
3.5 kb
gRNA#2
gRNA#3
Wildtype
FP
RP-WT
RP-MT
ssODN#2
5' HA (80bp)
Sph1
3' HA (80bp)
ssODN#3
5' HA (80bp)
Spe1
3' HA (80bp)
Sph1
Eo-null (Sph1)
Spe1
Eo-null (Spe1)
e
FP1:RP-WT = 499 bp
FP1:RP-MT = 633 bp
Sph1/Spe1 Digestion Products
221 and 412 bp
Eo Sph1/Spe1
Eo +/+
Sph1 Digest
650 bp
400 bp
Eo-null
Wild type
Spe1 Digest
650 bp
400 bp
Eo-null
Wild type

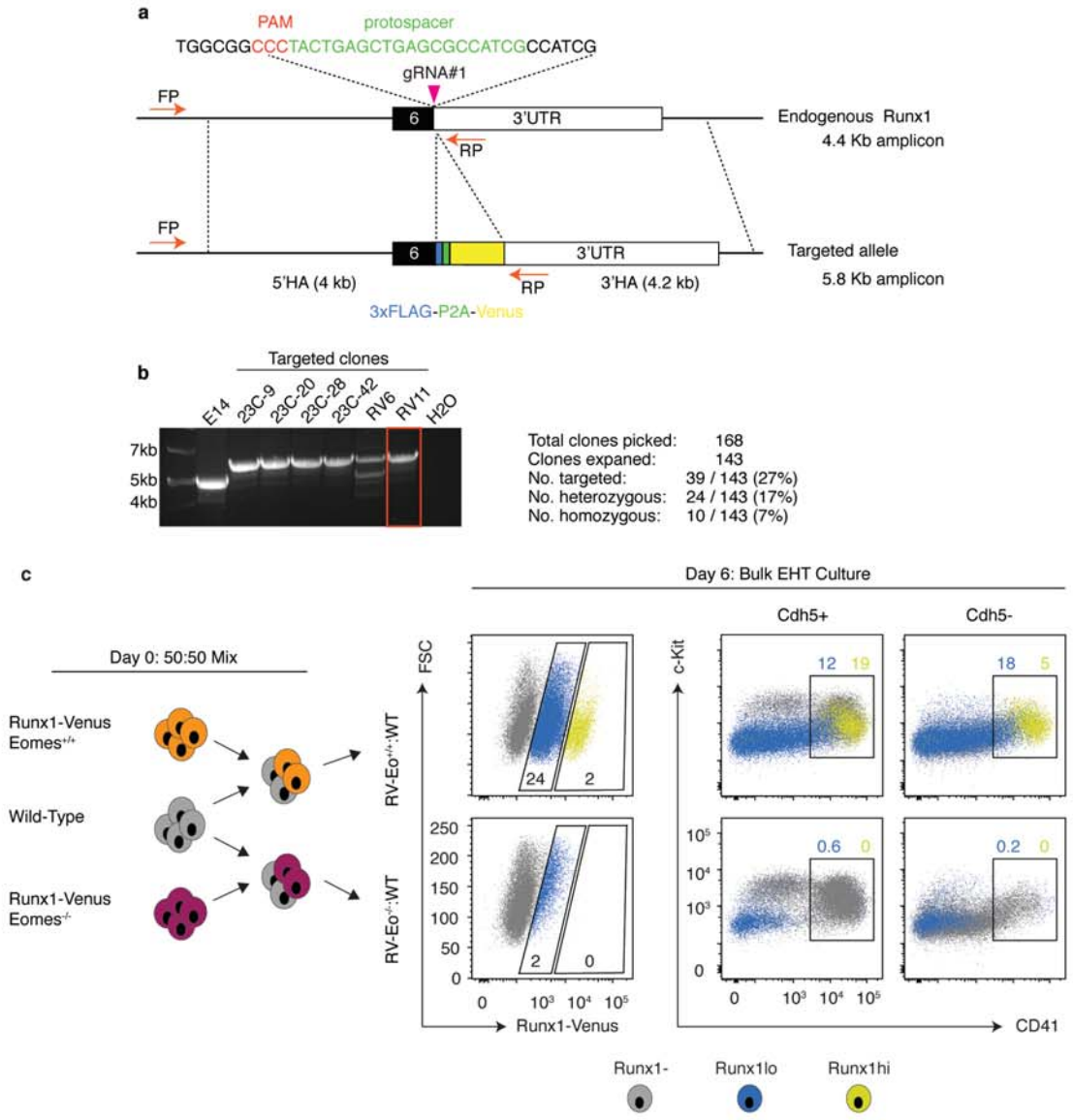
a
PAM
protospacer
TGGCGGCCCTACTGAGCTGAGCGCCATCGCCATCG
gRNA#1
FP
6
3'UTR
RP
Endogenous Runx1
4.4 Kb amplicon
FP
6
3'UTR
Targeted allele
5.8 Kb amplicon
5'HA (4 kb)
RP
3'HA (4.2 kb)
3xFLAG-P2A-Venus
b
Targeted clones
E14
23C-9
23C-20
23C-28
23C-42
RV6
RV11
H2O
7kb
5kb
4kb
Total clones picked: 168
Clones expaned: 143
No. targeted: 39 / 143 (27%)
No. heterozygous: 24 / 143 (17%)
No. homozygous: 10 / 143 (7%)
c
Day 0: 50:50 Mix
Runx1-Venus
Eomes+/+
Wild-Type
Runx1-Venus
Eomes-/-
Day 6: Bulk EHT Culture
Cdh5+
Cdh5-
FSC
c-Kit
RV-Eo+/+:WT
RV-Eo-/-:WT
24
2
12
19
18
5
2
0
0.6
0
0.2
0
Runx1-Venus
CD41
Runx1-
Runx1lo
Runx1hi

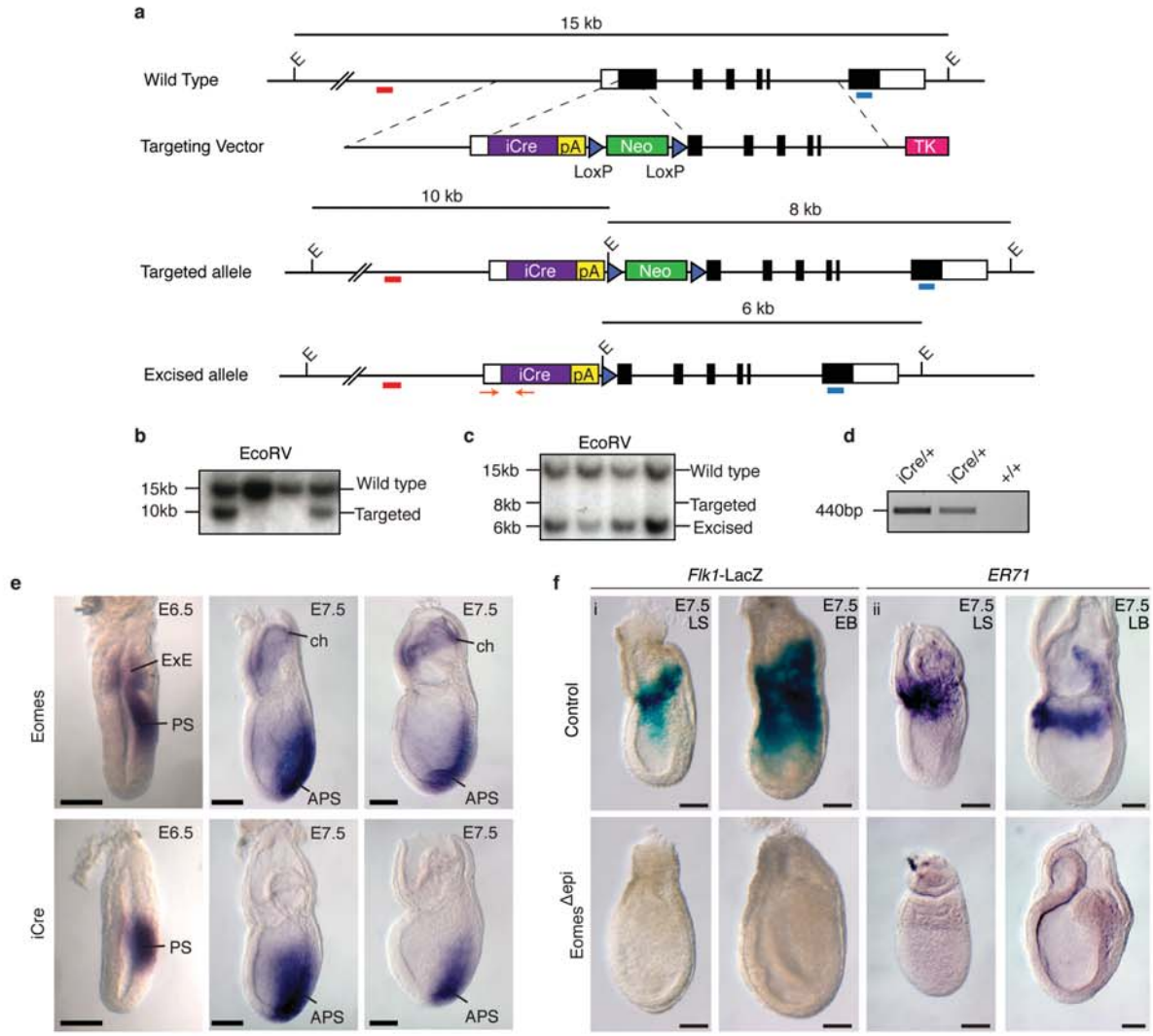
a
15 kb
Wild Type
E
E
Targeting Vector
iCre
pA
Neo
TK
LoxP
LoxP
10 kb
8 kb
Targeted allele
6 kb
Excised allele
b
EcoRV
15kb
10kb
Wild type
Targeted
c
EcoRV
15kb
8kb
6kb
Wild type
Targeted
Excised
d
iCre/+
iCre/+
+/+
440bp
e
Eomes
iCre
E6.5
E7.5
ExE
PS
ch
APS
f
Flk1-LacZ
ER71
Control
Eomes Δepi
i
ii
E7.5 LS
E7.5 EB
E7.5 LB

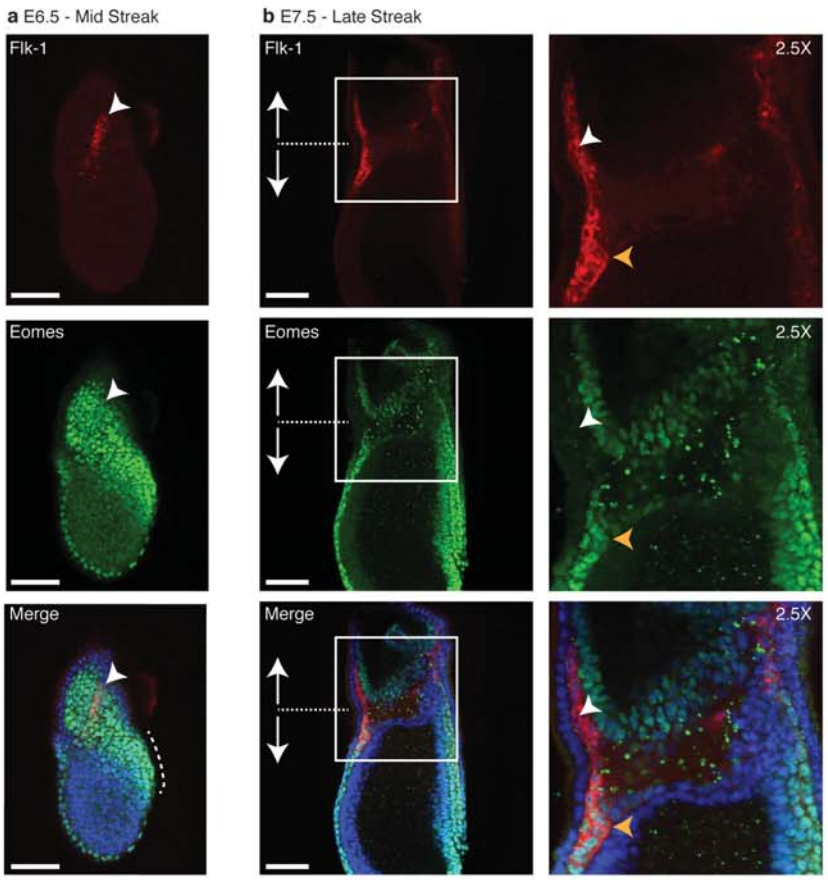
a E6.5 - Mid Streak
b E7.5 - Late Streak
Flk-1
Flk-1
2.5X
Eomes
Eomes
2.5X
Merge
Merge
2.5X